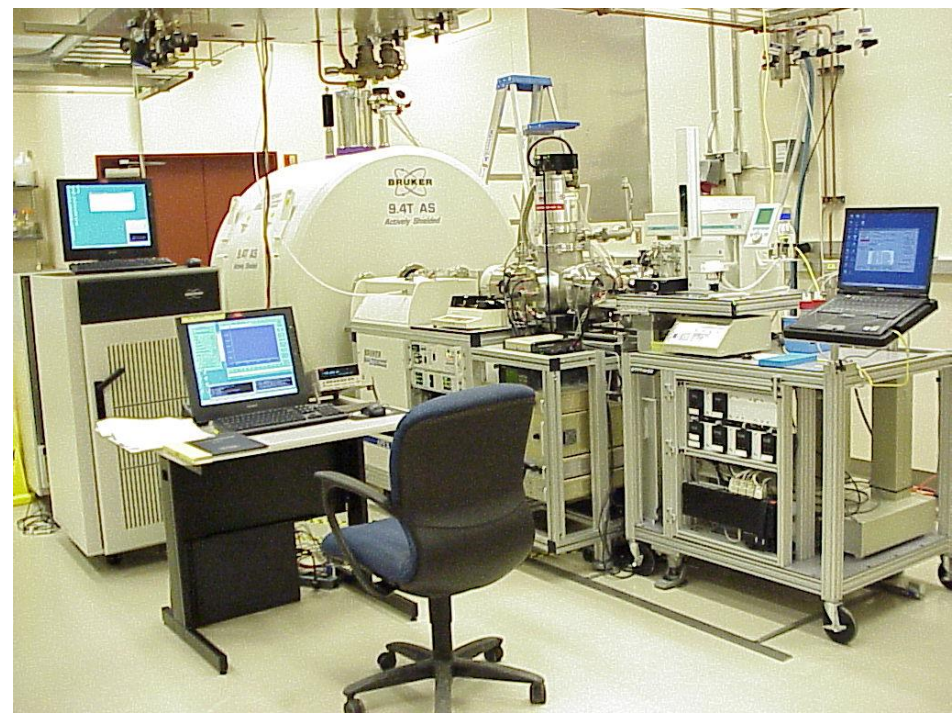
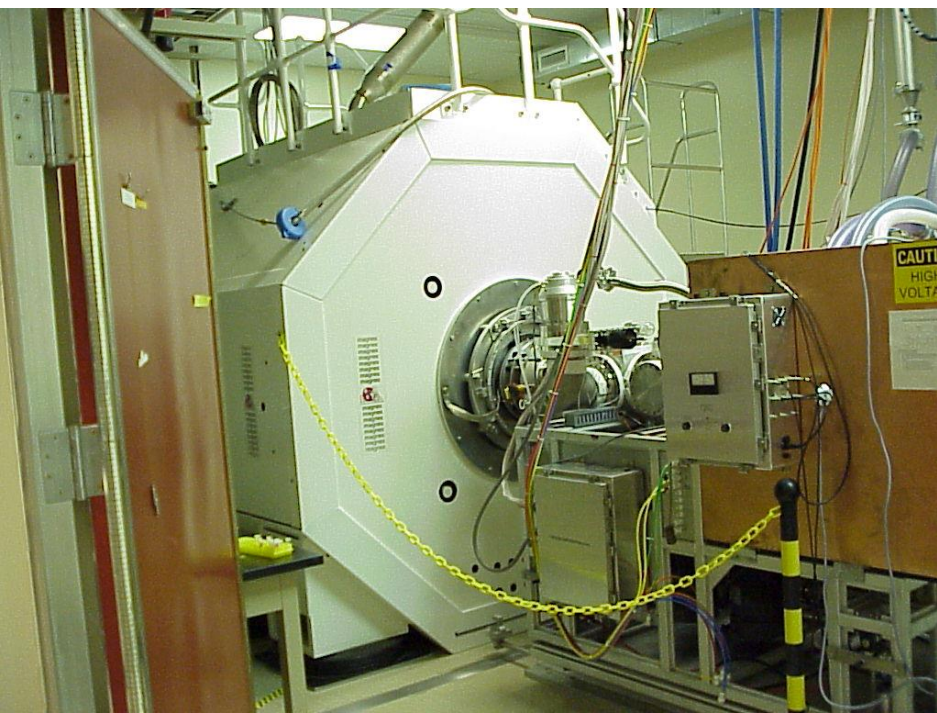
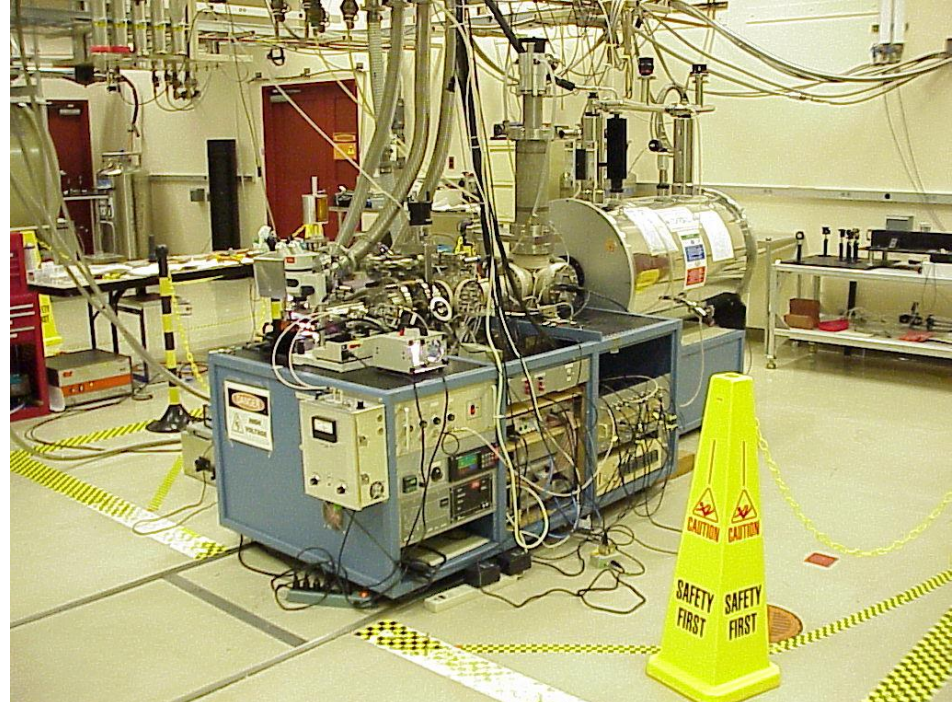
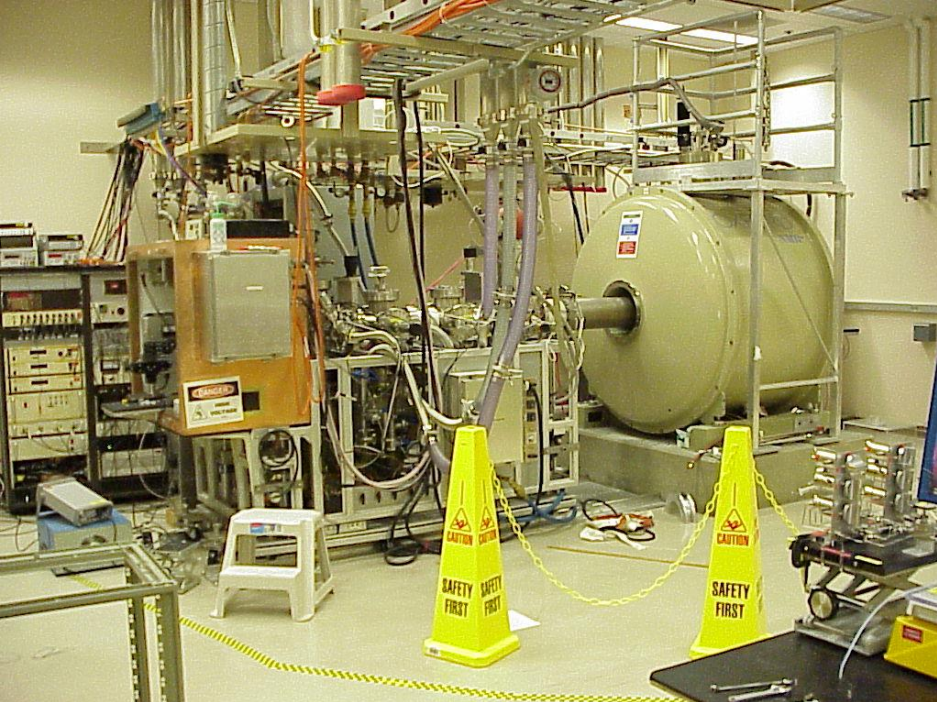


FT ICR cell: How to make the best

Evgeny Nikolaev
Skolkovo Institute of Science and Technology



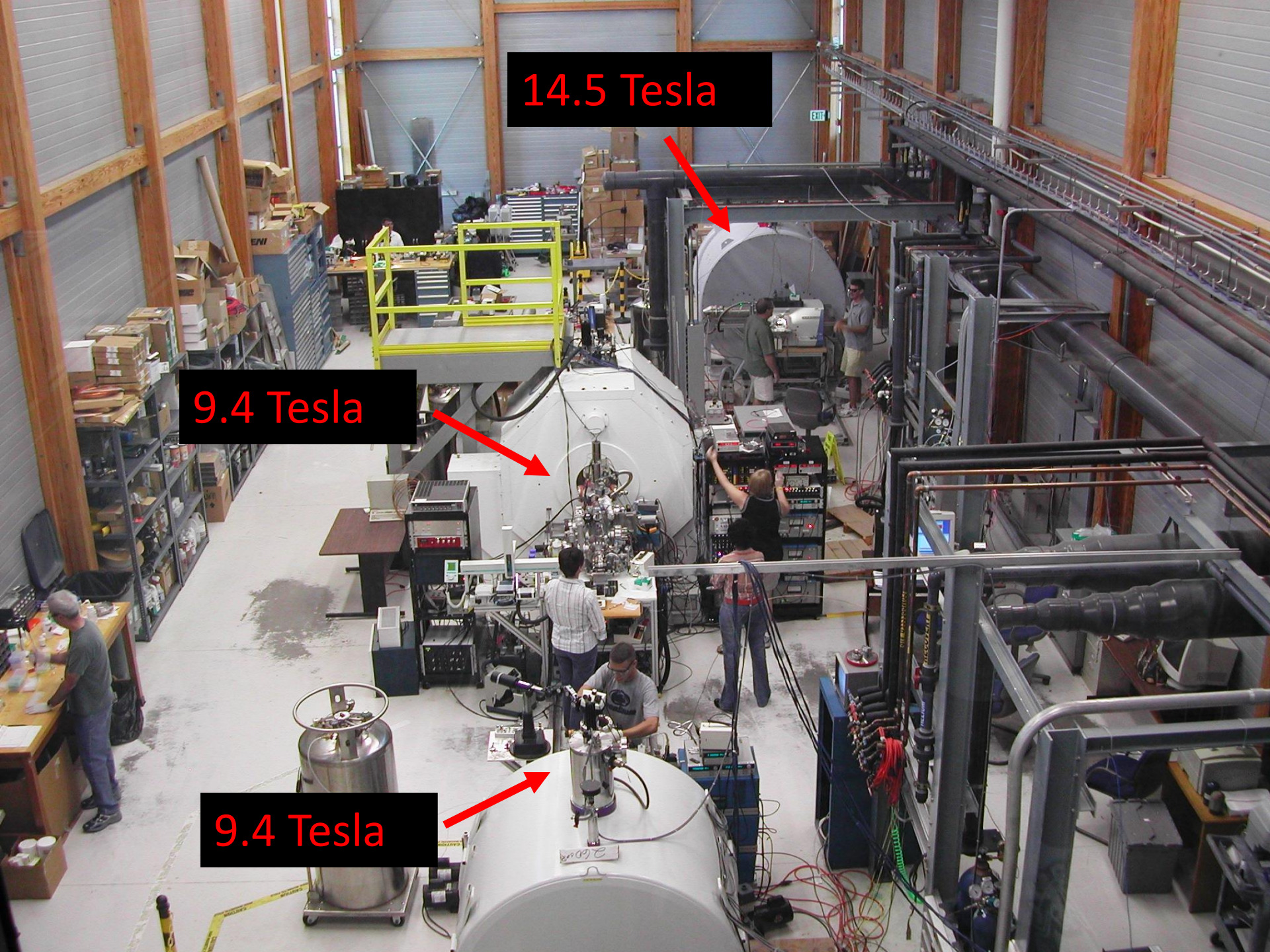
Since introduction in 1974 FT ICR continue to be the best in resolving power and mass measurement accuracy!



14.5 Tesla

9.4 Tesla

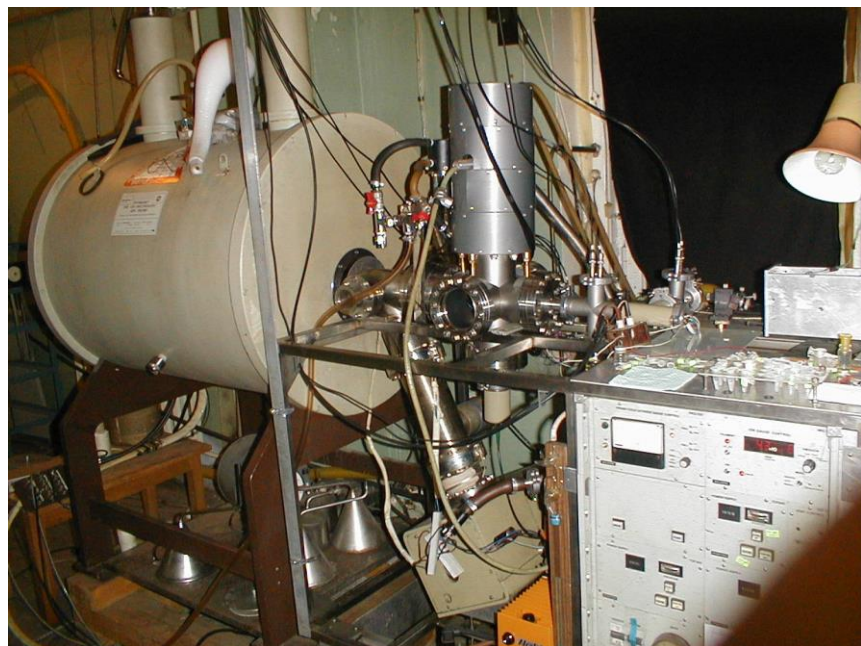
9.4 Tesla





National High Magnetic Field Laboratory NHMFL (Tallahassee Florida)

From Alan Marshall 10th NA FTMS 21 T talk



Moscow FT ICR
instruments

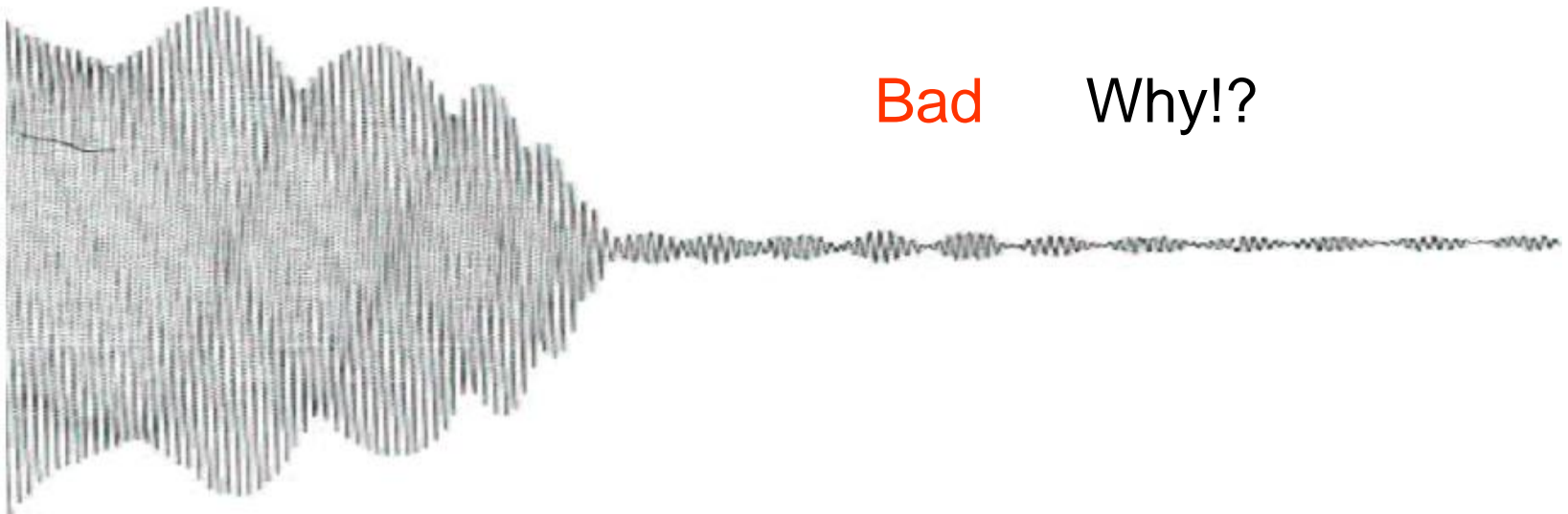
After 47 years since introduction of FT ICR
do we understand how it works?

Good!



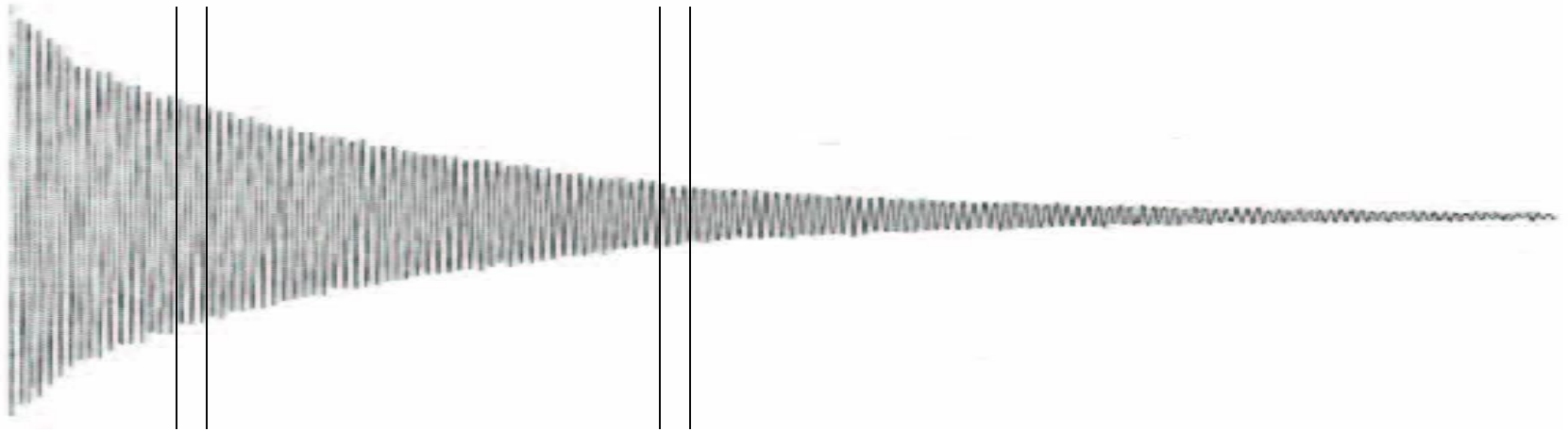
Signals from same m/z ions

Bad Why!?



$\Omega(t)$

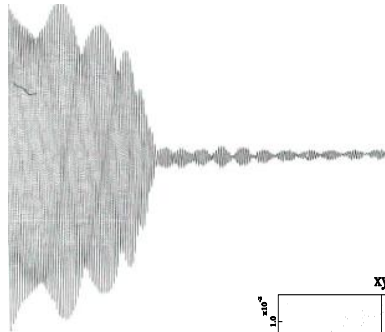
$\Omega(t+\Delta t)$



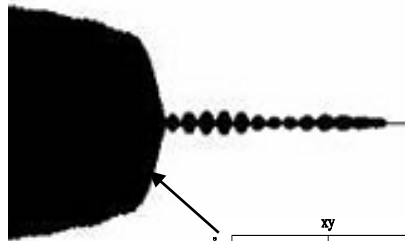
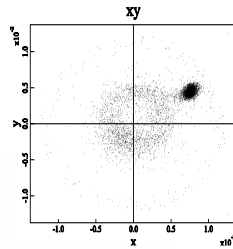
$\Omega(t+\Delta t) \neq \Omega(t)$

Why!?

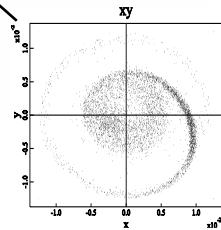
Strange signal forms



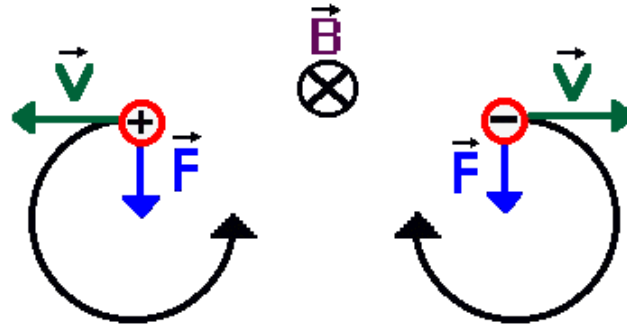
Experimental



Simulated



Charged particle in magnetic field



Lorentz force $F = ze \cdot v \cdot B = m \cdot v^2 / r$

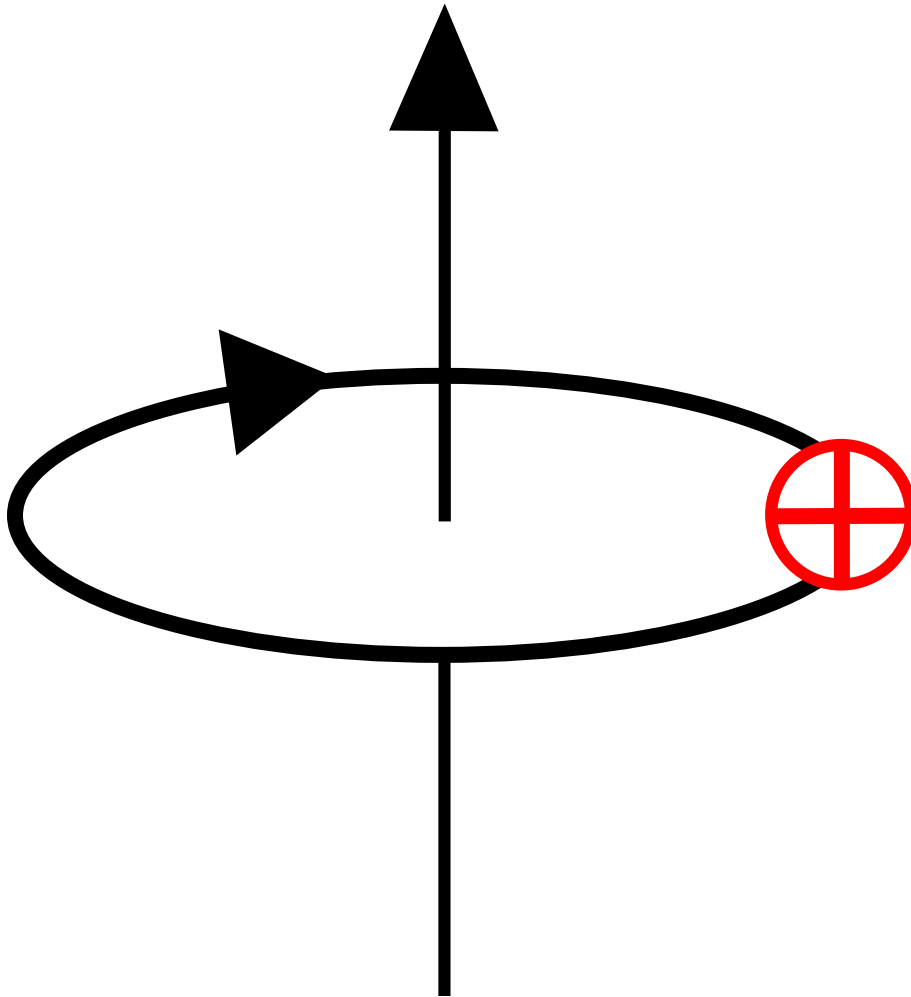
$$v/r = 2\pi\omega,$$

$$ze \cdot B = m \cdot 2\pi\omega$$

$$\omega = B \cdot ze / 2\pi m \text{ (cyclotron frequency)}$$

B

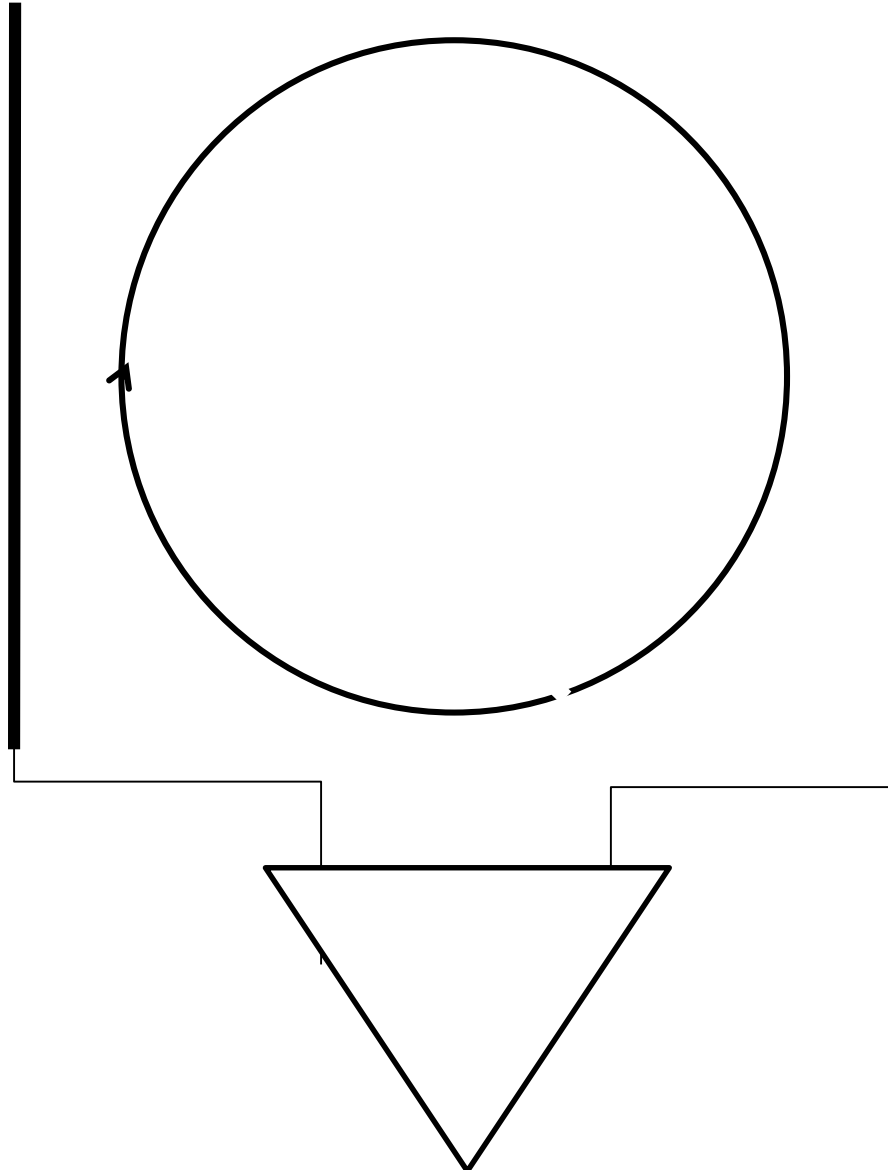
Cyclotron motion of ions



$$\omega = \frac{Z e B}{m}$$

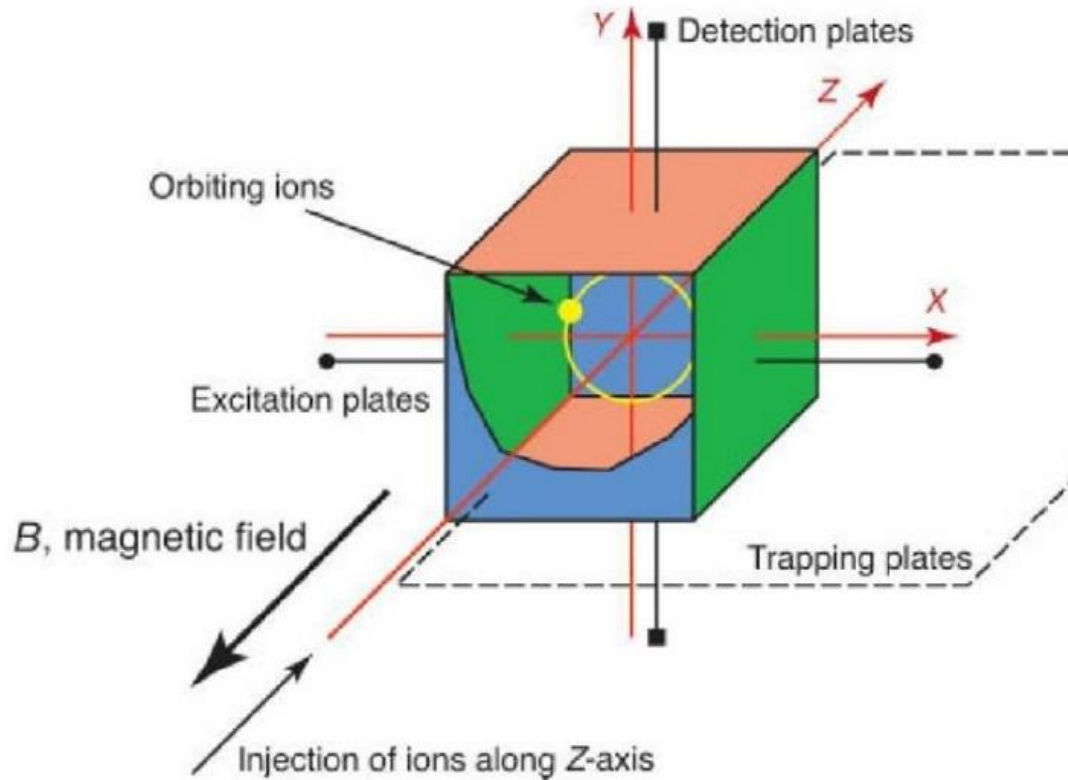
Ion motion in electric field free space

$$\omega_c = \frac{|eB|}{mc}$$

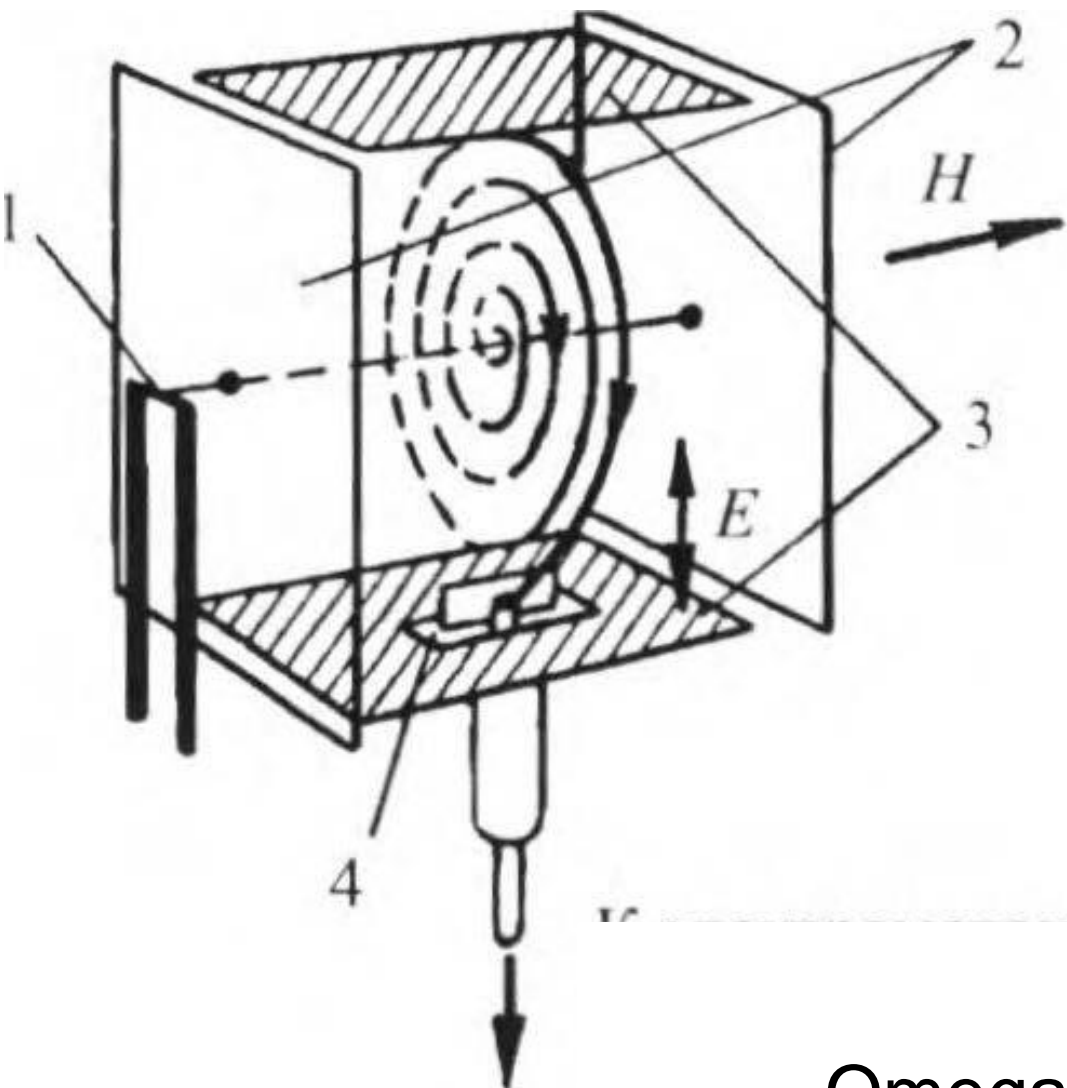


To excite cyclotron motion and detect the signal we need to trap ions

ICR Cells (Penning trap)

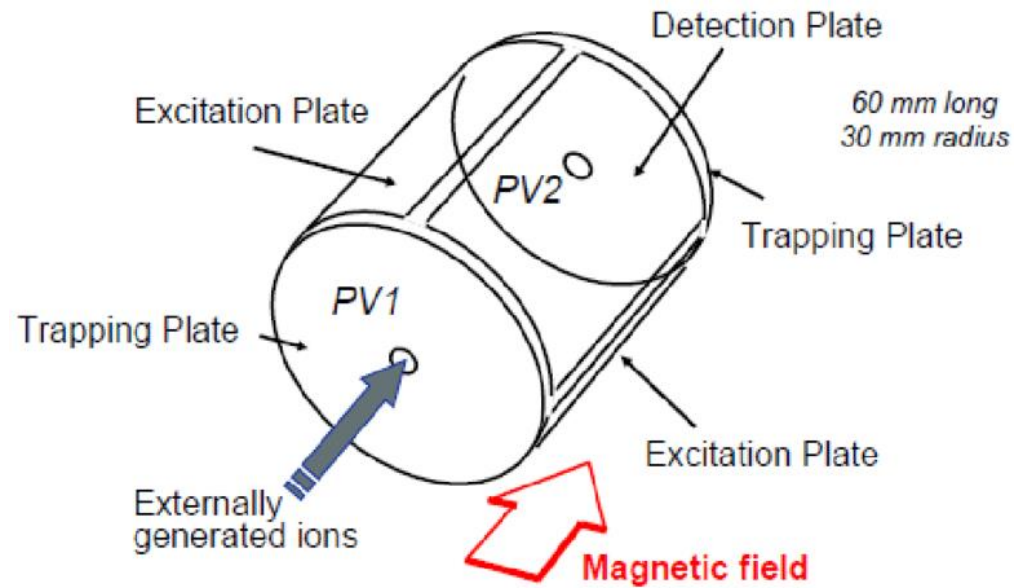


Was used in electromagnet Based FT ICR instruments



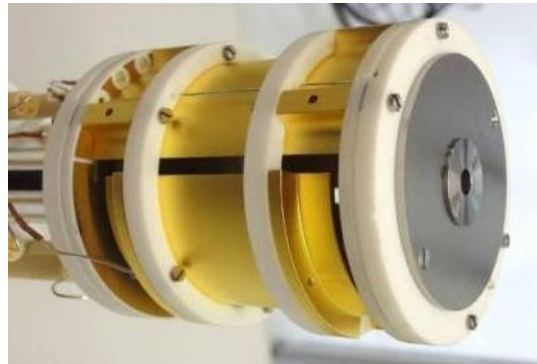
Omegatron

For superconductive magnets with cylindrical symmetry

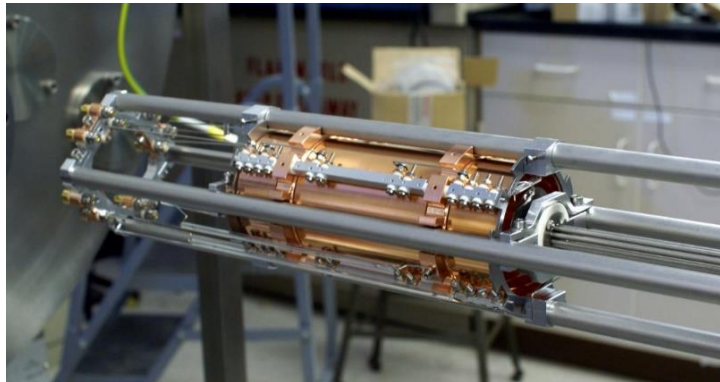


Most used cells

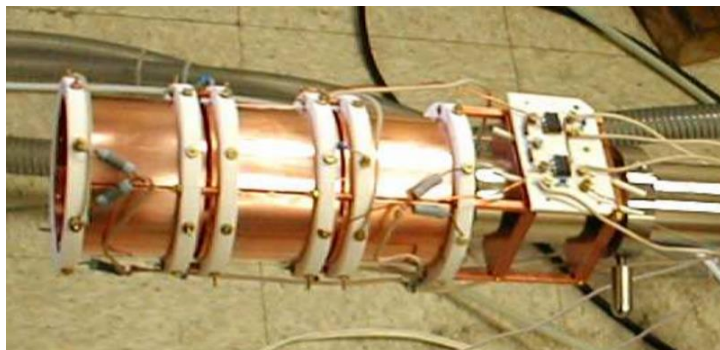
Bruker
Infinity cell
(until 2014)



Thermo
LTQ FT
(until 2006)

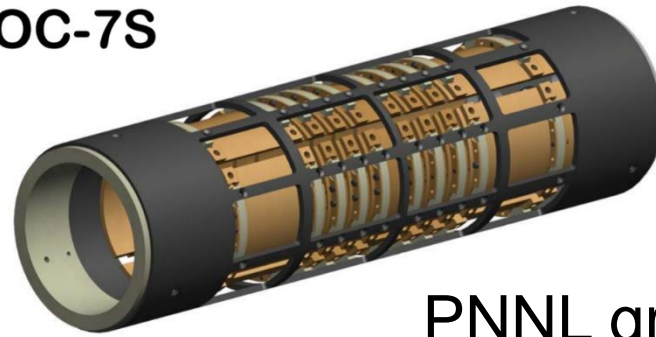


IonSpec Varian



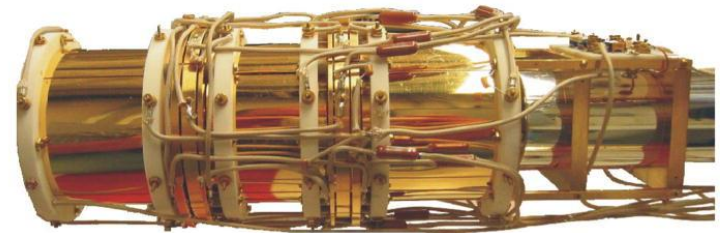
Compensated cells

OC-7S

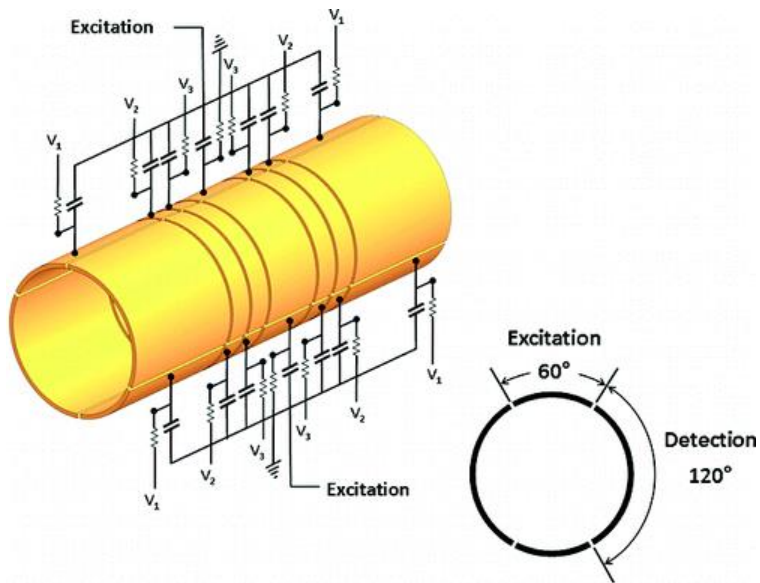
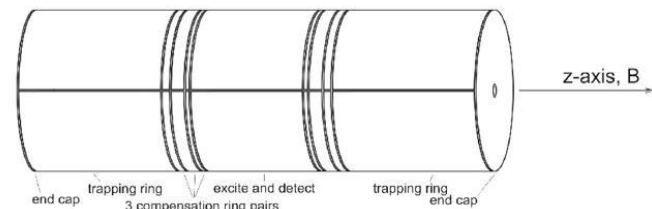


PNNL group

(a)



(b)



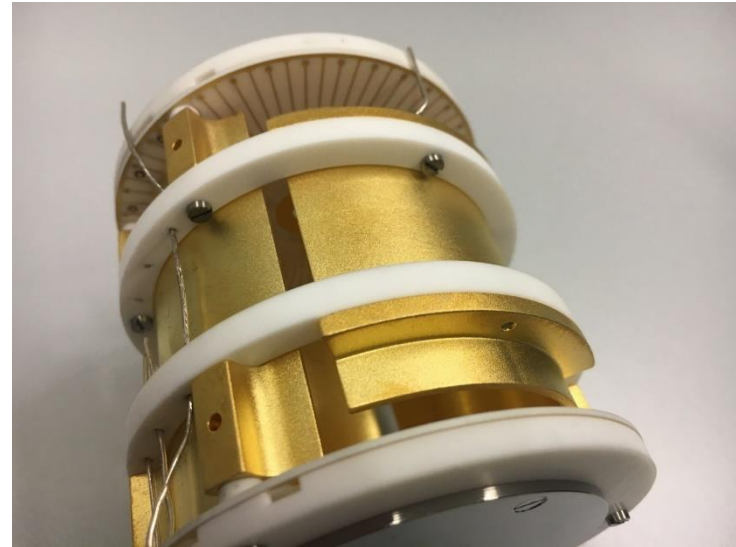
Marshall group

Gross group

Cells with trapping by pseudopotential

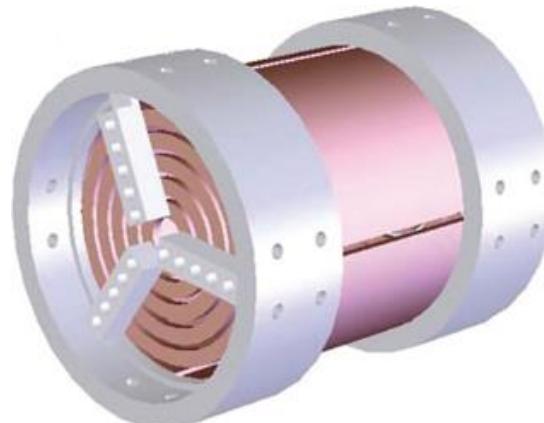


Nikolaev



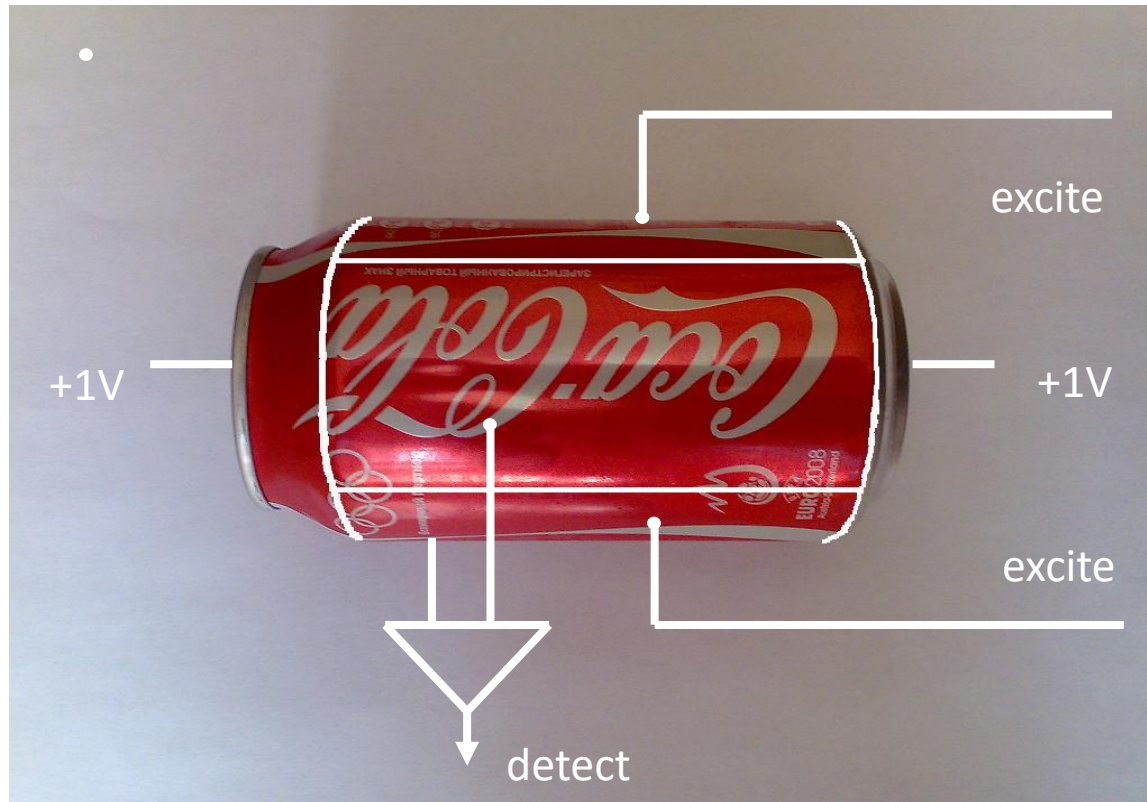
Bruker-Nikolaev

Cell with segmented trapping electrodes



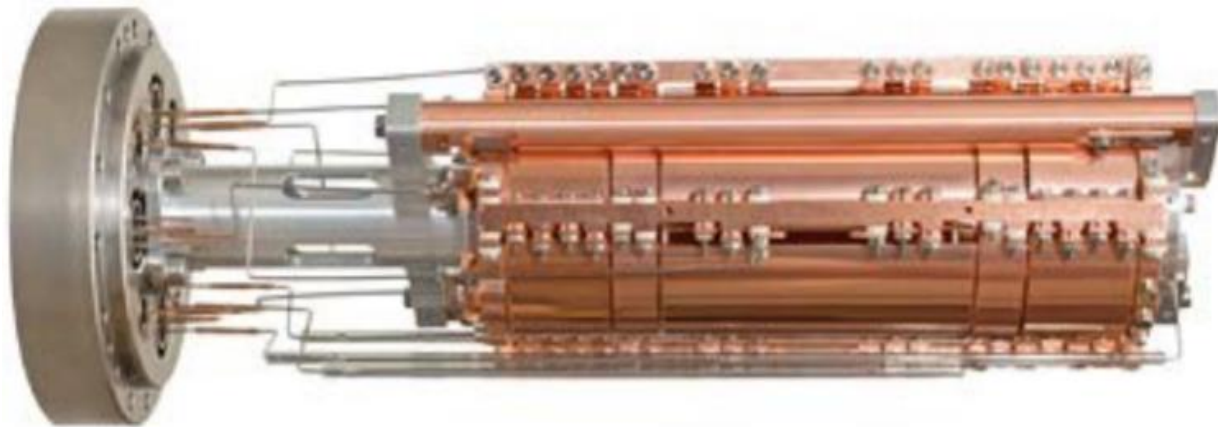
Bruce

Fancy cells

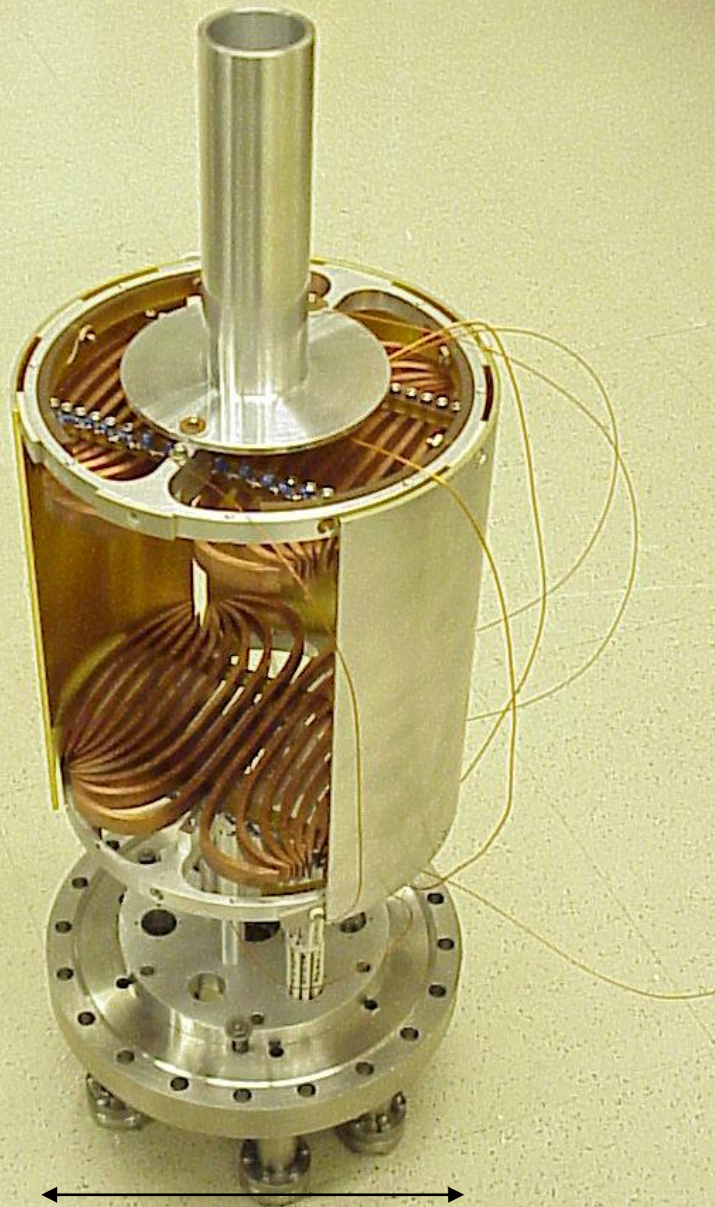


Coca-Cola cell

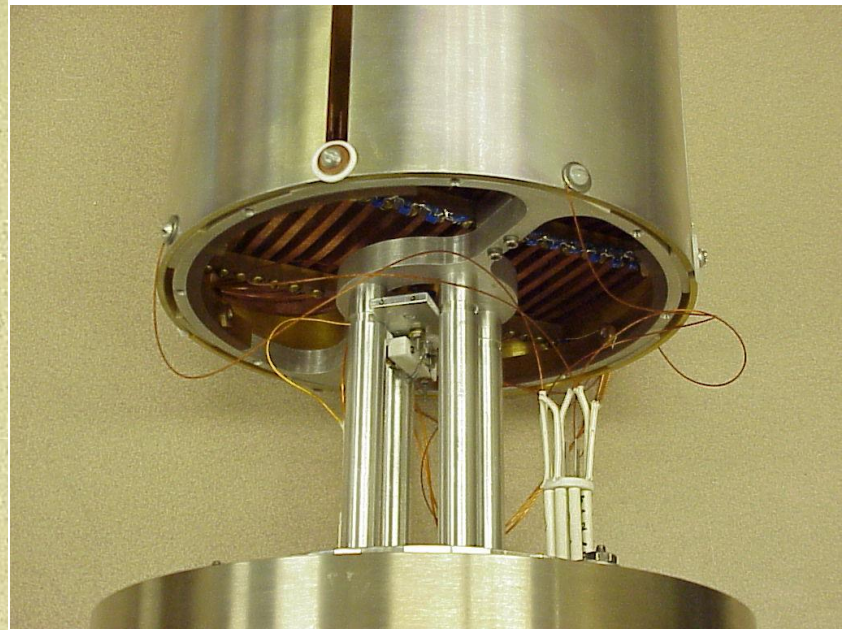
Spectroswiss NADEL cell



BIG
7 inches FT ICR cell



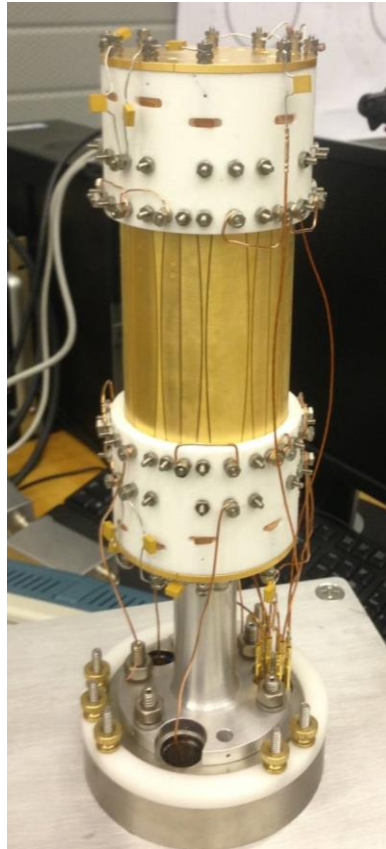
7 inches



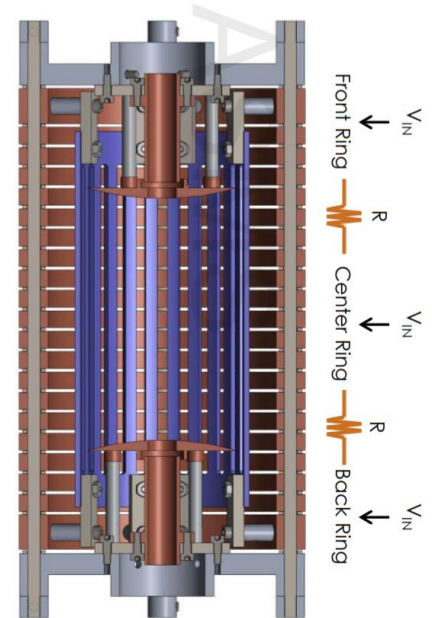
Dynamically harmonized cells



Bruker Solarix
R&D



NHMFL cell From
Alan Marshall 21 T
talk



PNNL window
cell

Dynamically harmonized
FT ICR cell for
Thermo LTQ FT

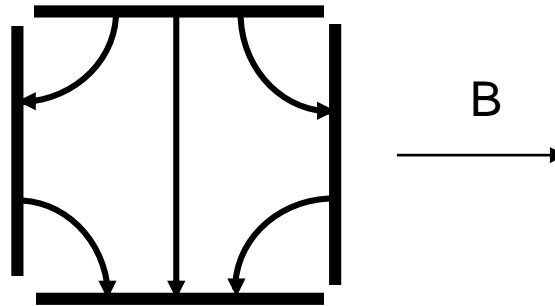


Why so many designs?

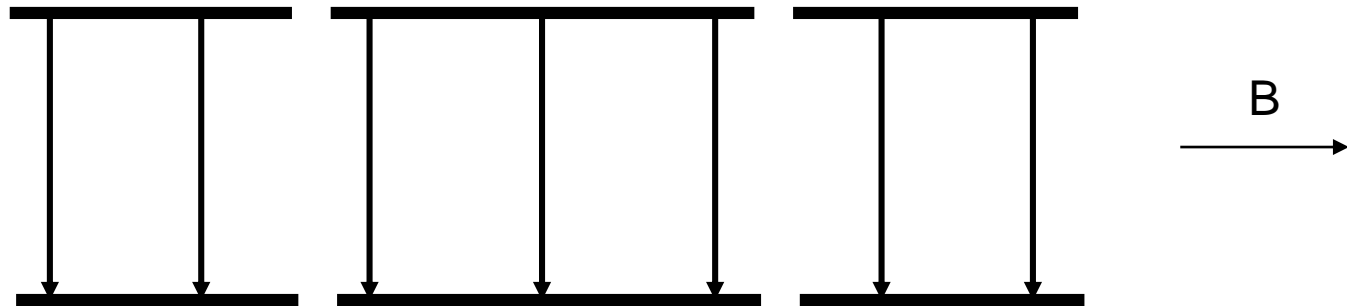
What is the problem?

The first problem was homogeneity of excitation Field distribution

Cubic and cylindrical

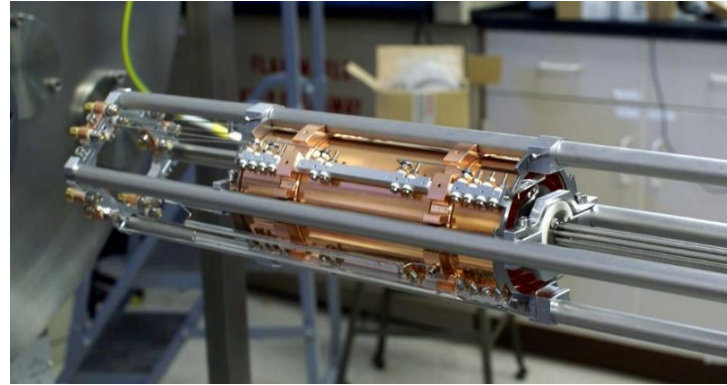


Elongated open cell

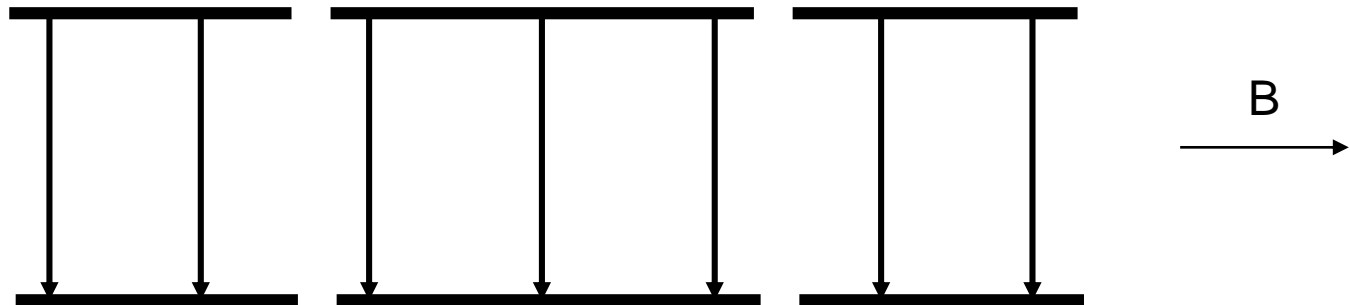
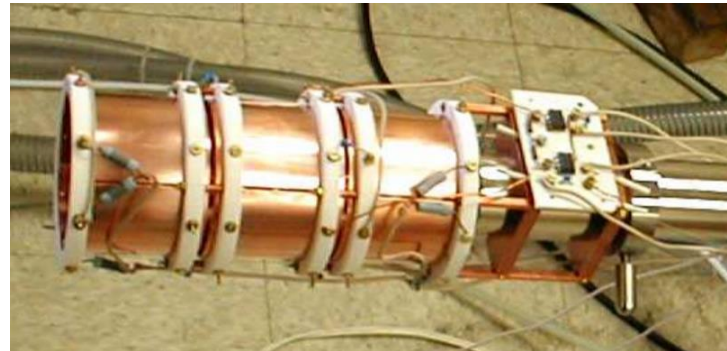


Elongated open cells

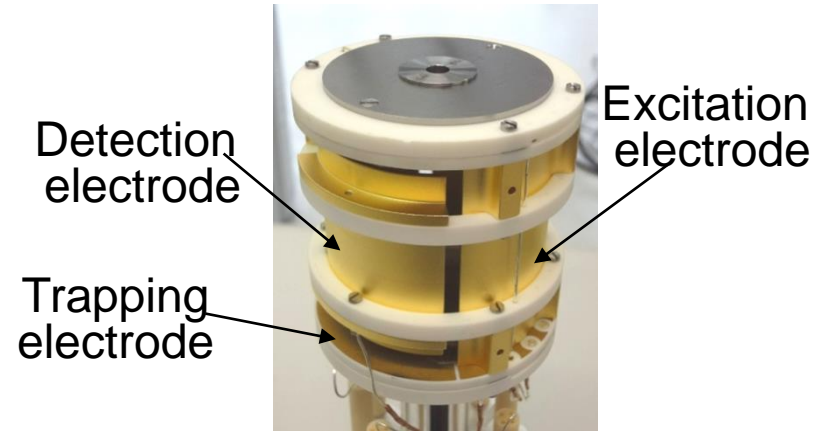
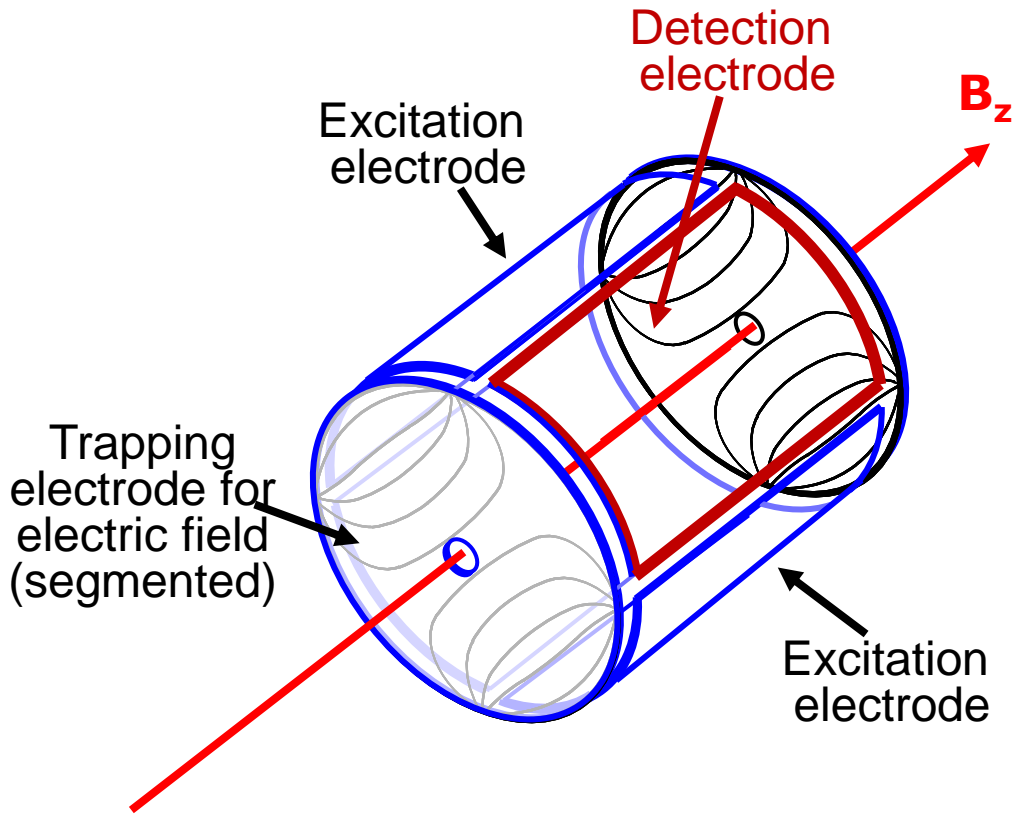
Thermo
LTQ FT
(until 2006)



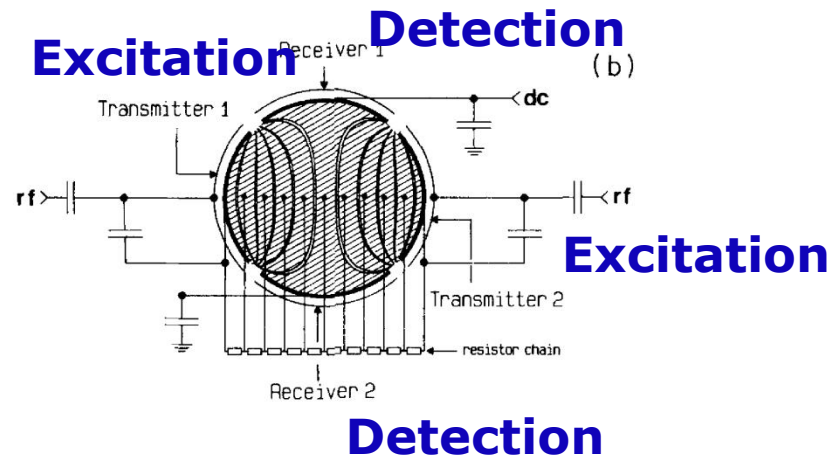
IonSpec Varian



Infinity cell

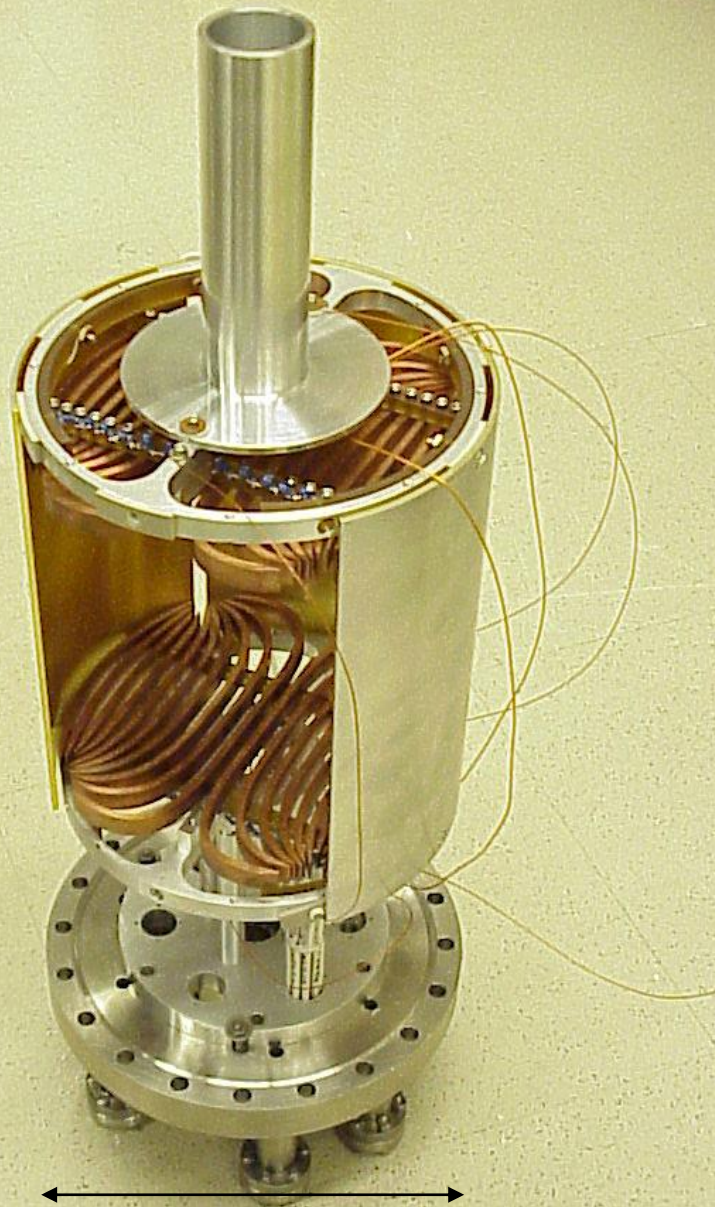


diameter: 60 mm
length: 60 mm

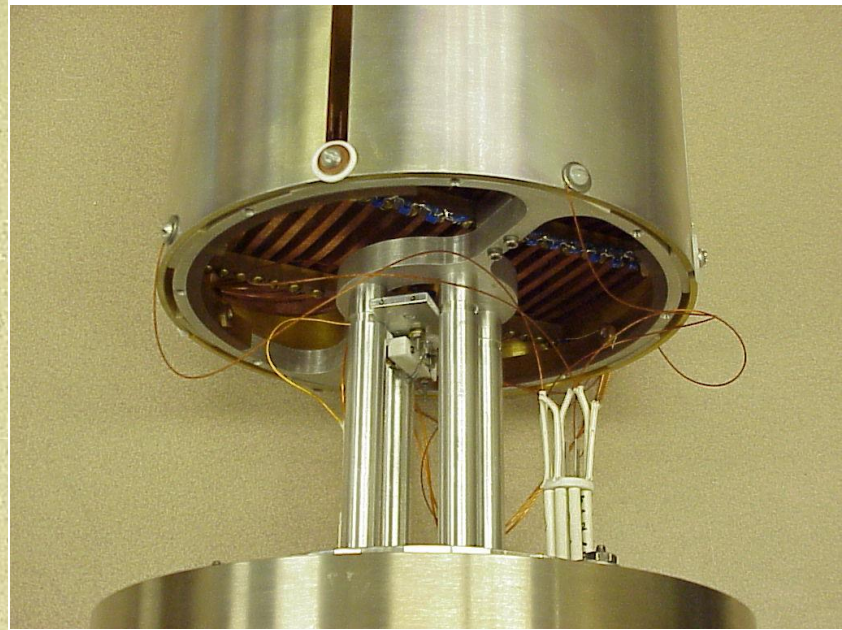


→ Infinity trapping segments realize a dipolar excitation field, as if the ICR cell would be “infinitely” long.

BIG
7 inches FT ICR cell



7 inches

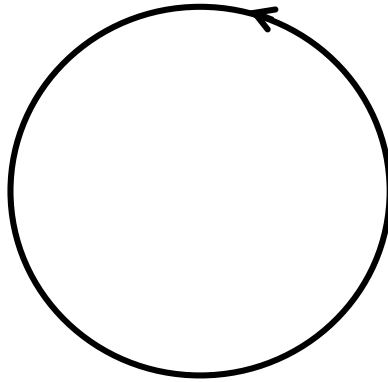


The second problem was:

Why we could not reach resolving power of more than 1 million at m/z close to 1000 Da?

Is it the vacuum problem?

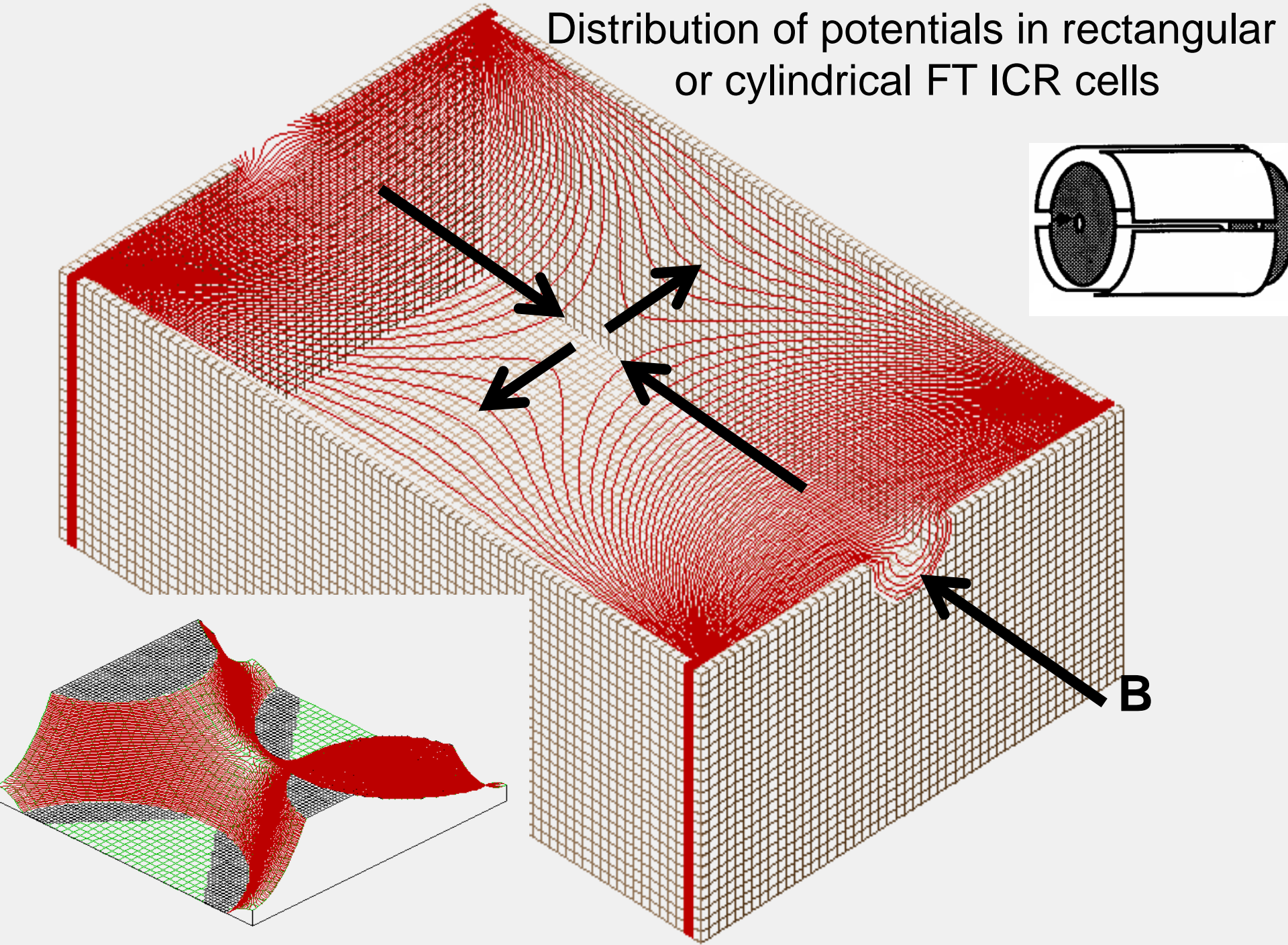
Ion motion in electric field free space



Cyclotron
rotation

$$\omega_c = \frac{|eB|}{mc}$$

Distribution of potentials in rectangular or cylindrical FT ICR cells



Motion of ions in crossed E/B fields

Cell potential plot in the xy plane of a cubic FT ICR cell.
3 V potential is applied to the trapping electrodes

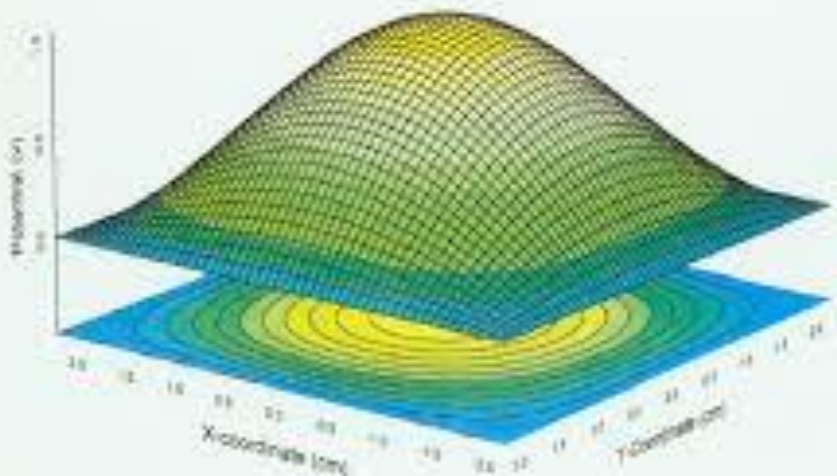
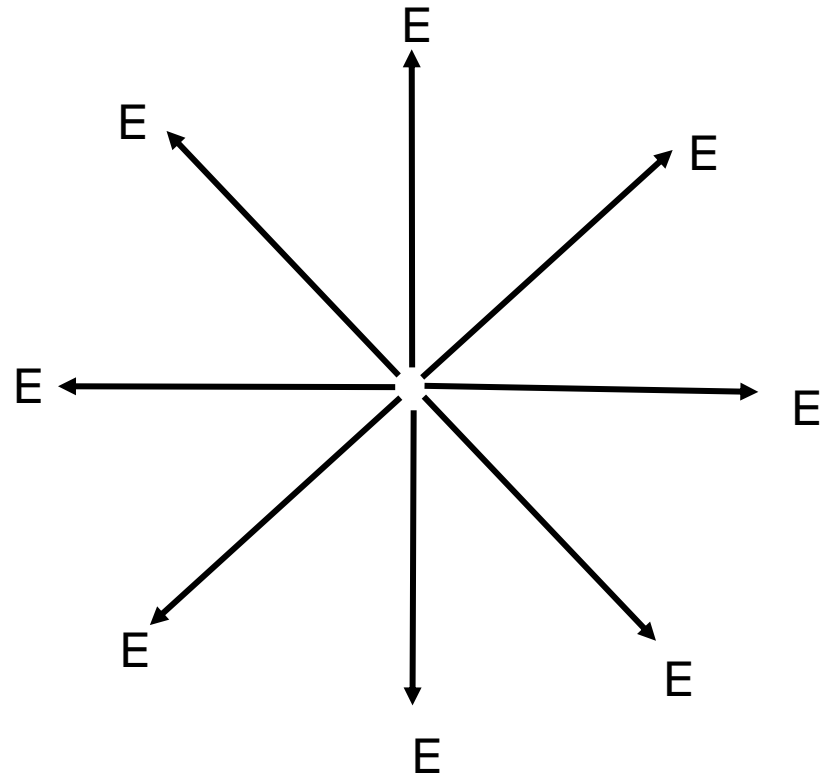
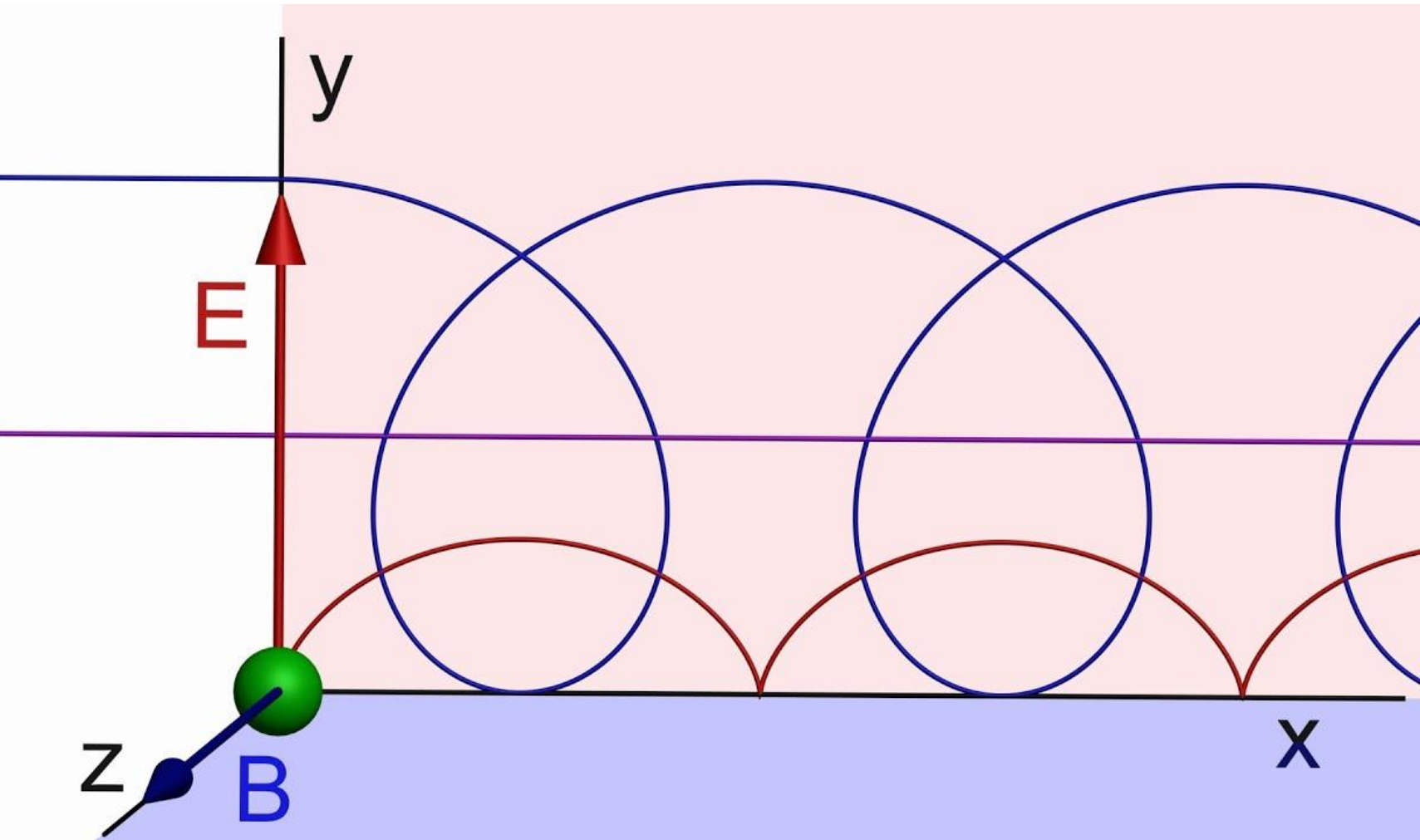


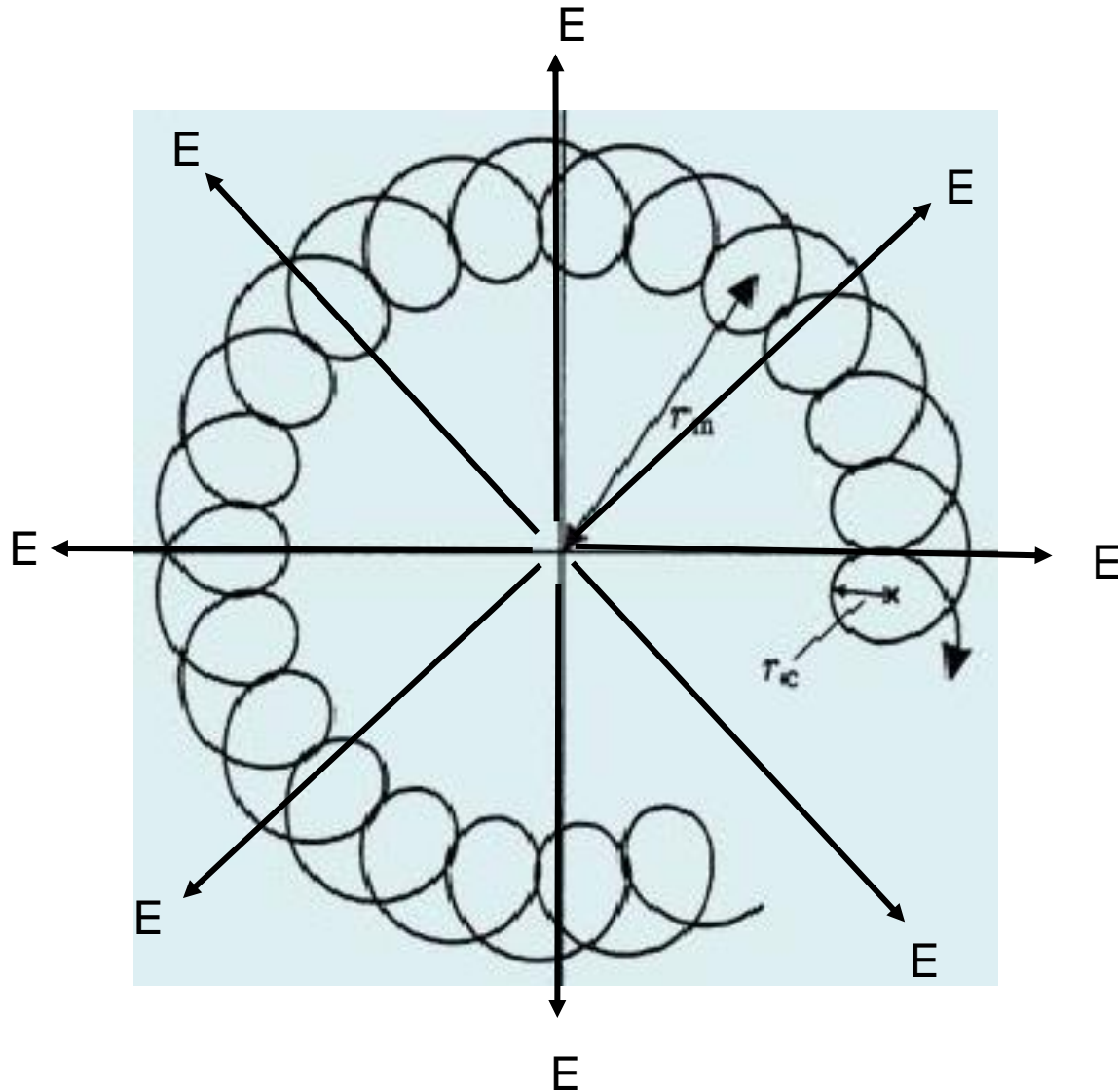
Figure 4. Plot of the electric potential due to the trapping voltage in a cubic cell in the plane that is perpendicular to the magnetic field, and that passes through the center of the cell. The potential has its maximum in the center of the cell, producing an inward-directed force on ions.



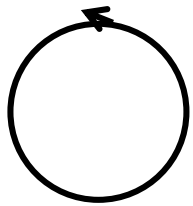
Motion of ions in crossed E/B fields



Magnetron motion. No excitation of cyclotron motion



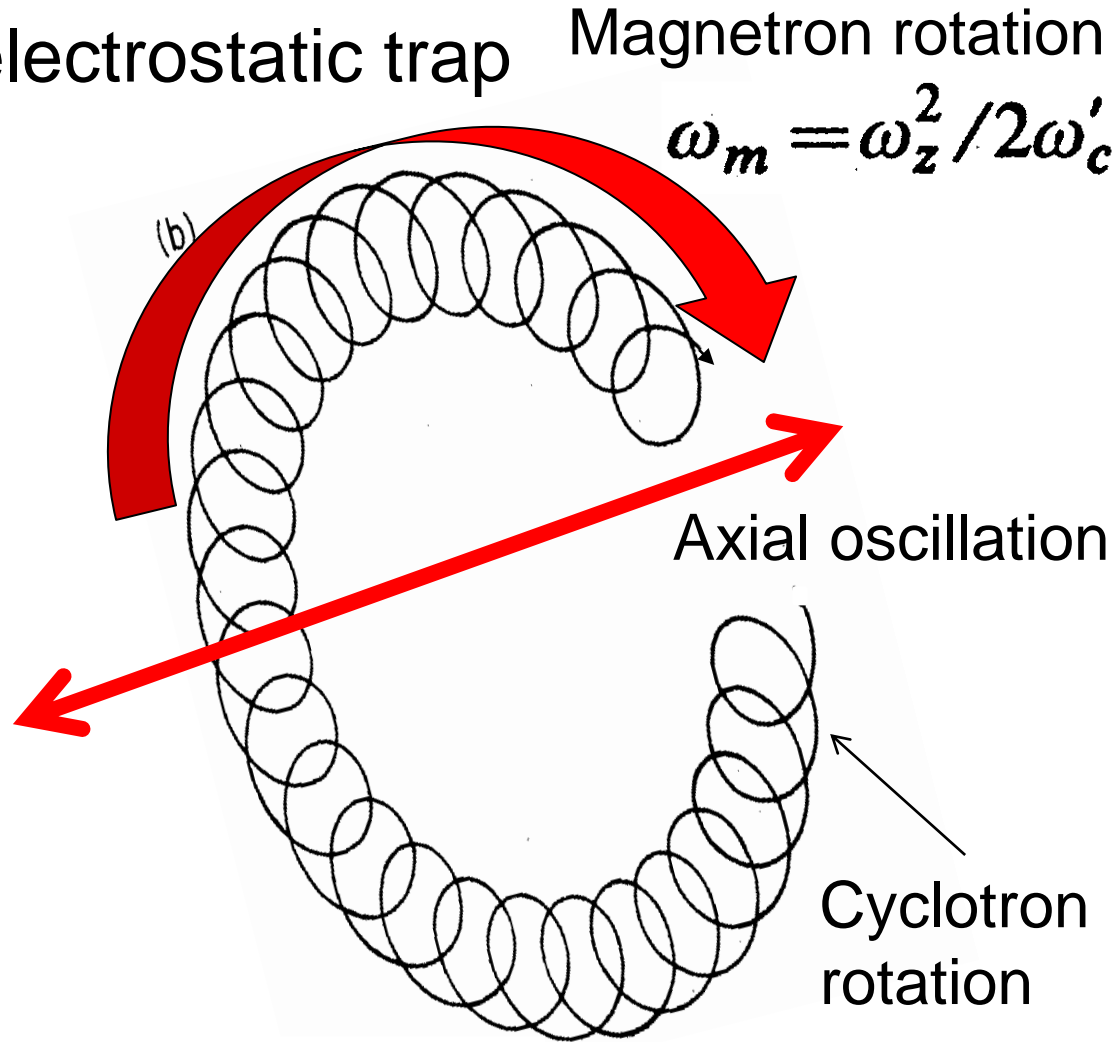
Ion motion in electric field free space



Cyclotron rotation

$$\omega_c = \frac{|eB|}{mc}$$

Ion motion in an electrostatic trap



Magnetron rotation

$$\omega_m = \omega_z^2 / 2\omega'_c$$

Axial oscillation

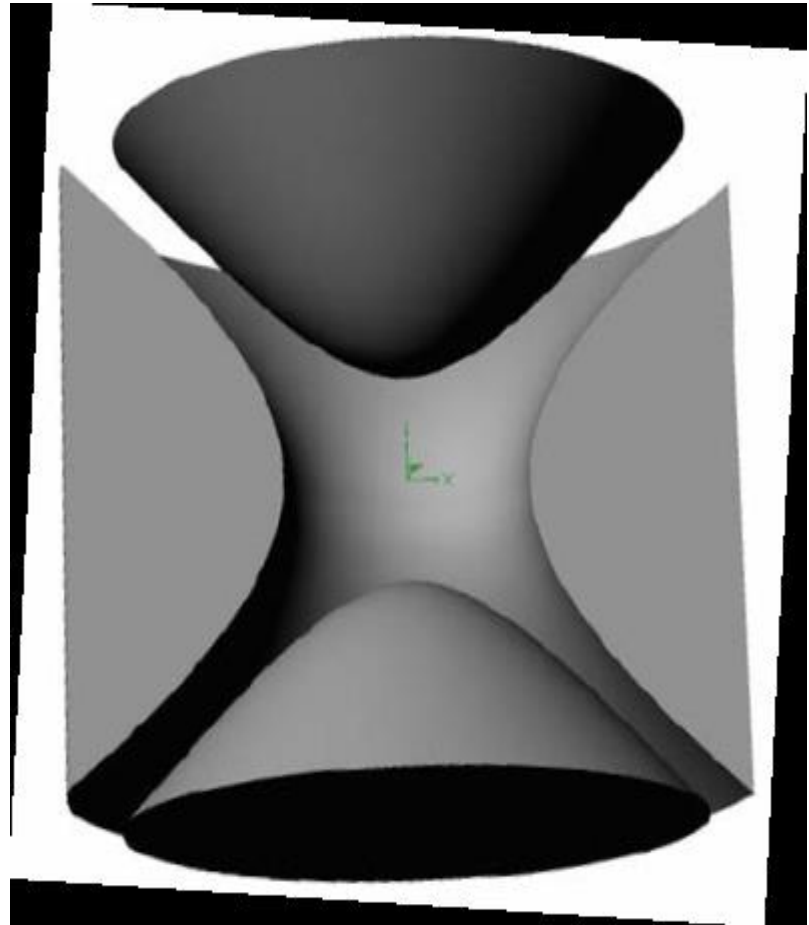
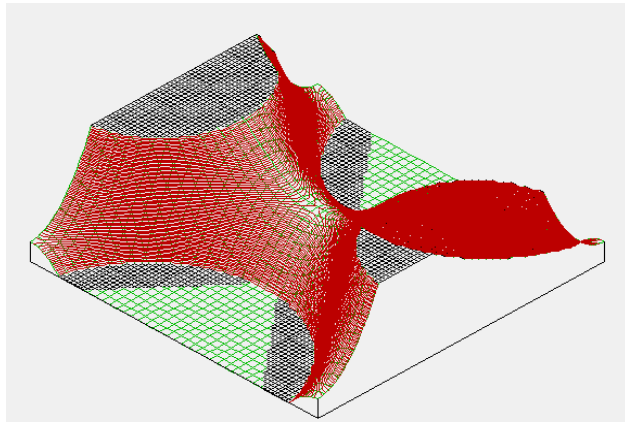
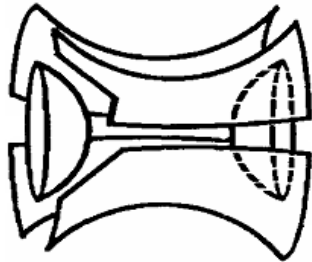
Cyclotron rotation

$$\omega'_c = \omega_c - \omega_m$$

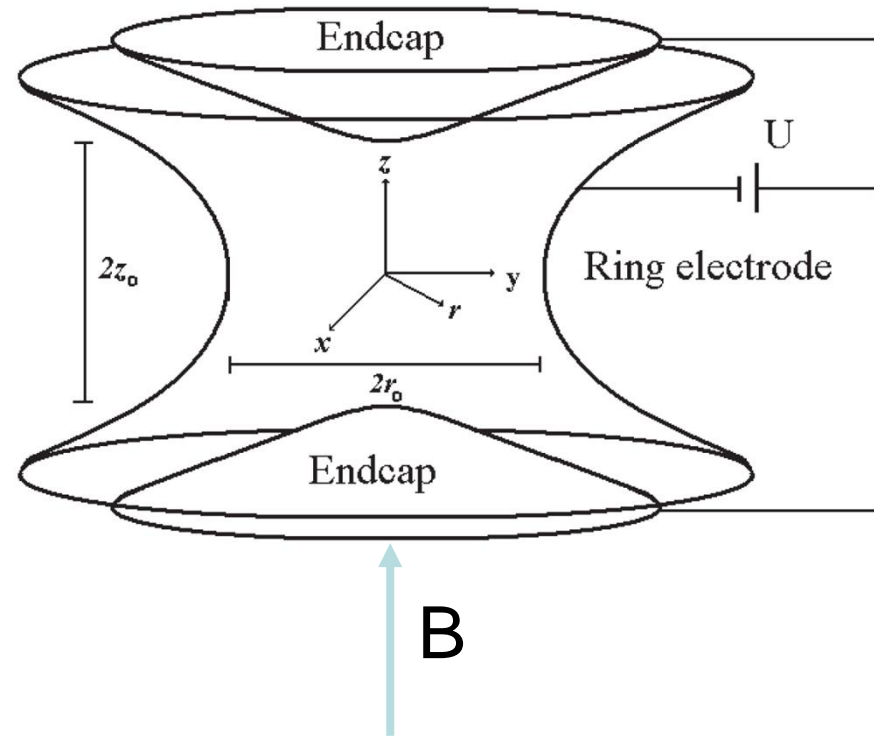
Measured frequency

$$\omega_c = \frac{|eB|}{mc}$$

Hyperbolic cell

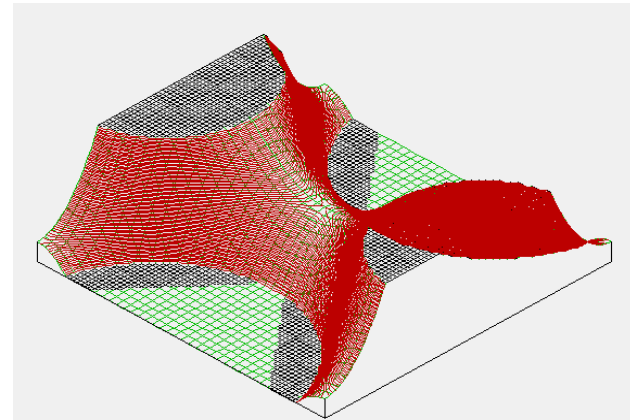


Hyperbolic Penning trap



$$\phi(r, z) = \frac{U_0}{R_0^2} (r^2 - 2z^2)$$

$$R_0^2 = r_0^2 + 2z_0^2$$



$$\vec{F} = q(\vec{E} + \vec{v} \times \vec{B})$$

Linear dependence of electric field on coordinates in hyperbolic ion trap

Electric field distribution

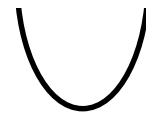
$$E_x = -\frac{\partial\phi(x, y, z)}{\partial x} = -\frac{2U_0}{R_0^2}x$$



$$E_y = -\frac{\partial\phi(x, y, z)}{\partial y} = -\frac{2U_0}{R_0^2}y$$



$$E_z = -\frac{\partial\phi(x, y, z)}{\partial z} = \frac{4U_0}{R_0^2}z$$



Potential distribution

$$\frac{\partial^2 x}{\partial t^2} = \frac{qB}{m} \frac{\partial y}{\partial t} - \frac{2qU_0}{mR_0^2} x$$

$$\frac{\partial^2 y}{\partial t^2} = -\frac{qB}{m} \frac{\partial x}{\partial t} - \frac{2qU_0}{mR_0^2} y$$

$$\frac{\partial^2 z}{\partial t^2} = \frac{4qU_0}{mR_0^2} z$$

$$\ddot{x} = \omega_c \dot{y} + \frac{\omega_z^2 x}{2}$$

$$u = x + iy$$

$$\ddot{y} = -\omega_c \dot{x} + \frac{\omega_z^2 y}{2}$$

$$\ddot{u} = -i\omega_c \dot{u} + \frac{1}{2}\omega_z^2 u$$

$$\ddot{z} = -\omega_z^2 z$$

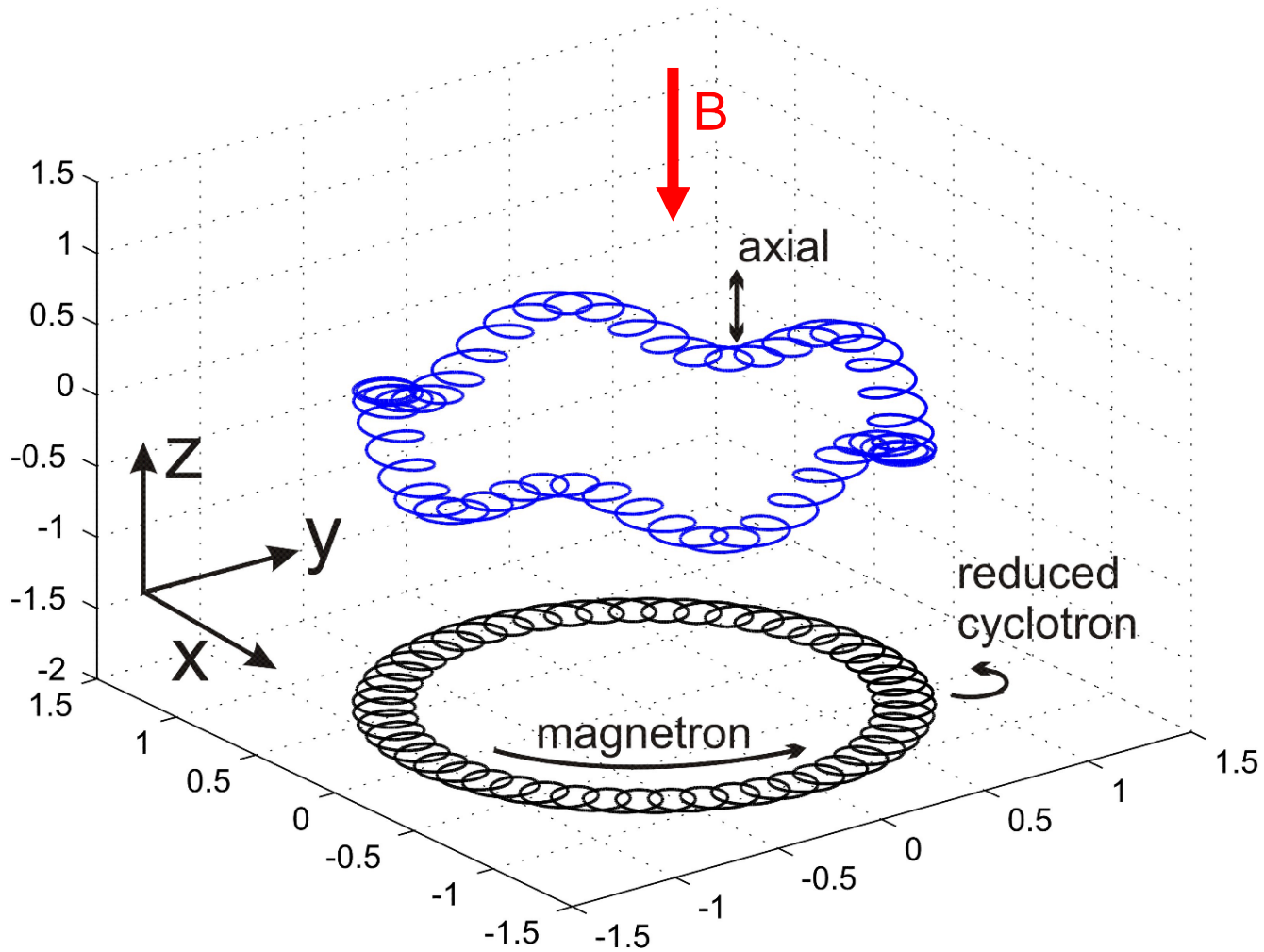
$$u = e^{-i\omega t}$$

$$\omega'_c = \frac{\omega_c + \sqrt{\omega_c^2 - 2\omega_z^2}}{2}$$

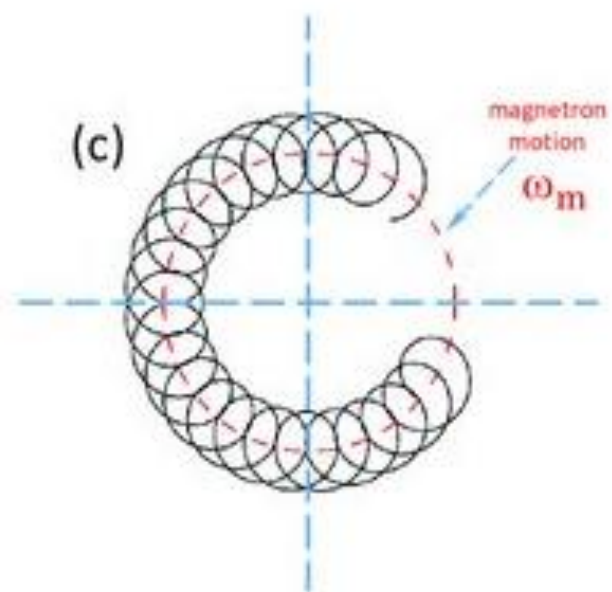
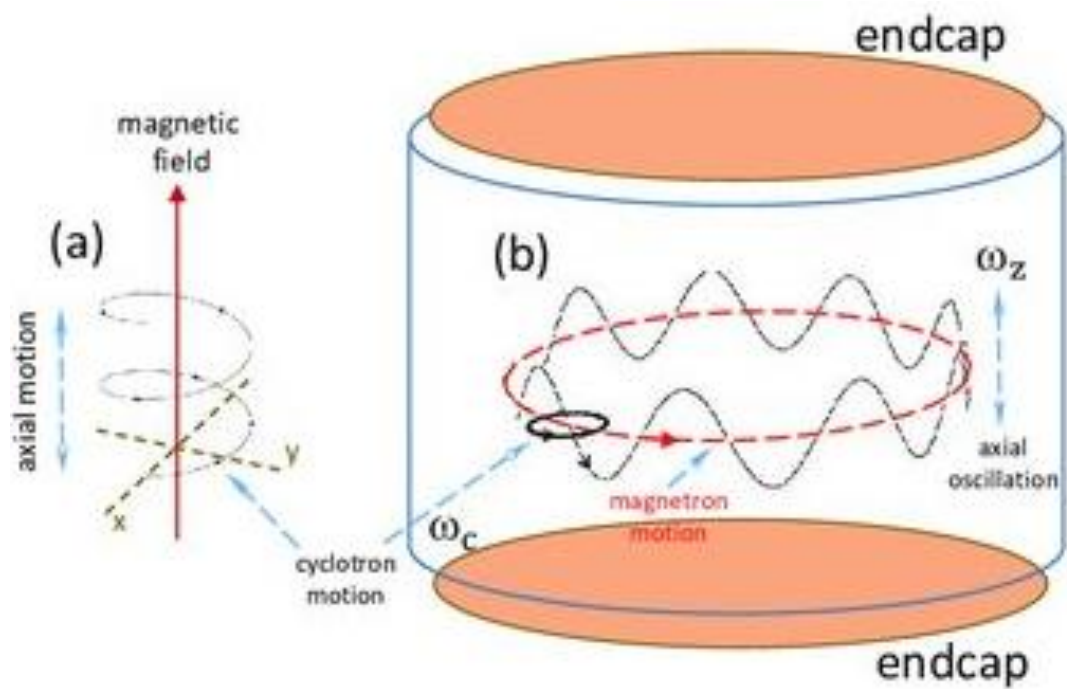
$$\omega_m = \frac{\omega_c - \sqrt{\omega_c^2 - 2\omega_z^2}}{2}$$

$$\omega_c^2 > 2\omega_z^2$$

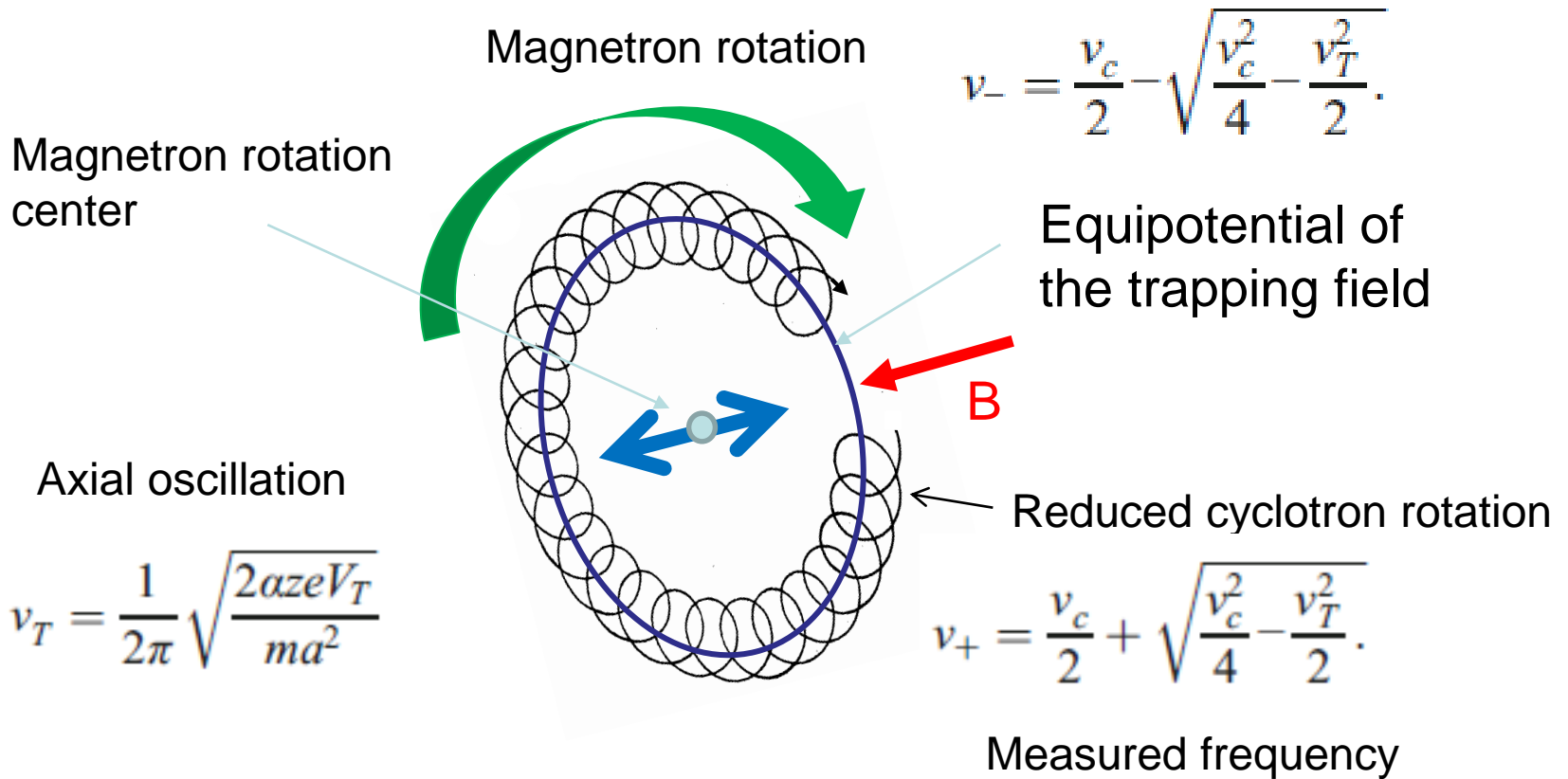
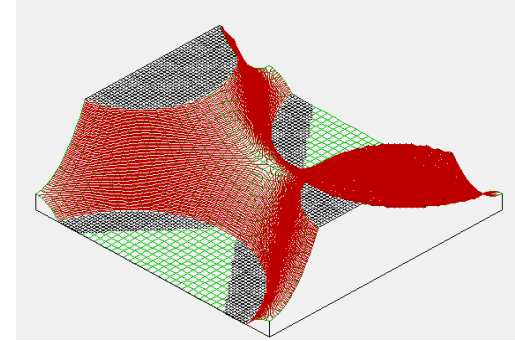
$$\omega'_c \approx \omega_c \gg \omega_z \gg \omega_m$$



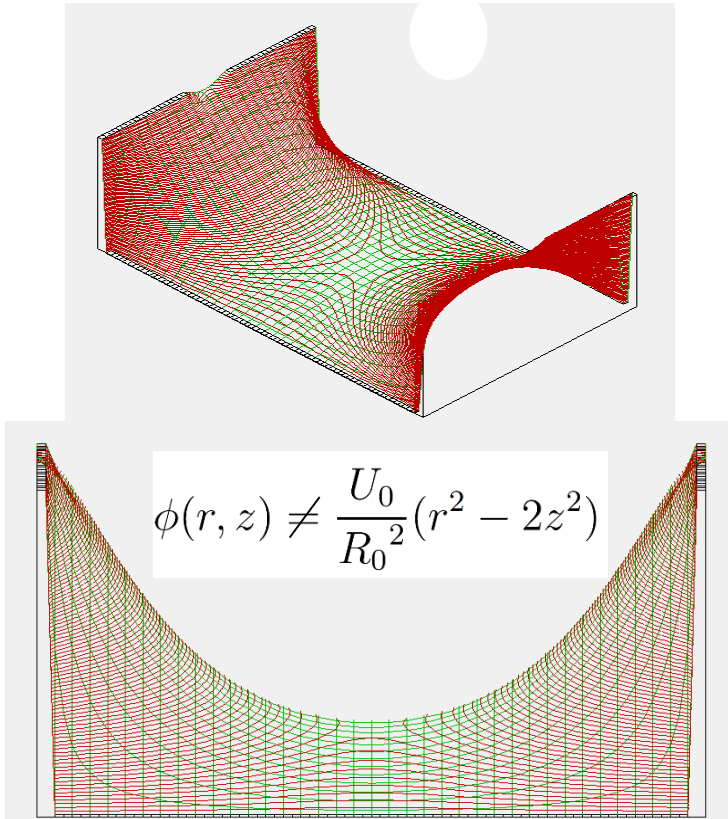
<https://www.diva-portal.org/smash/get/diva2:413035/FULLTEXT01.pdf>



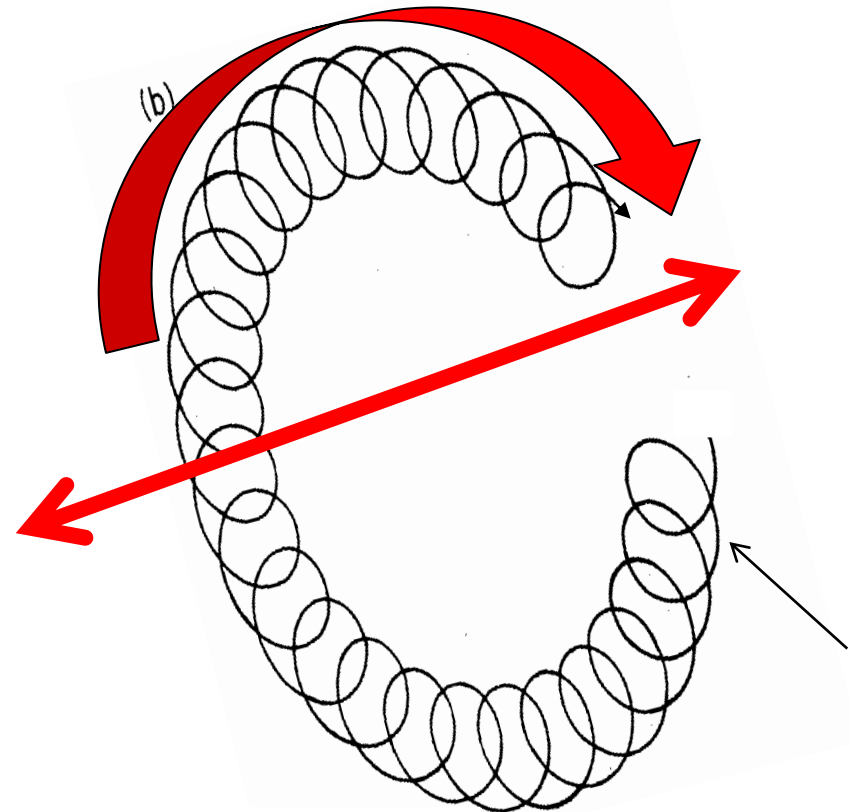
In ideal hyperbolic trap all modes of ion motion are independent



Distribution of potentials in rectangular or cylindrical FT ICR cells



Axial and magnetron frequencies depend on axial oscillation amplitude

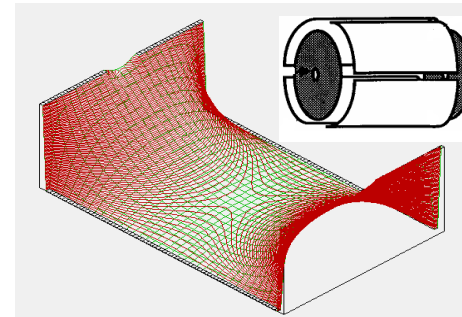
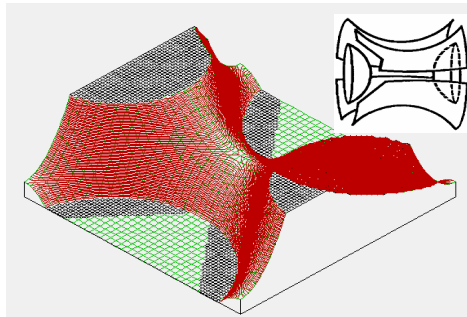


$$\omega'_c = \omega_c - \omega_m(z)$$

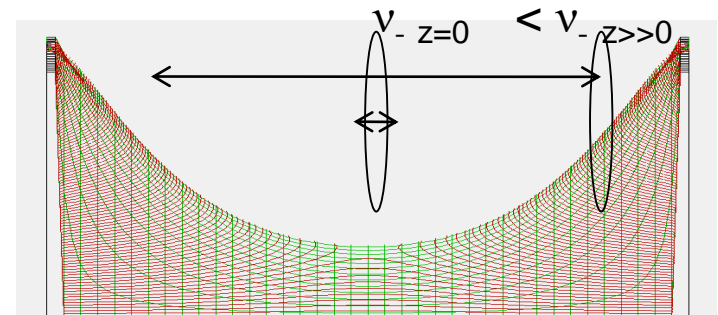
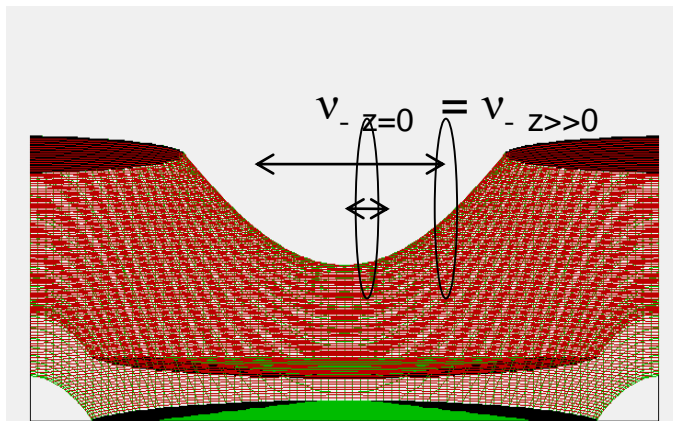
Measured frequency

$$\omega_c = \frac{|eB|}{mc}$$

The lost of phase coherence is a result of Inharmonicity of a regular FT ICR cell field



Distribution of potentials in hyperbolic (left) and rectangular or cylindrical FT ICR cells (right)

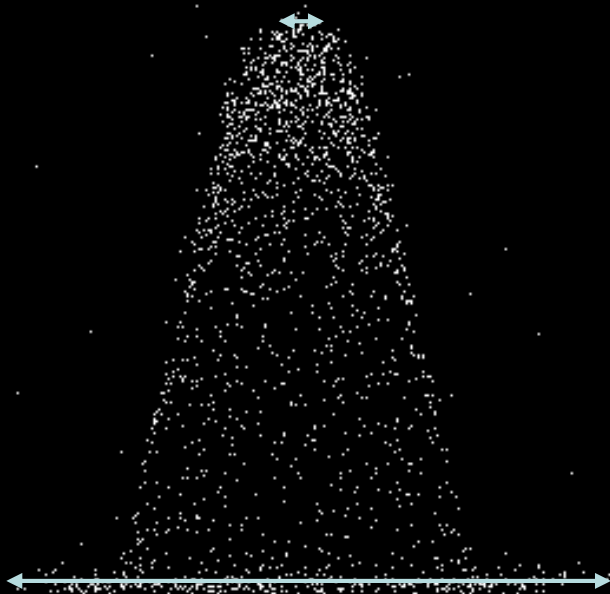


Cyclotron and magnetron frequencies are Independent on axial oscillation amplitude

Cyclotron and magnetron frequencies depend on axial oscillation amplitude

Comets in conventional FT ICR cell

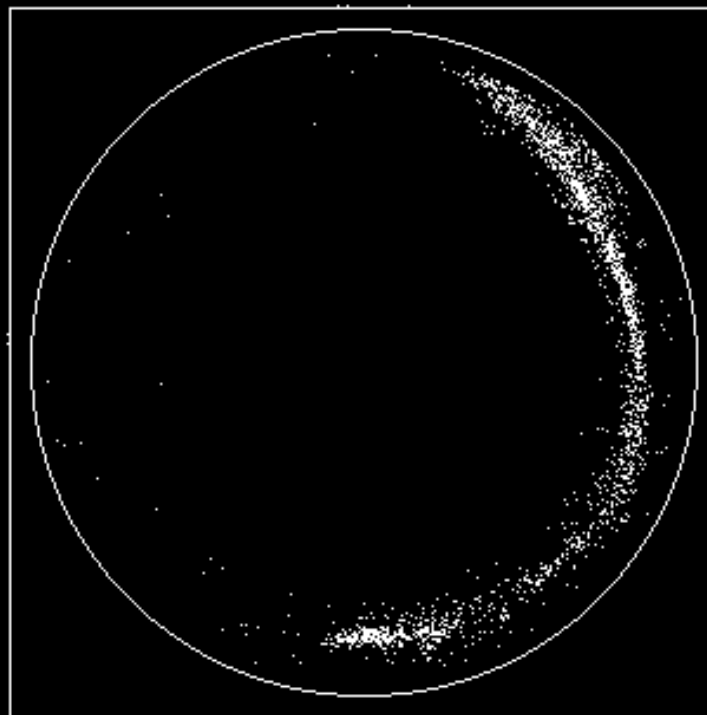
Small axial oscillation amplitude ions



Large axial oscillation amplitude ions

Xming X

New

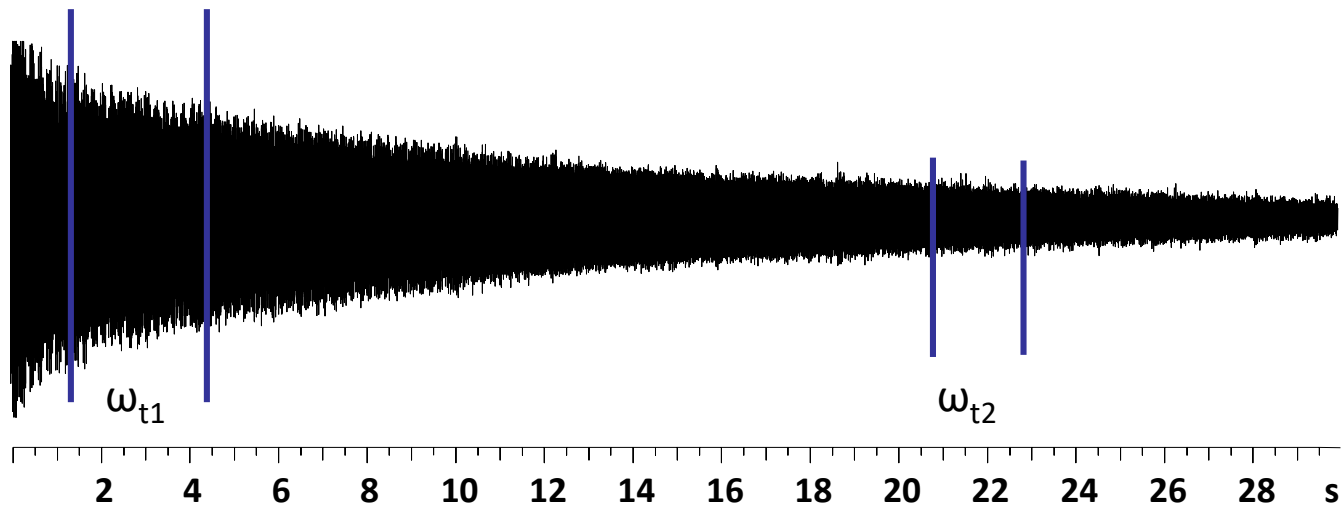


Comet in conventional
(cubic, cylindrical, “infinity” ..)
FT ICR cells



$$\omega_{t1} \neq \omega_{t2}$$

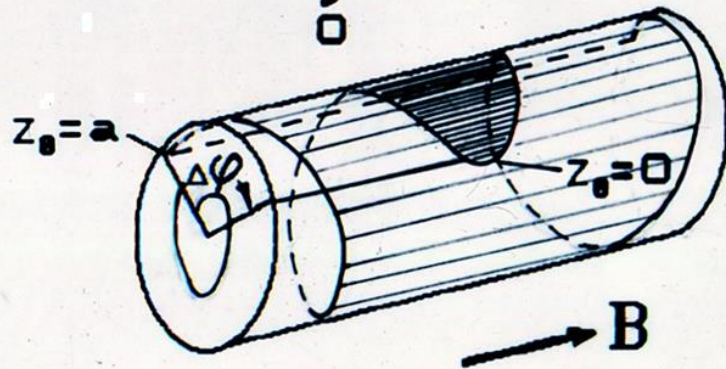
Because ion-ion interaction inside
comets is changing in time



How do we know about comets?

Phase shift accumulation

$$(1) \varphi(t, z_0) = \int_0^t \omega_{\text{eff}}(\tau, z_0) d\tau$$



$$(2) G(\Omega) = \text{Fur} \{ \langle \cos(\varphi(t)) \rangle \}$$

Nikolaev EN. 9th
Asilomar Conference on
Mass Spectrometry,
Trapped Ions: Principle,
Instrumentation and
Applications, Sep 27–
Oct 1, 1992

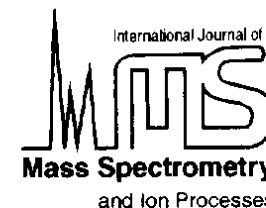
Two different approaches to simulation of ion cloud dynamics in FT ICR cell

1. Calculation of ion-ion and ion image charges interaction directly
2. Solving Poisson equation



ELSEVIER

International Journal of Mass Spectrometry and Ion Processes 148 (1995) 145–157



Evolution of an ion cloud in a Fourier transform ion cyclotron resonance mass spectrometer during signal detection: its influence on spectral line shape and position

Eugene N. Nikolaev^a, Nickolay V. Miluchihin^{b,1}, Masao Inoue^{b,*}

^a*Institute for Energy Problems of Chemical Physics, Russian Academy of Sciences, Moscow 117829, Russian Federation*

^b*Department of Applied Physics and Chemistry, University of Electro-Communications, Chofu-shi, Tokyo 182, Japan*

Received 19 August 1994; accepted 31 May 1995

Simulation was carried out on a Fujitsu AP1000 parallel computer, which is a “multiple instruction multiple data” (MIMD) machine with 512 independent 25 MHz processors. **(One processor per ion)**

We were trying to explain:

Why ICR frequency is changing during detection?

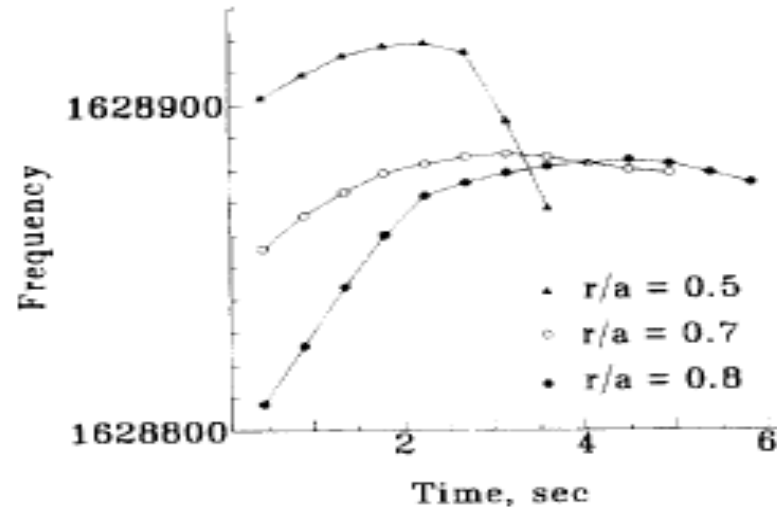
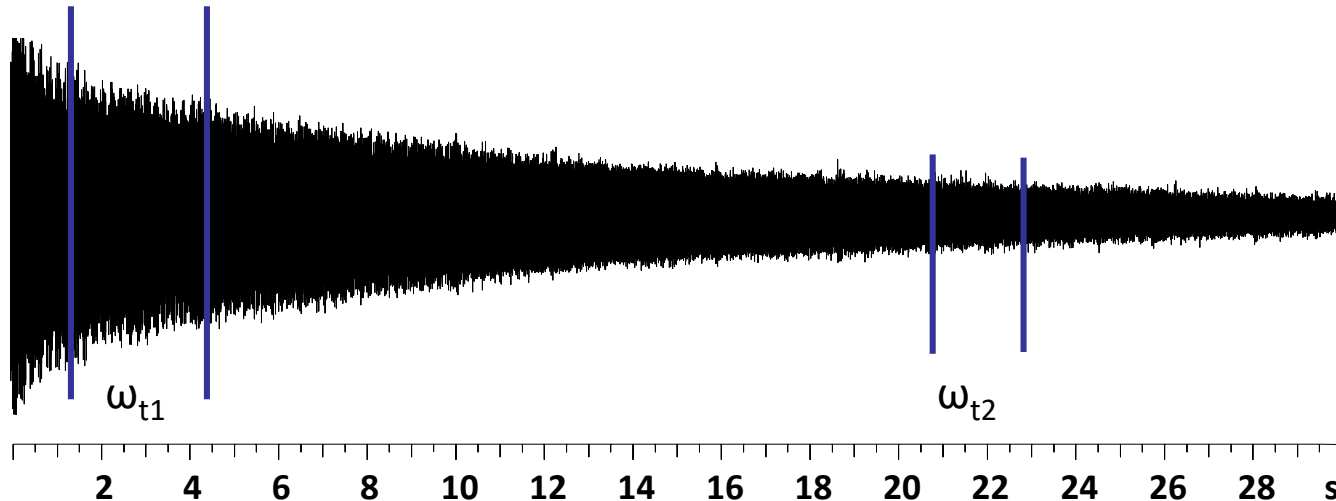


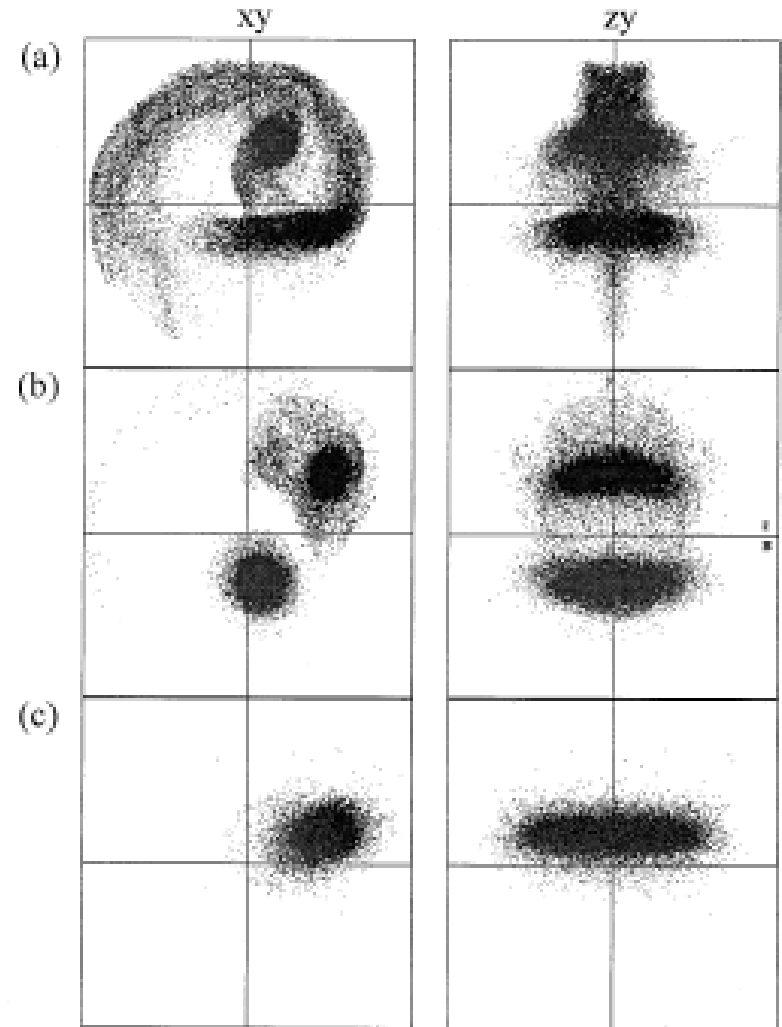
Fig. 1. Experimental ICR frequency of externally produced Cs^- ions as a function of time. The three curves correspond to different ratios of cyclotron radius to cell radius.



The Particle-Mesh Method

Dale Mitchell and Richard Smith

1996



Snapshots in xy perspective (left) and zy perspective (right) at a late time during the detection period. **(a)** 50,000, **(b)** 150,000, and **(c)** 350,000 ions.

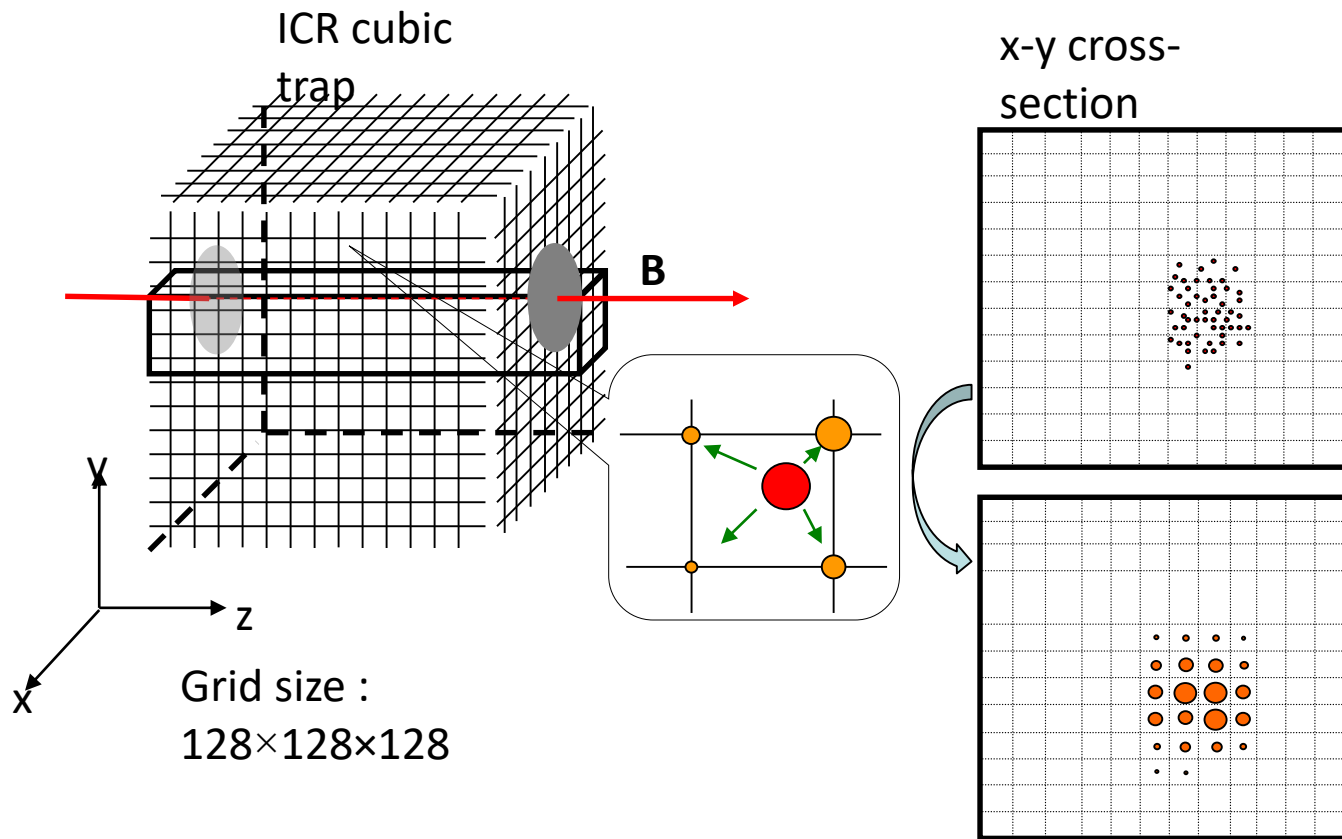
Solving Poisson equation using supercomputer

Eugene N. Nikolaev; Ron M.A. Heeren; Alexander M. Popov;
Alexander V Pozdneev;
Konstantin S Chingin;

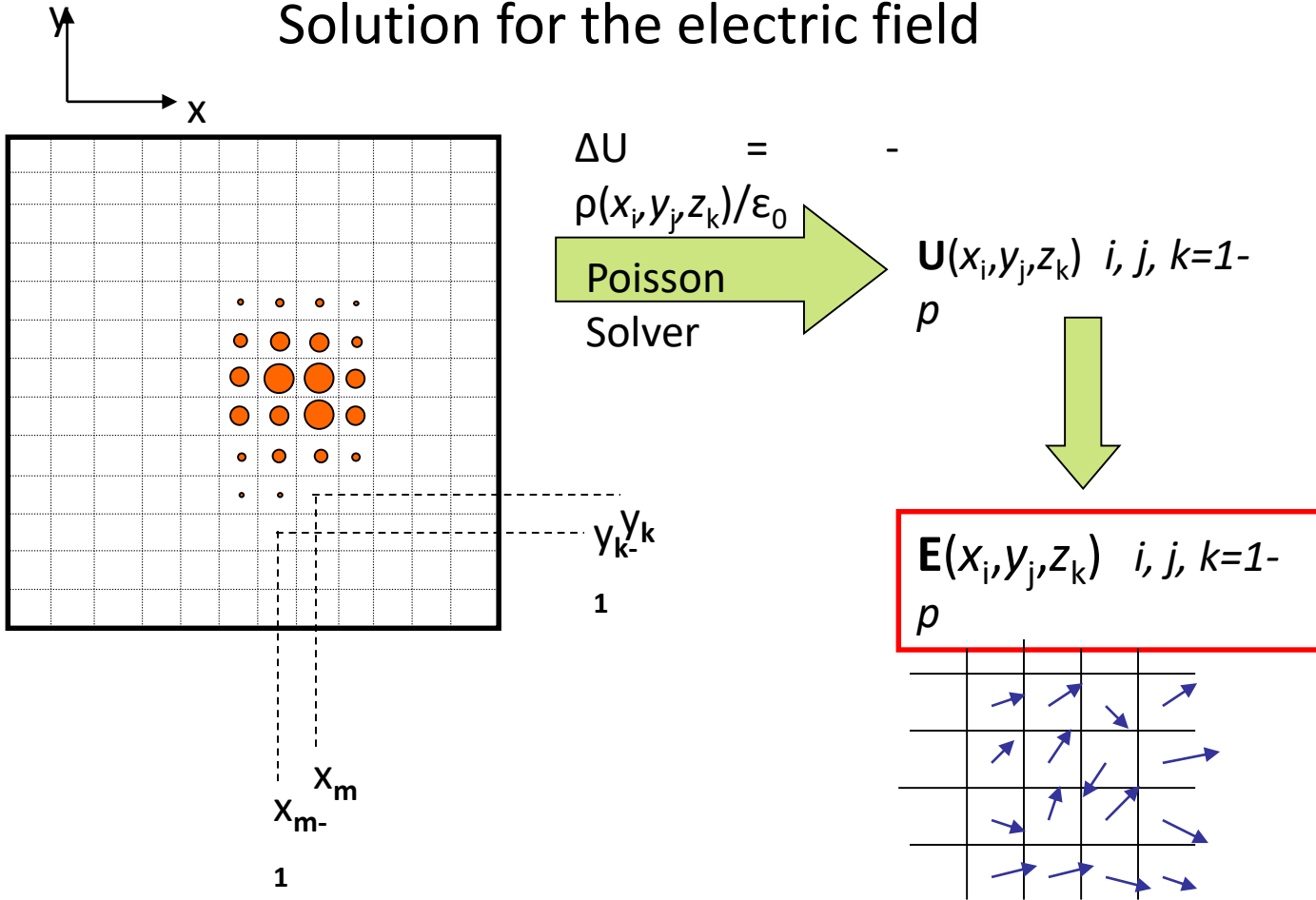
***Realistic modeling of ion cloud motion in Fourier transform
ion cyclotron resonance cell by use of a particle-in-cell
approach***

Rapid Commun. Mass Spectrom. 2007; 21,1-20

Particle-In-Cell Algorithm (first used to describe ion behavior in FT ICR cell by Dale Mitchell and Richard Smith)

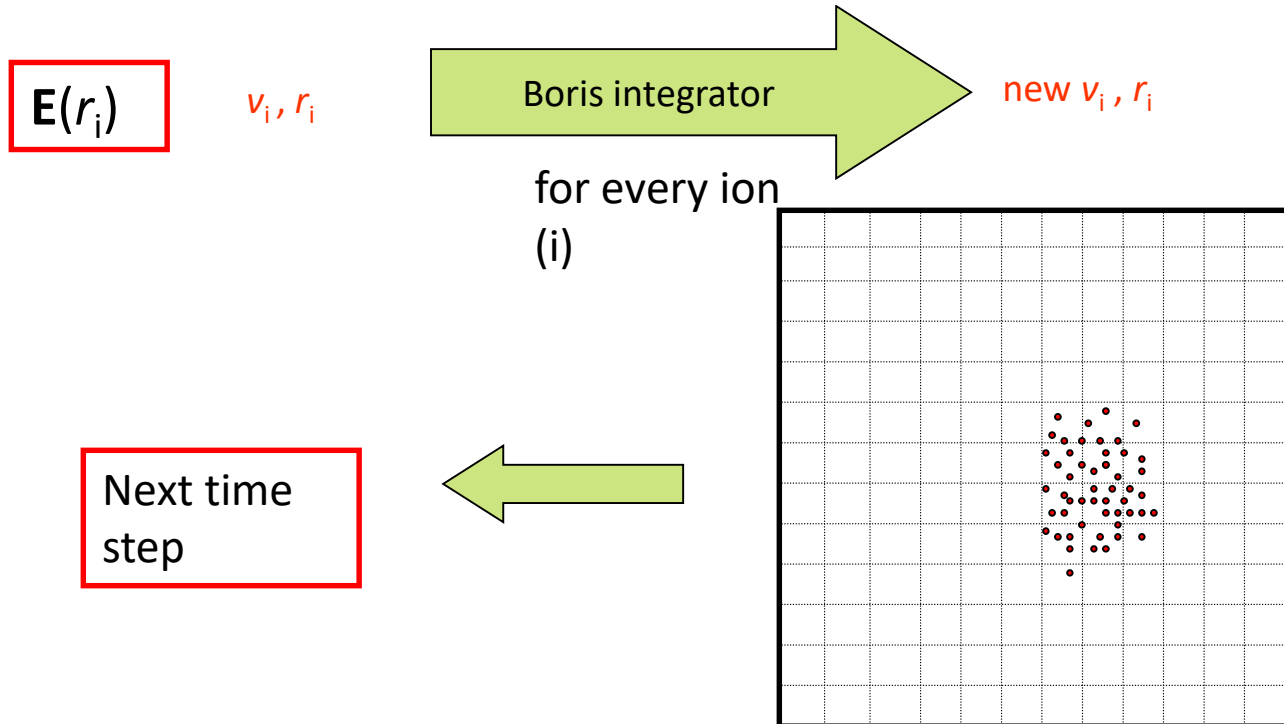


Solution for the electric field



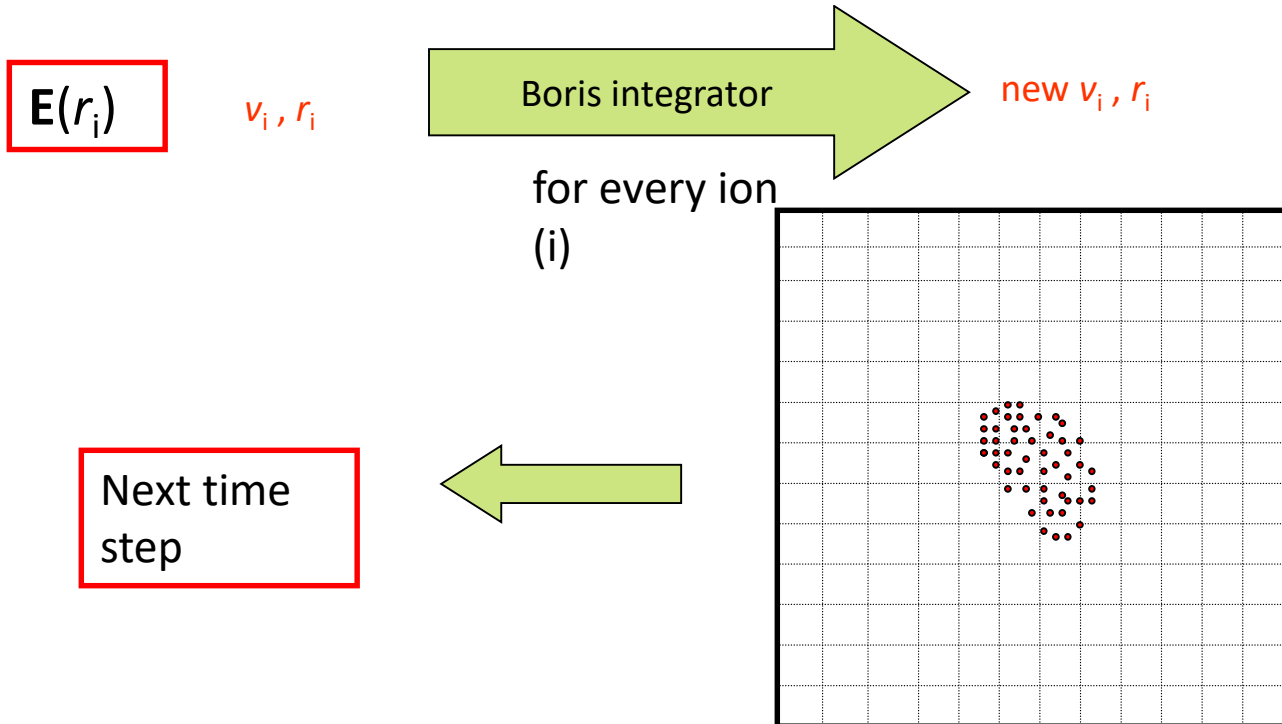
Integration the equation of motion

$$m \frac{d^2 \vec{r}}{dt^2} = q \vec{E} + q \left(\frac{d\vec{r}}{dt} \times \vec{B} \right)$$

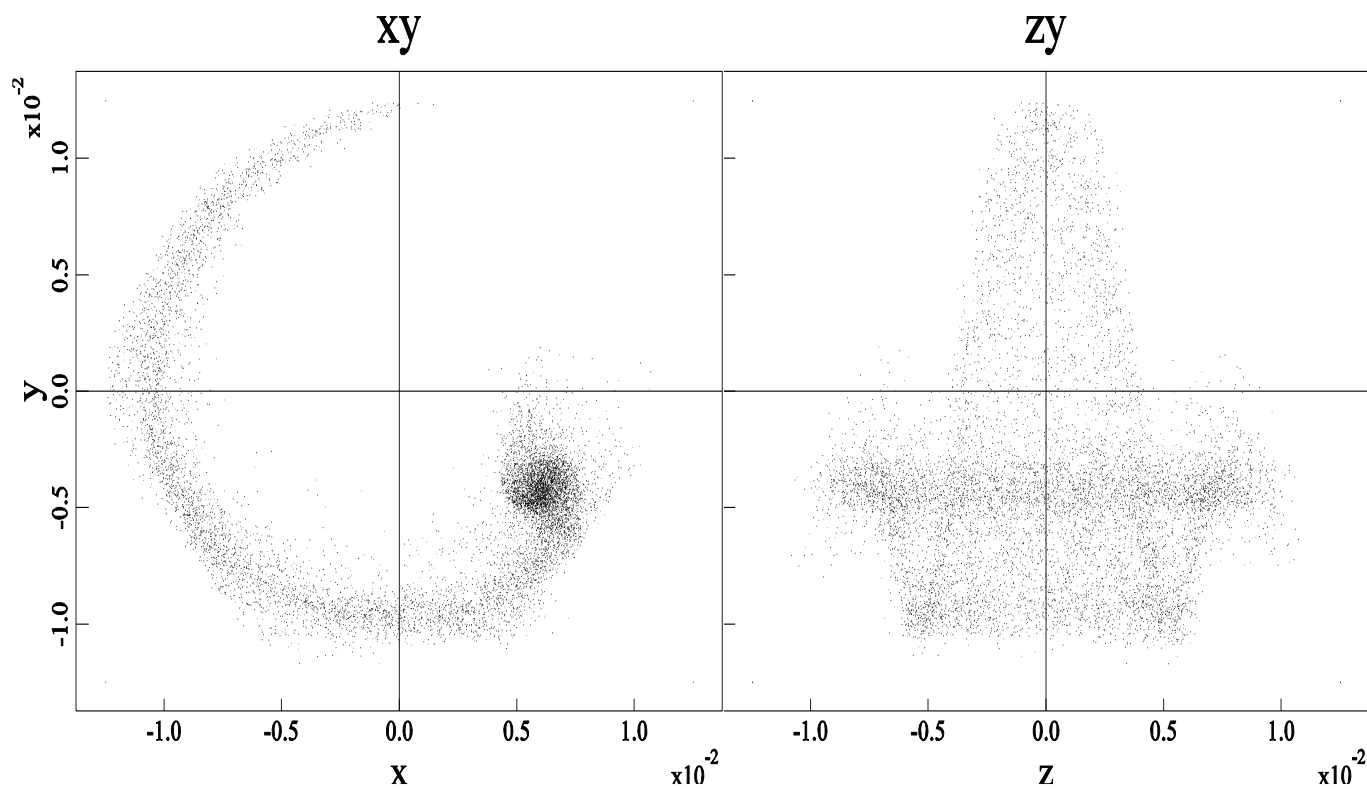


Integration the equation of motion

$$m \frac{d^2 \vec{r}}{dt^2} = q \vec{E} + q \left(\frac{d\vec{r}}{dt} \times \vec{B} \right)$$

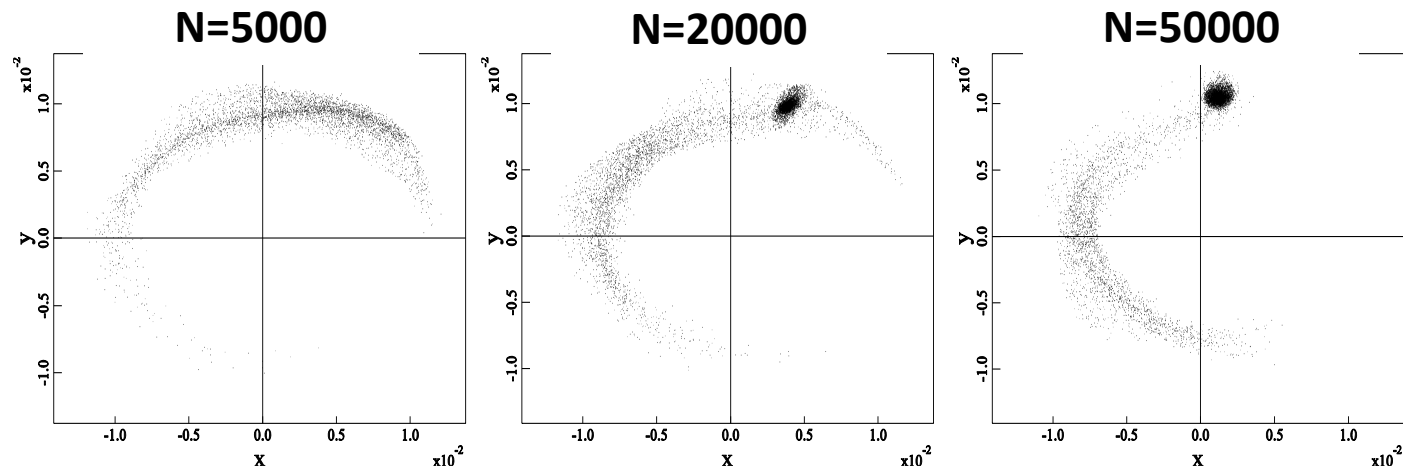


Cloud of one m/z ions in a cylindrical geometry FT ICR cell



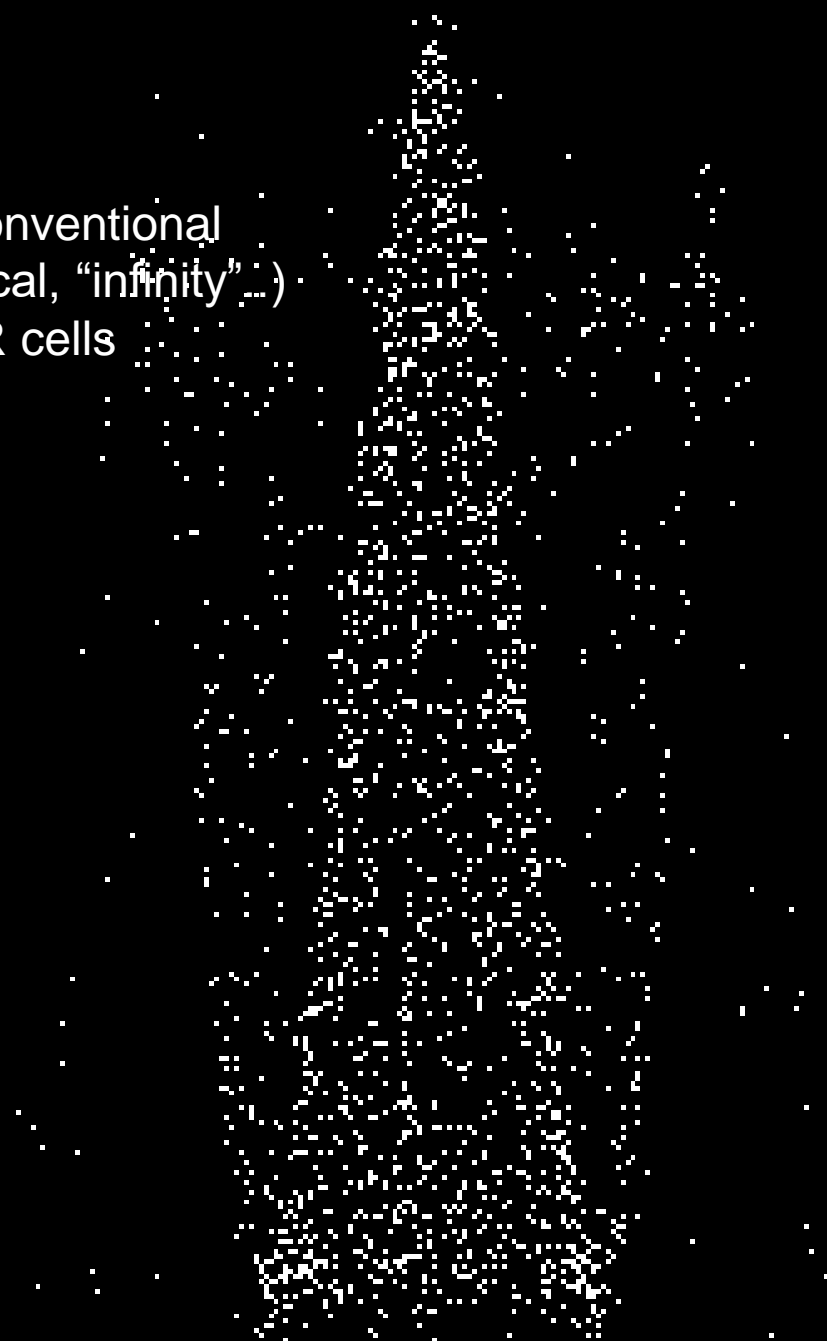
Evolution of ion clouds with different amount of ions in the cell

cloud initial radius 0.15 cm
cloud initial length 0.10 cm
 $T_{\text{exc}} = 0.07 \text{ ms}$, $T_{\text{detect}} = 30 \text{ ms}$
ms

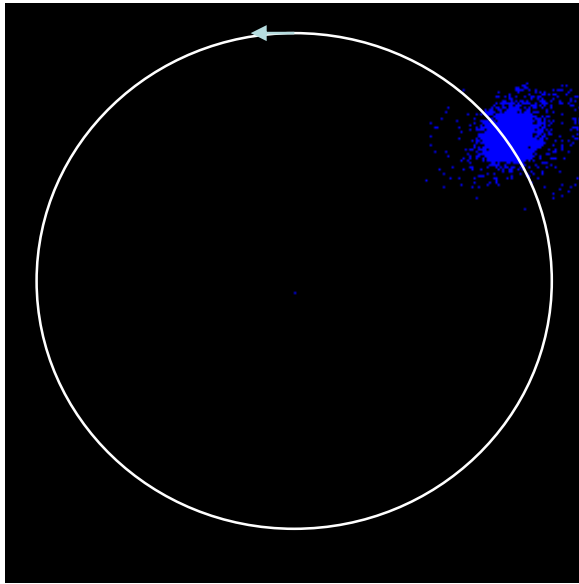


$t = 3.24 \text{ ms}$

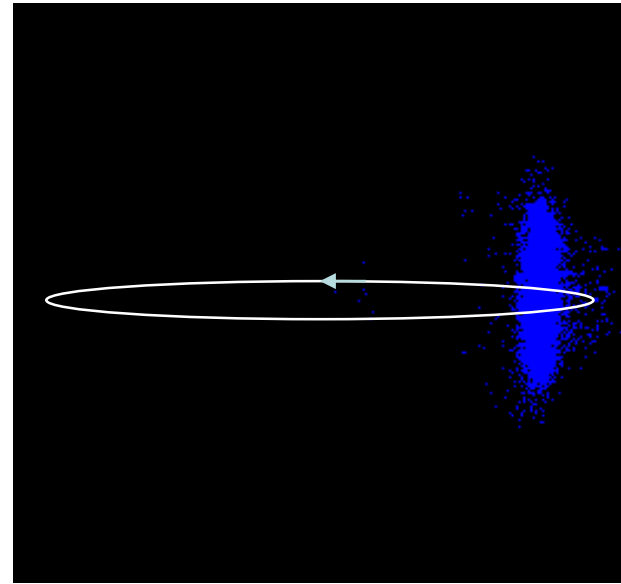
Comet in conventional
(cubic, cylindrical, "infinity" ...)
FT ICR cells



Ion clouds in harmonized cells have elliptical cigar like forms



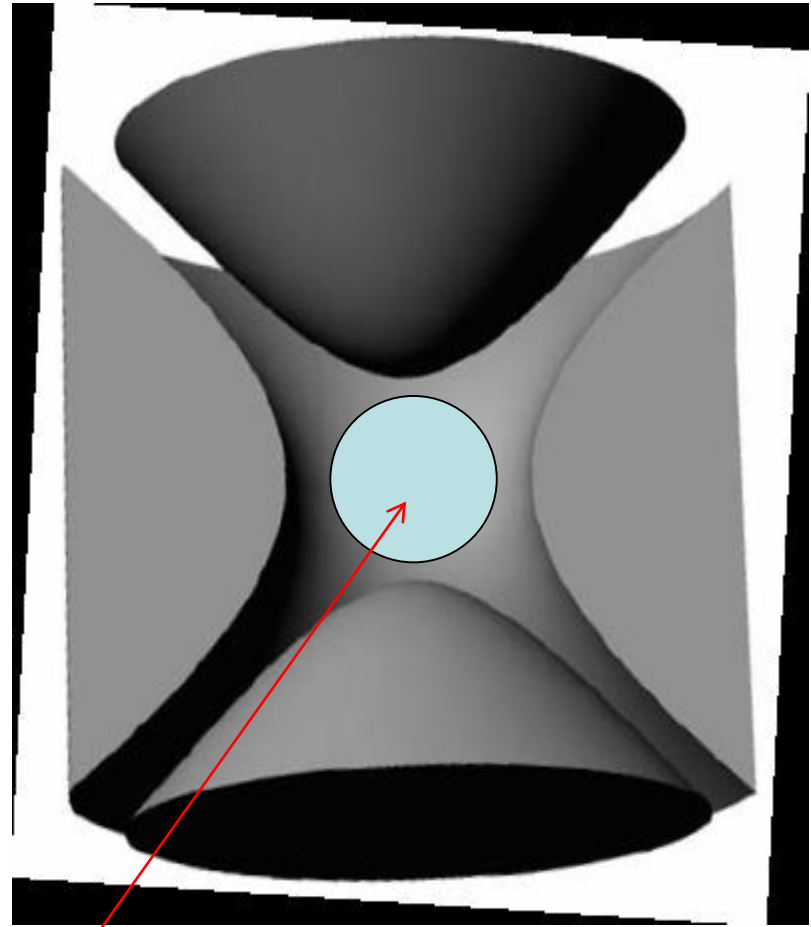
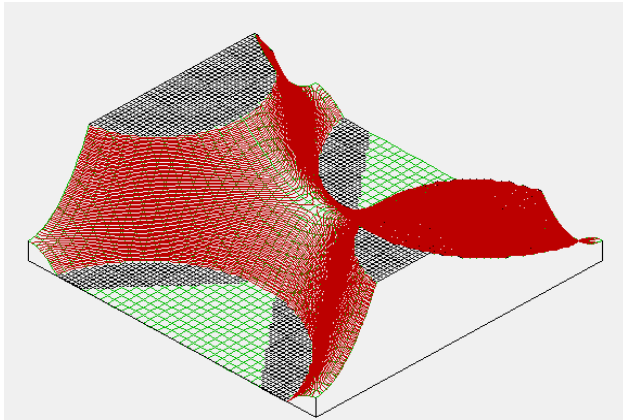
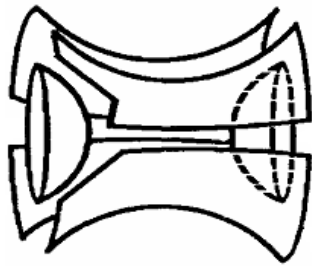
Projection on the plane
orthogonal to the magnetic field



Projection on the plane almost
Parallel to the magnetic field

How to get rid of these comets?

The simple solution: use hyperbolic cell

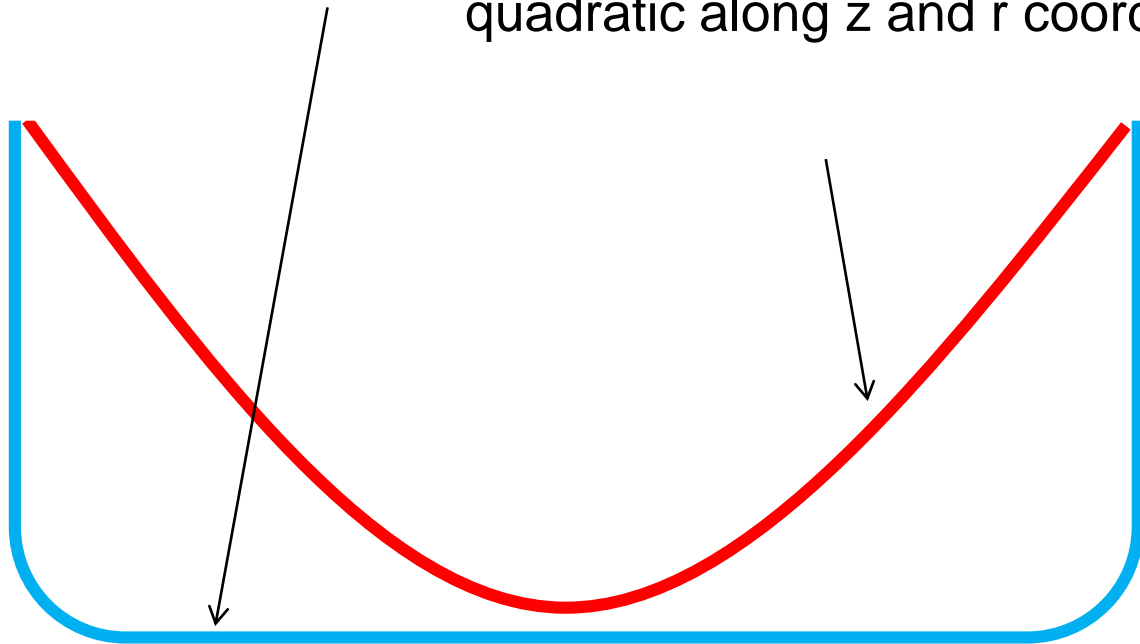


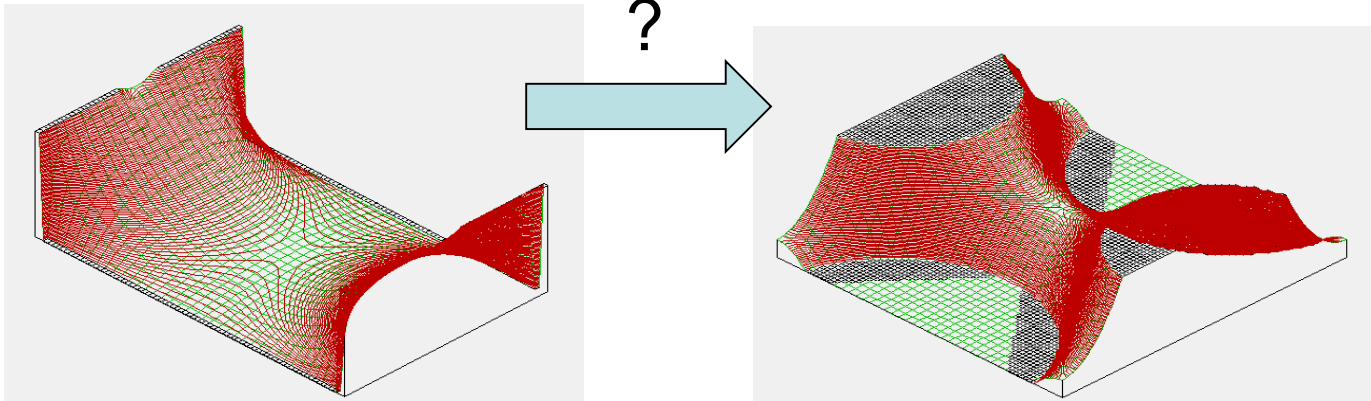
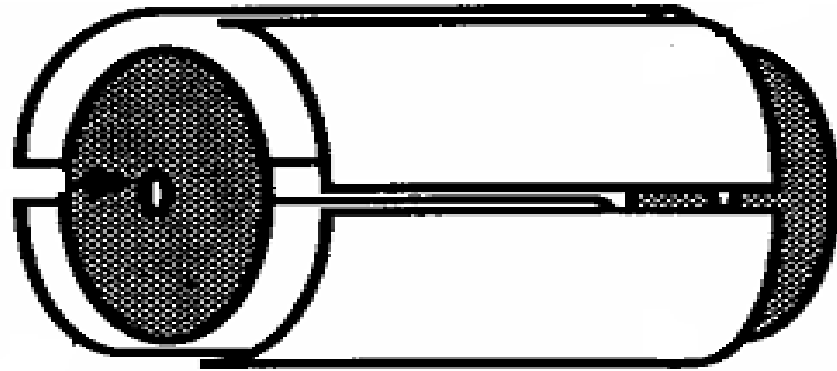
Used space

Other approaches

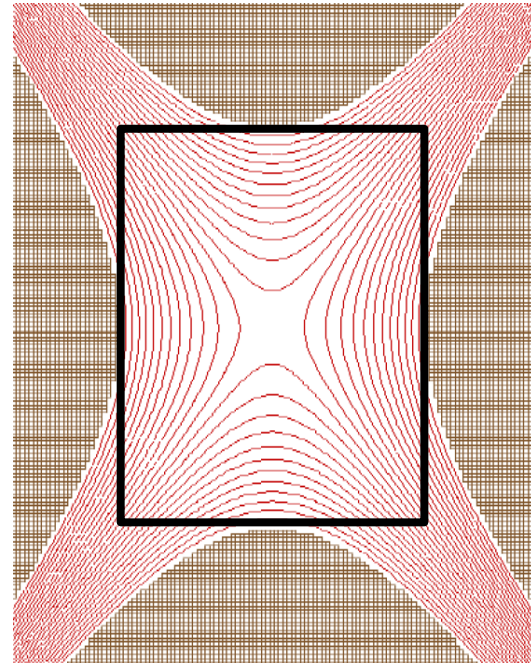
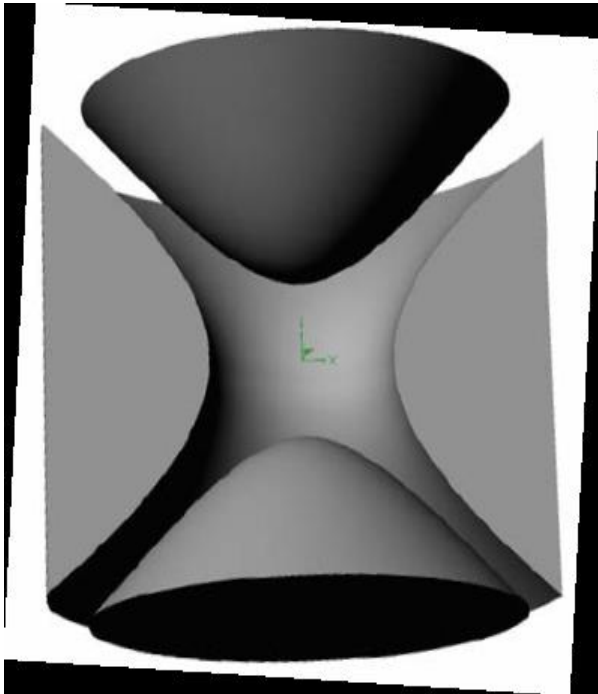
Flattering potential

Harmonization - making the field quadratic along z and r coordinates

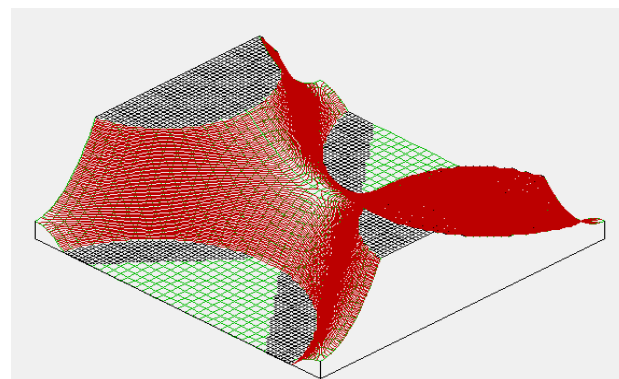
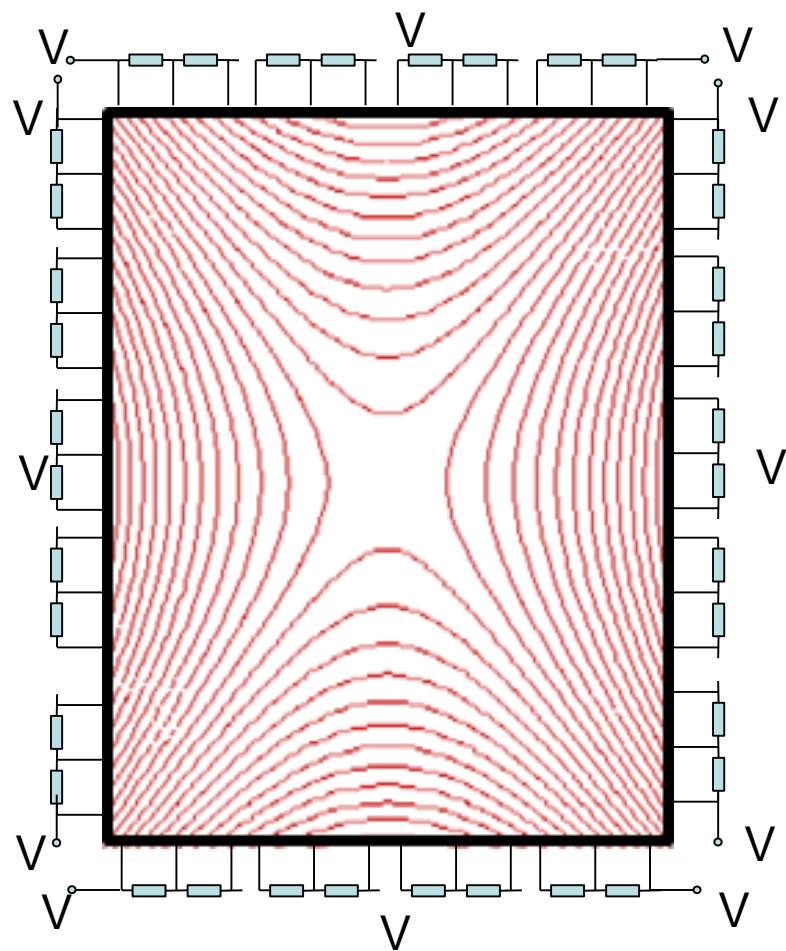


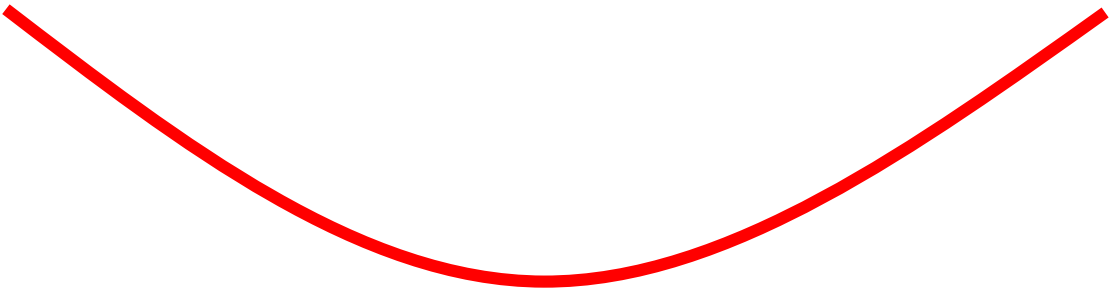
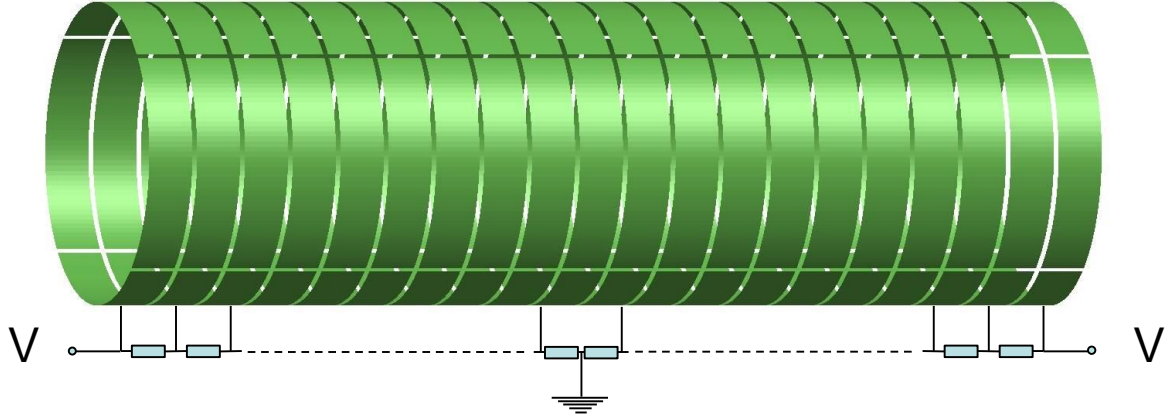


An instrument with a hyperbolic trap, however, suffers at least from inefficient use of the magnet bore and a relatively inaccessible trap interior.



The quadrupolar potential well can also be approximated in a cylindrical or cubic trap by using simple electrode shapes and by optimizing the aspect ratio or by segmenting the electrodes
(Gerald Gabrielse)

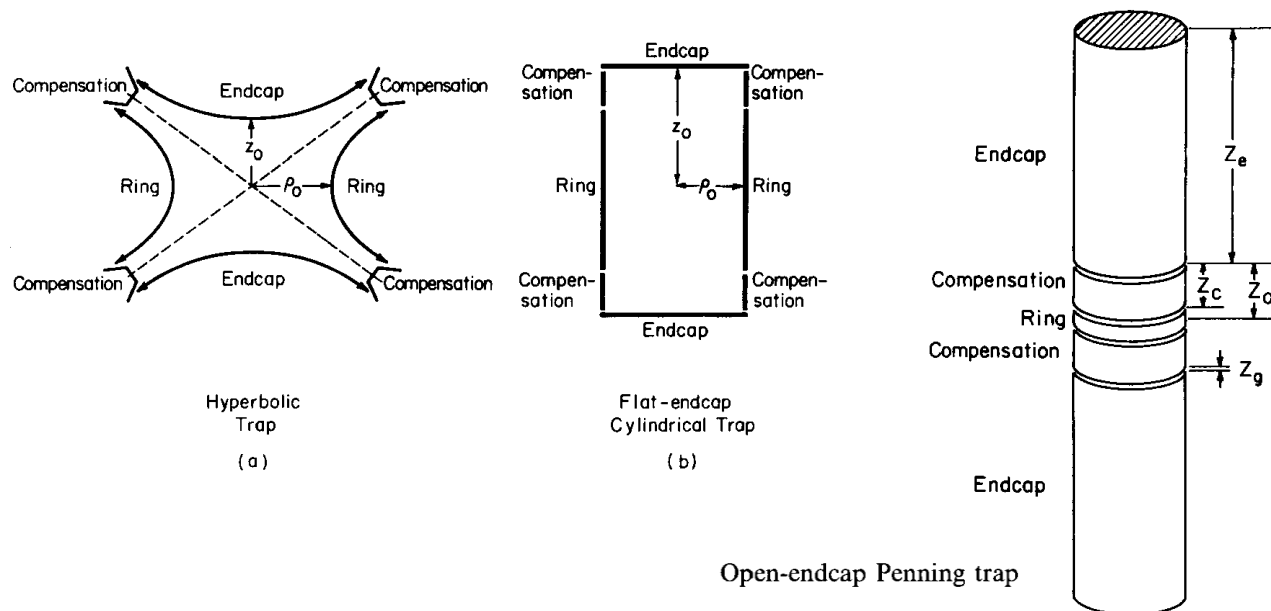




G. GABRIELSE, L. HAARSMA and S.L. ROLSTON

OPEN-ENDCAP PENNING TRAPS FOR HIGH PRECISION EXPERIMENTS

International Journal of Mass Spectrometry and Ion Processes, 88 (1989) 319–332

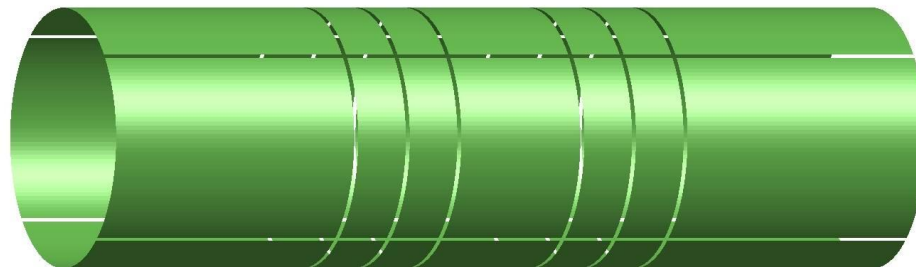
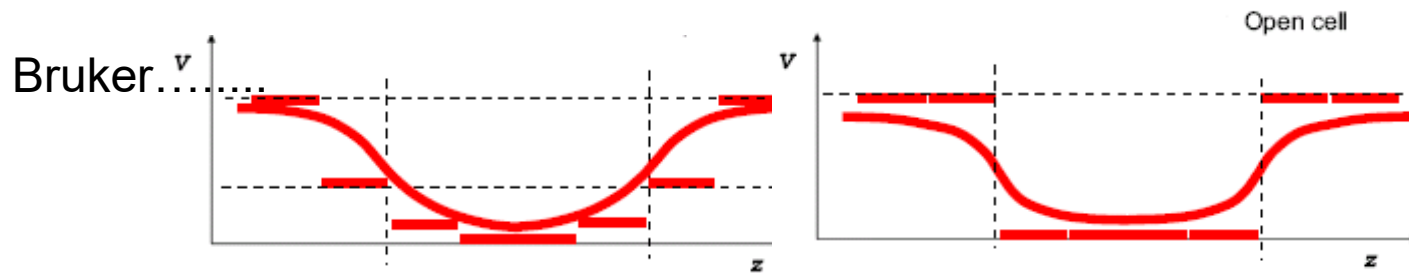


Harmonization of cell's electric potential (G.Gabrielse 1989)

Tolmachev, A. V.; Robinson, E. W.; Wu, S.; Kang, H.; Lourette, N. M.; Pasa-Tolic, L.; Smith, R. D. Trapped-Ion Cell with Improved DC Potential Harmonicity for FT-ICR MS

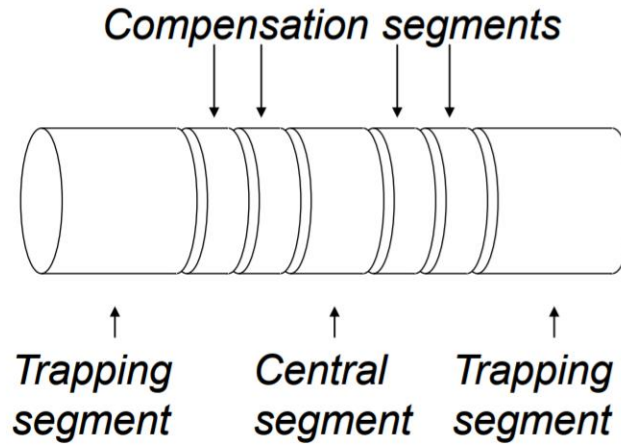
Brustkern A.M., Rempel D.L., Gross M.L. An Electrically Compensated Trap Designed to Eighth Order for FT-ICR Mass Spectrometry. J Am Soc Mass Spectrom 2008, 19, 1281–1285

Marshall's group,

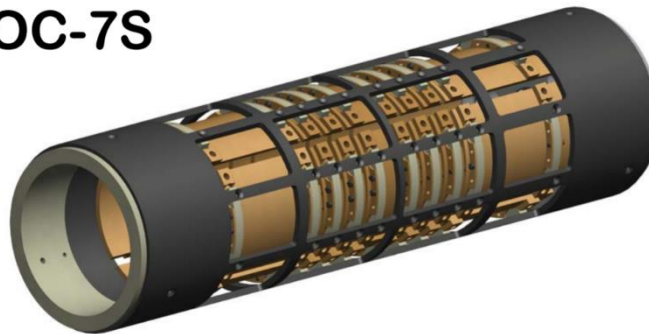


PNNL cell

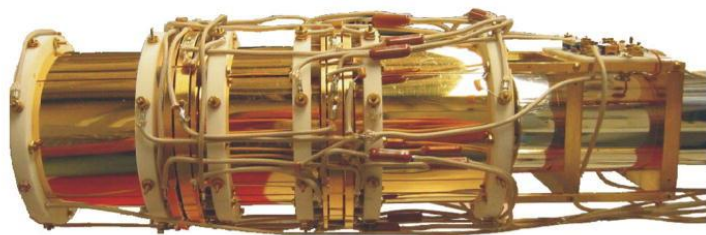
OC-7S compensation configuration



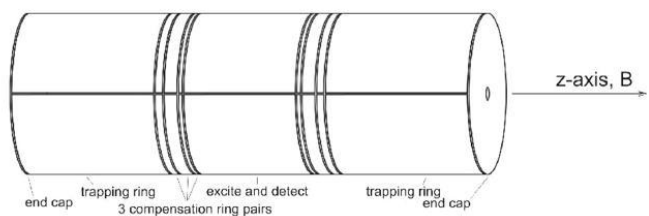
OC-7S



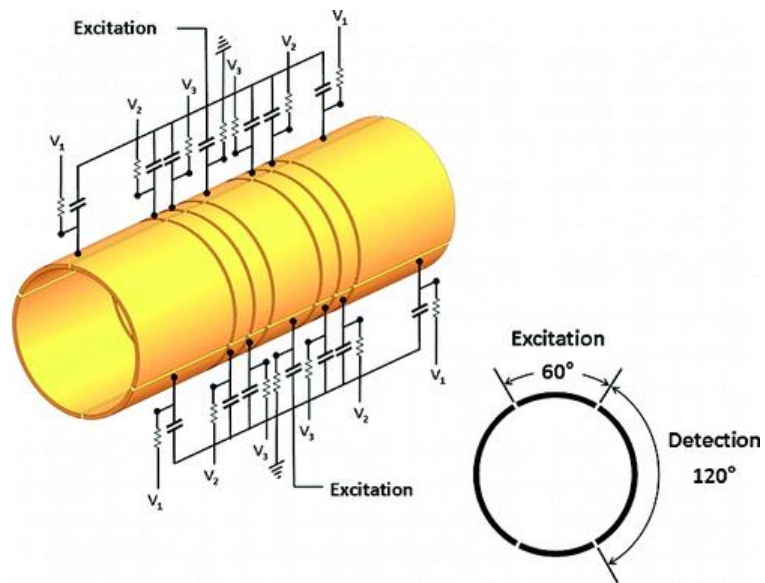
(a)



(b)



Gross group

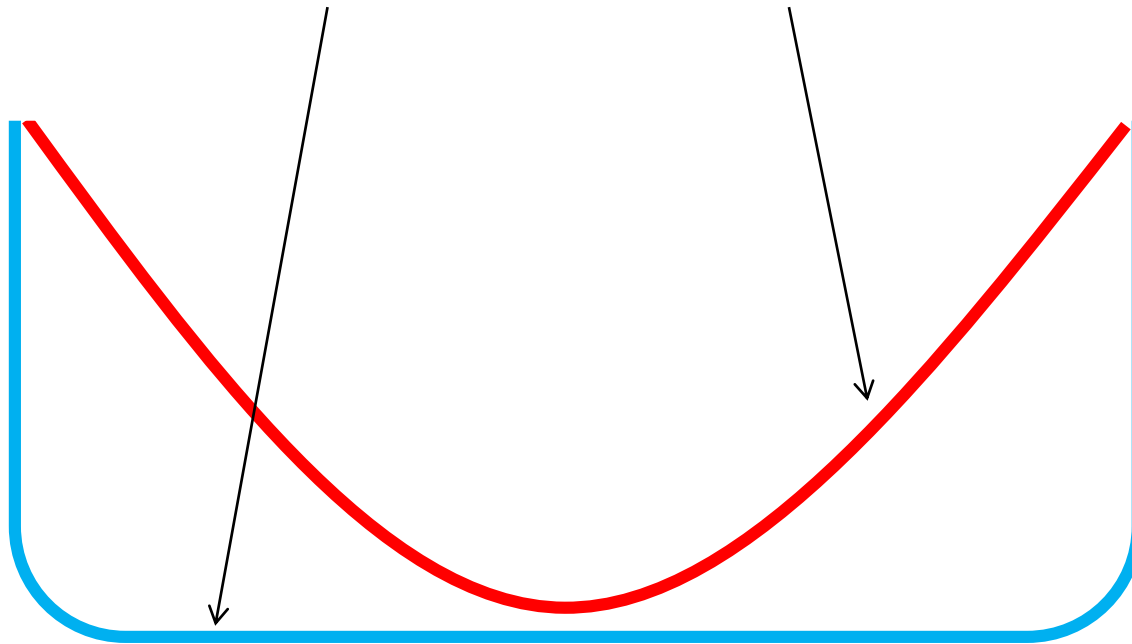


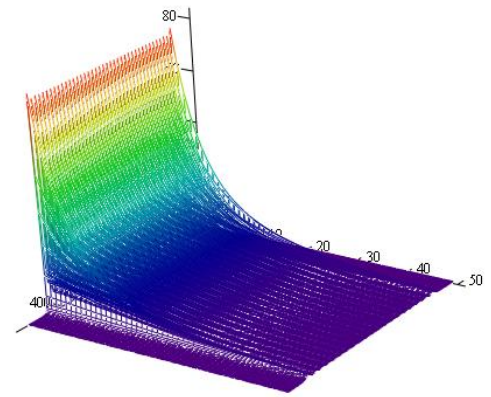
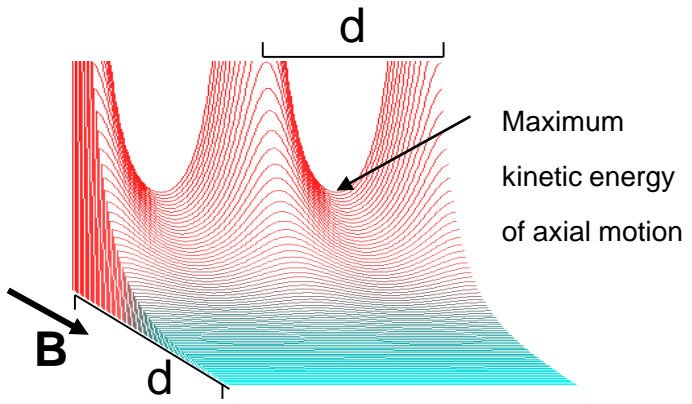
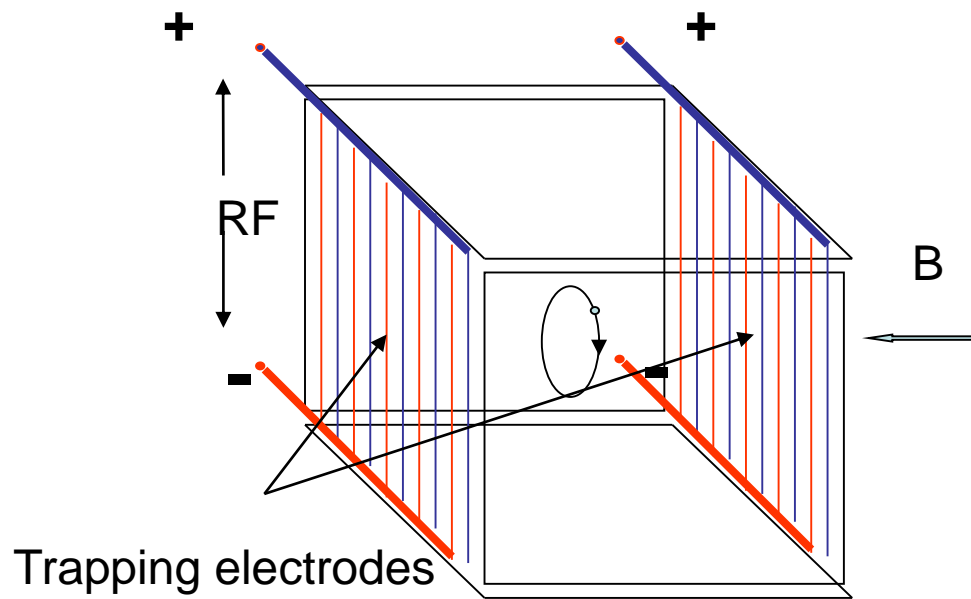
Marshall group

Two main approaches

Flattering potential

Harmonization

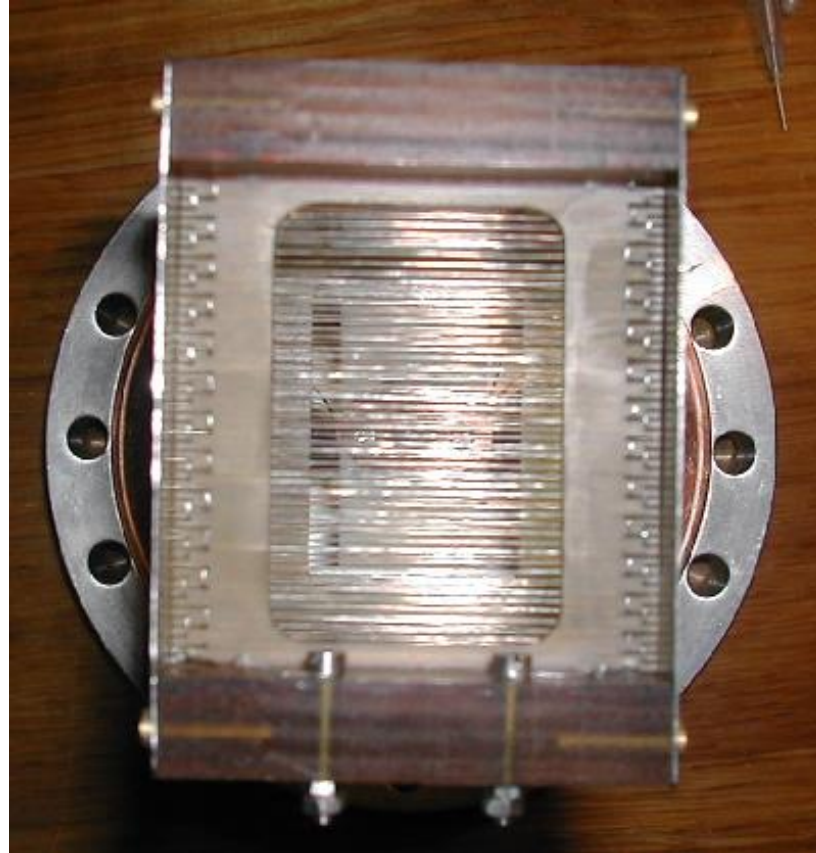




FT ICR cell with mesh trapping electrodes creating pseudopotential



Wire cell trapping electrode (1 mm distance between adjacent wires)





US 20050242280A1

(19) **United States**

(12) **Patent Application Publication** (10) **Pub. No.: US 2005/0242280 A1**

Nikolaev

(43) **Pub. Date:**

Nov. 3, 2005

(54) **ION CYCLOTRON RESONANCE MASS SPECTROMETER**

(52) **U.S. Cl.** **250/291**

(75) **Inventor: Evgenij Nikolaev, Moscow (RU)**

Correspondence Address:
**KUDIRKA & JOBSE, LLP
ONE STATE STREET
SUITE 800
BOSTON, MA 02109 (US)**

(57) **ABSTRACT**

The invention describes an ion cyclotron resonance (ICR) mass spectrometer with an ICR trap, the ICR trap having as trapping electrodes two ion reflecting electrode structures operated by RF voltages without any DC voltage. The usual apertured ion trapping electrodes are replaced by multitudes of structural elements, electrically conducting, and repeating spatially in one or two directions of a surface, neighboring structure elements being connected each to different phases of an RF voltage. In the simplest case a grid of parallel wires can be used. The surface of such structures reflects ions of both polarities, if the mass-to-charge ratio of the ions is higher than a threshold.

(73) **Assignee: Bruker Daltonik GMBH, Bremen (DE)**

(21) **Appl. No.: 10/833,938**

(22) **Filed: Apr. 28, 2004**

Publication Classification

(51) **Int. Cl.⁷ H01J 49/38**

(12) **United States Patent**
Franzen et al.

(10) **Patent No.:** **US 7,368,711 B2**

(45) **Date of Patent:** **May 6, 2008**

(54) **MEASURING CELL FOR ION CYCLOTRON
RESONANCE MASS SPECTROMETER**

5,019,706 A * 5/1991 Allemann et al. 250/291

5,572,035 A 11/1996 Franzen

6,403,955 B1 6/2002 Senko

7,223,965 B2 * 5/2007 Davis 250/282

(75) Inventors: **Jochen Franzen**, Bremen (DE);
Evgenij Nikolaev, Moscow (RU)

(73) Assignee: **Bruker Daltonik GmbH**, Bremen (DE)

FOREIGN PATENT DOCUMENTS

U.S. Patent

May 6, 2008

Sheet 3 of 5

US 7,368,711 B2

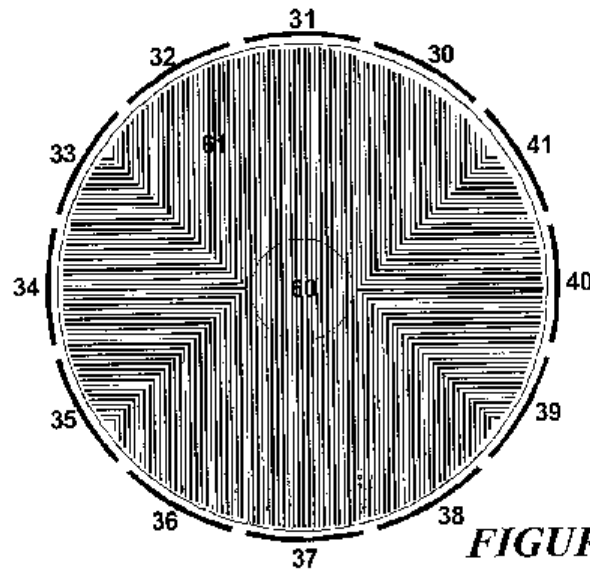
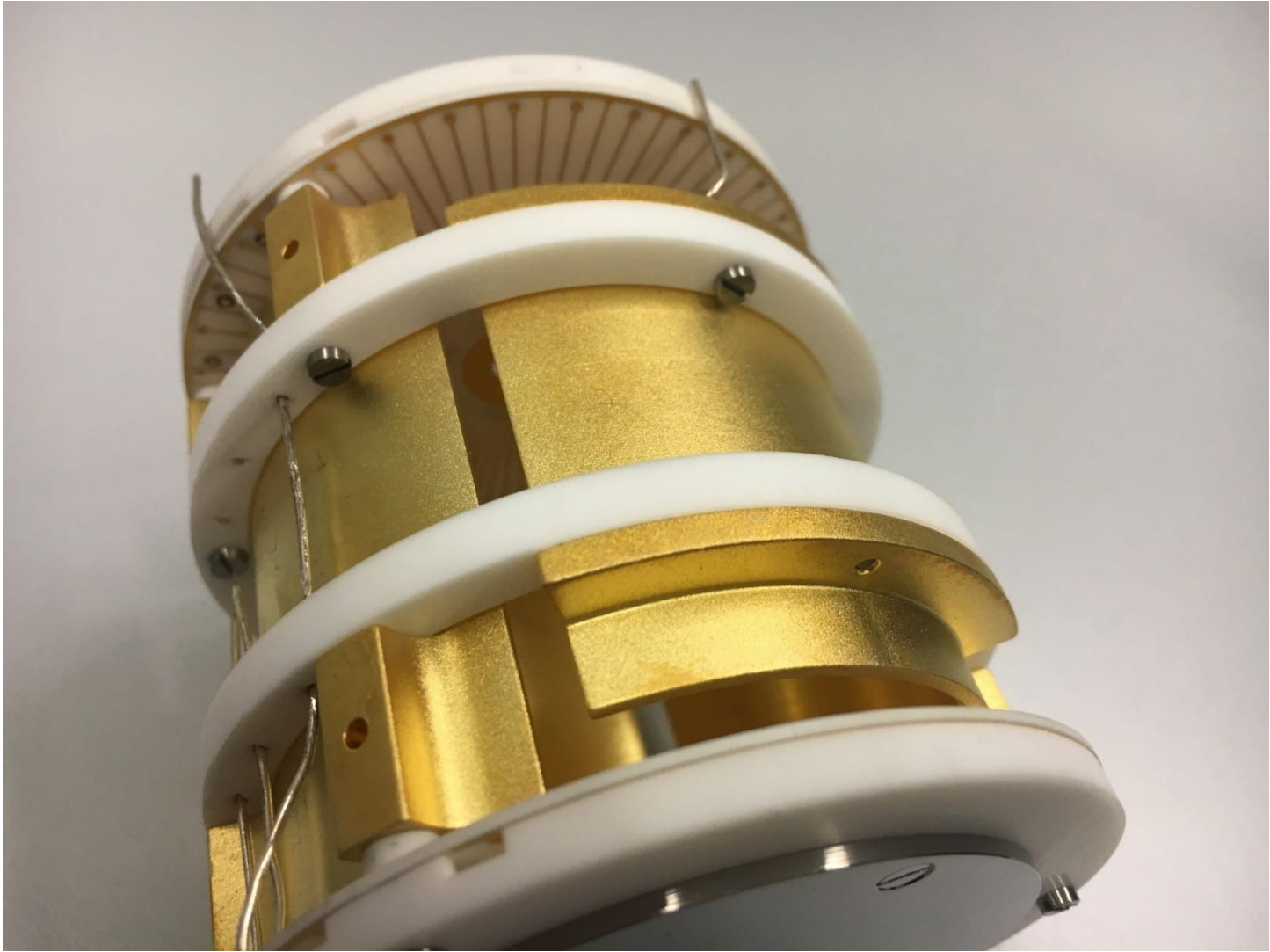
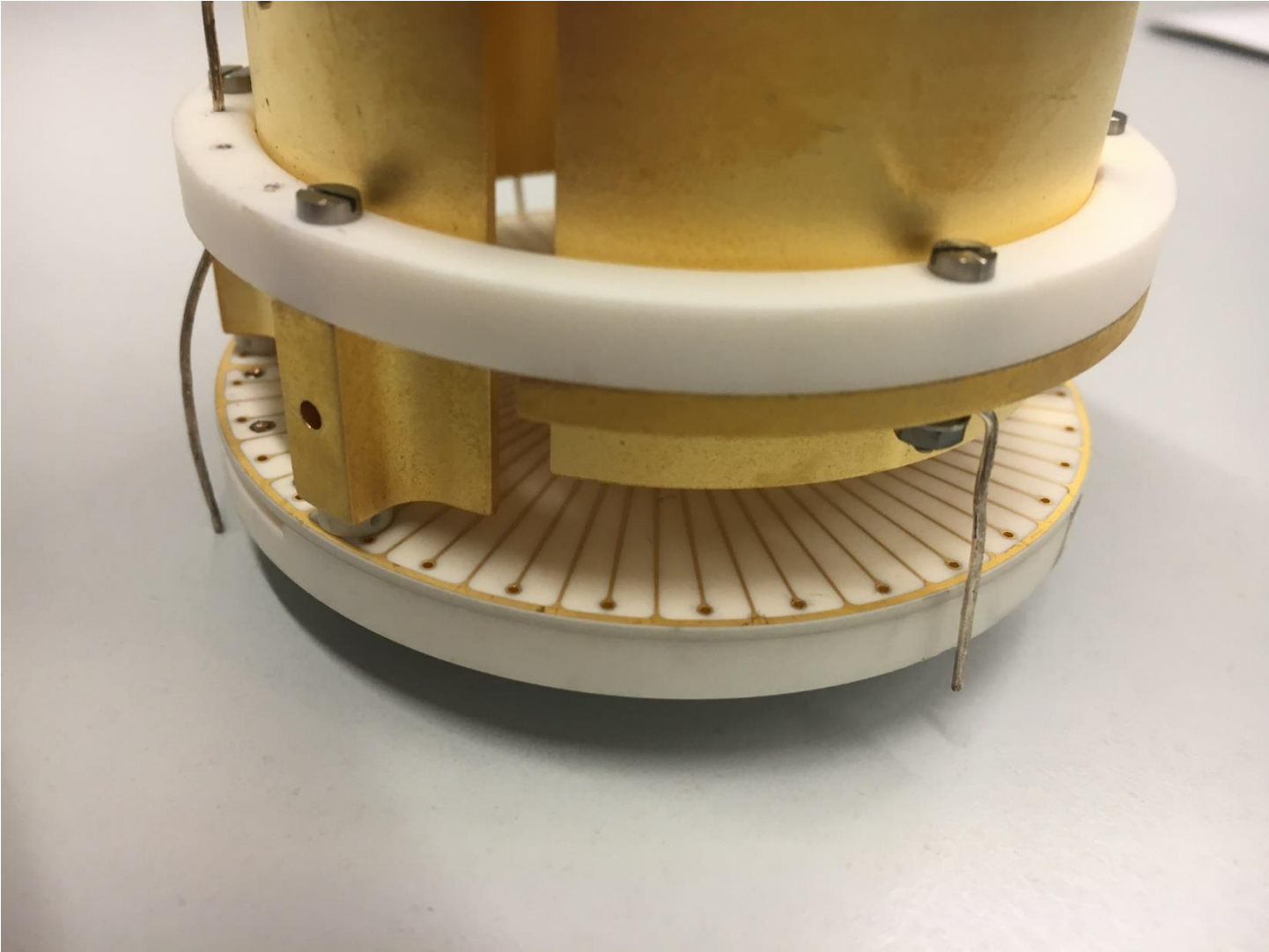


FIGURE 7

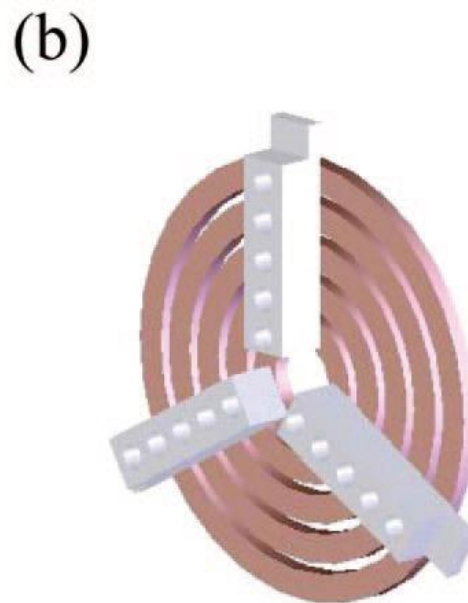
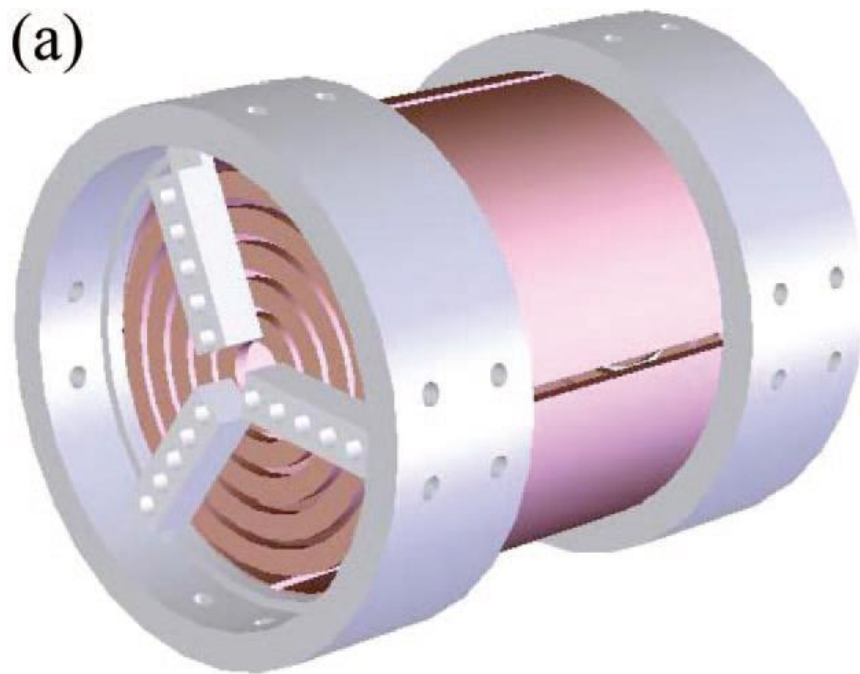




Cell with trapping electrodes segmented to rings

Chad R. Weisbrod, Nathan K. Kaiser, Gunnar E. Skulason, and James E. Bruce*

Trapping Ring Electrode Cell: A FTICR Mass Spectrometer Cell for Improved Signal-to-Noise and Resolving Power *Anal. Chem.* 2008, 80, 6545–6553



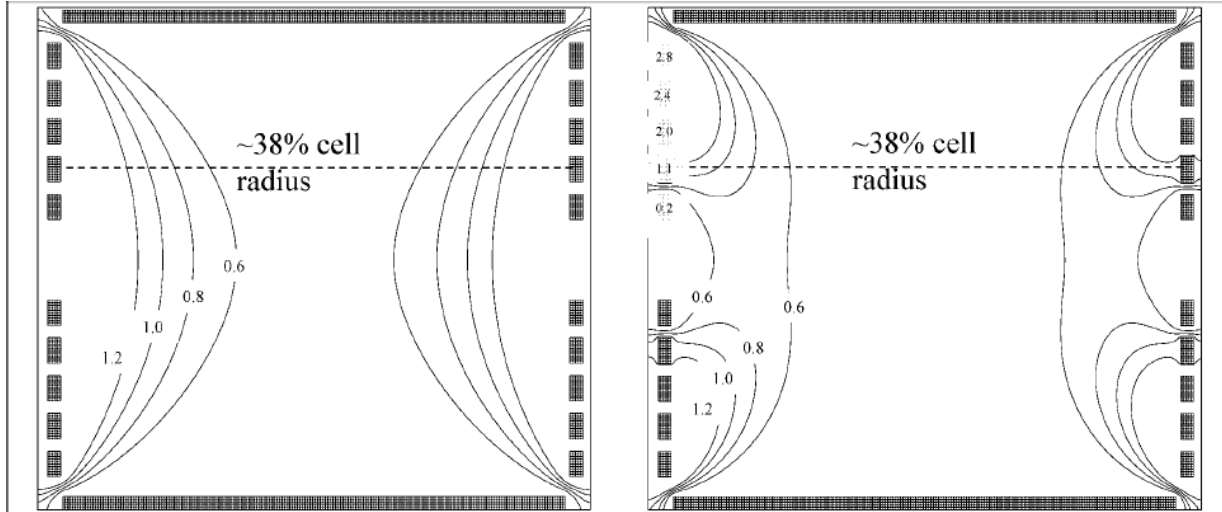


Figure 2. Equipotential contour plots are shown for (a) common 2.0 V trapping conditions and (b) the TREC trapping conditions. The voltages for the modulated (TREC) trapping conditions with increasing electrode radius are 0.2, 1.1, 2.0, 2.4, and 2.8 V respectively, as shown on the rings. A dashed line through the cell located at 38% cell radius is depicted.

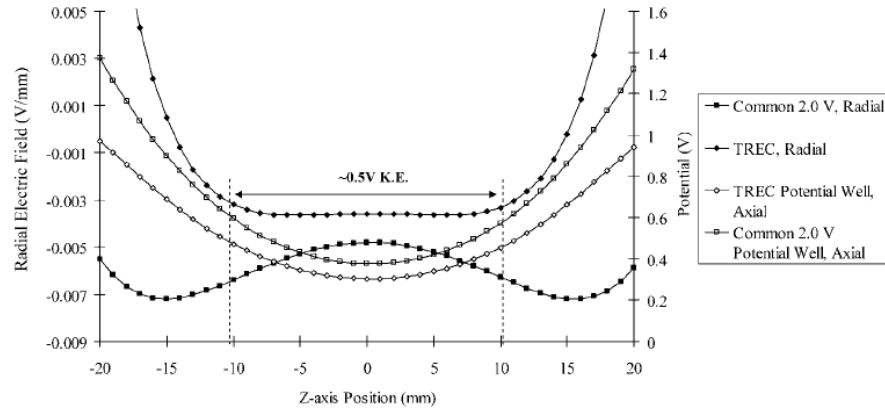
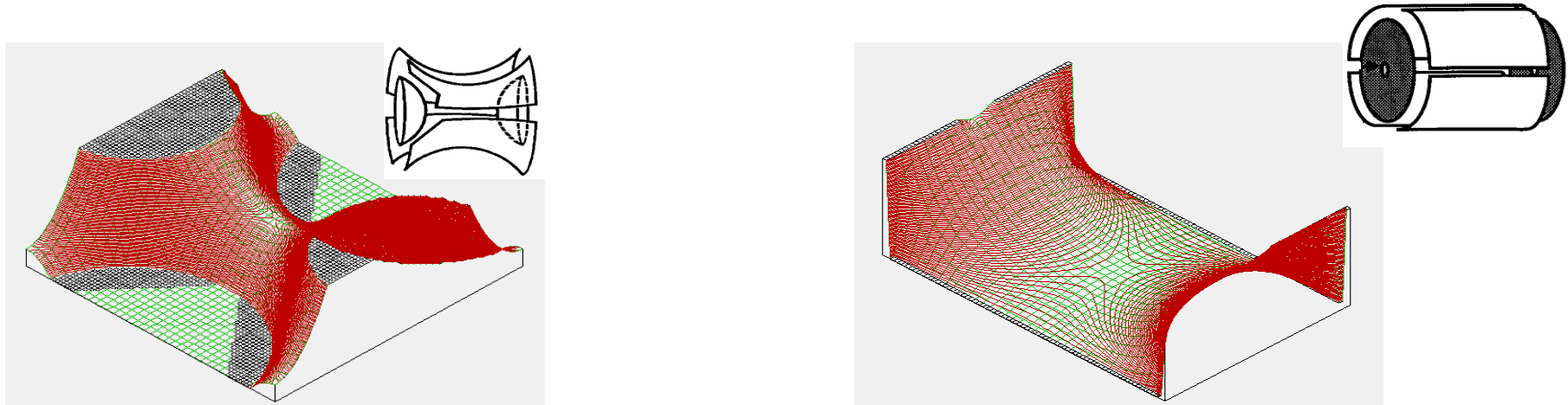
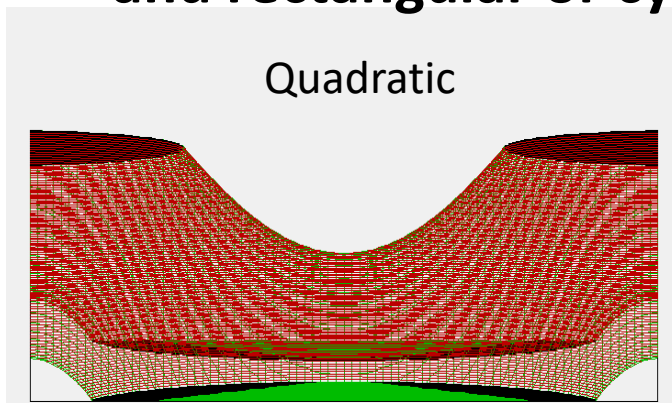


Figure 3. Radial electric field plots generated at 38% cell radius for both common 2.0 V trapping conditions and the TREC modulated conditions. A trapping potential well generated from the TREC conditions is overlaid to provide perspective.

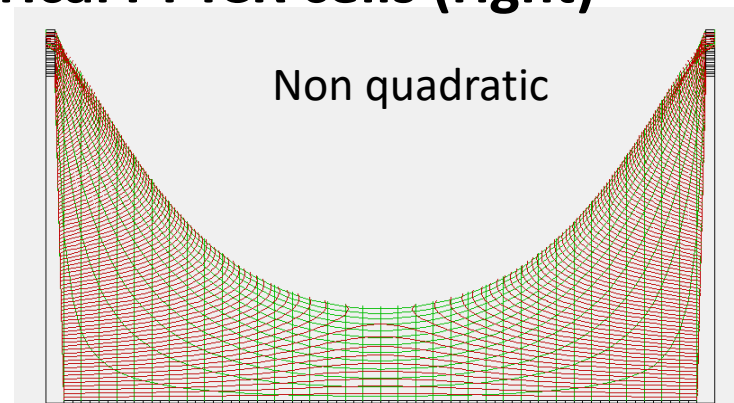
The lost of phase coherence is a result of Unharmonicity of a regular FT ICR cell field



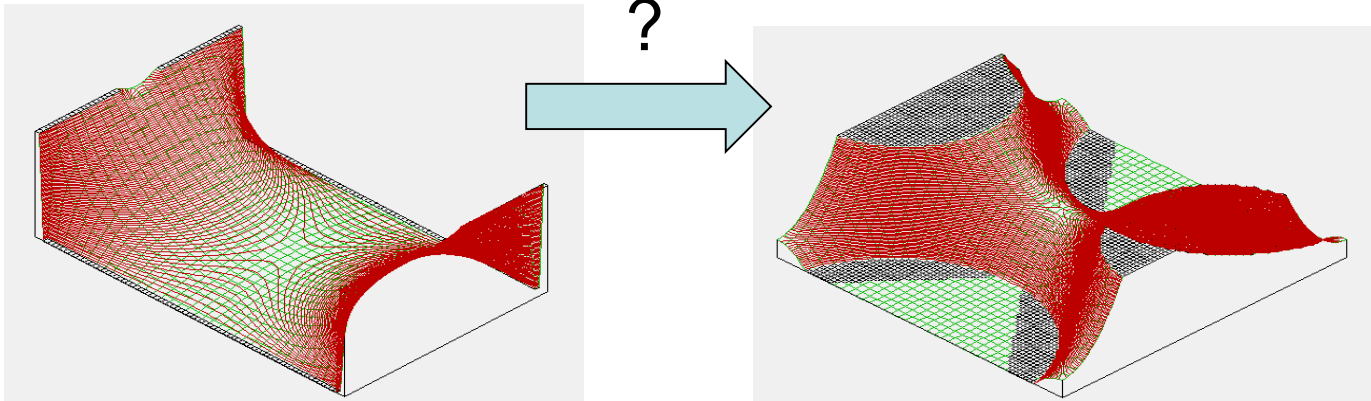
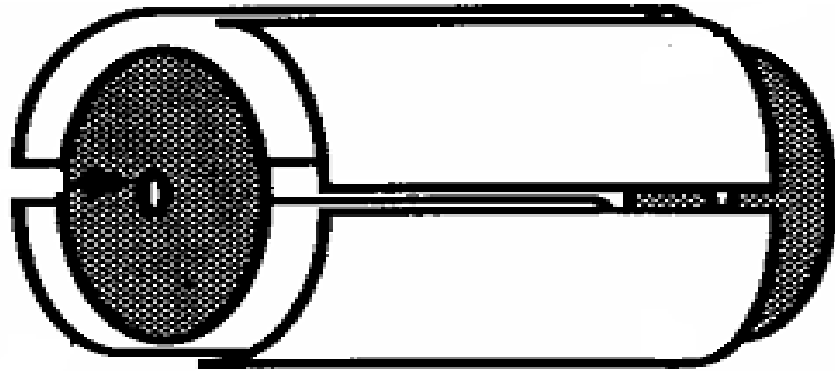
Distribution of potentials in hyperbolic (left) and rectangular or cylindrical FT ICR cells (right)



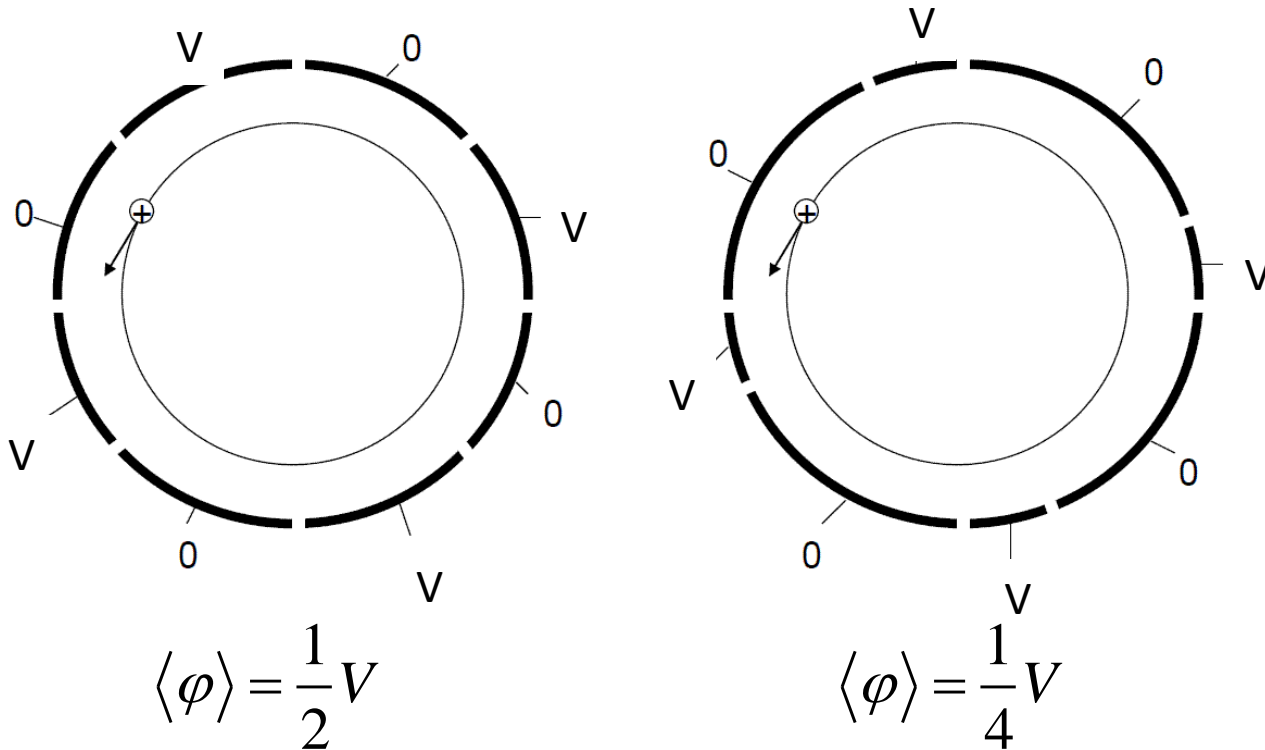
Axial and magnetron frequencies are Independent on axial oscillation amplitude

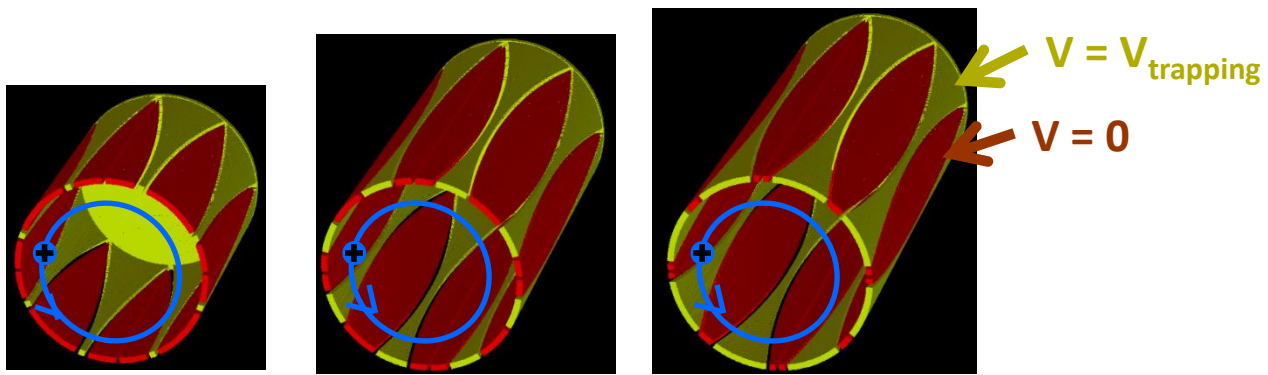


Axial and magnetron frequencies depend on axial oscillation amplitude

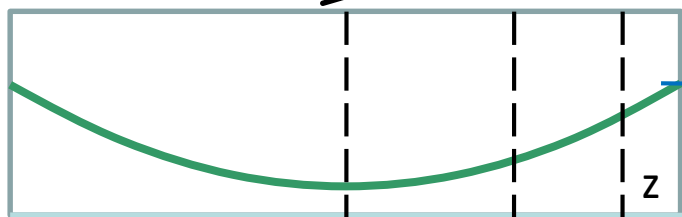


Averaging over cyclotron motion

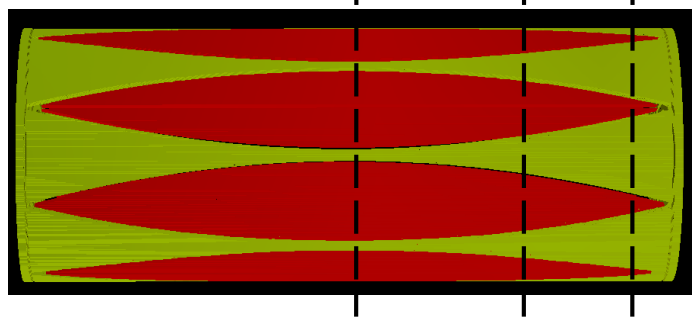




$\langle \phi \rangle \approx 1/4 * V_{trapping}$
 $\langle \phi \rangle \approx 1/2 * V_{trapping}$
 $\langle \phi \rangle \approx 3/4 * V_{trapping}$



$\langle \phi \rangle(z)$ – potential
 averaged over cyclotron
 orbit

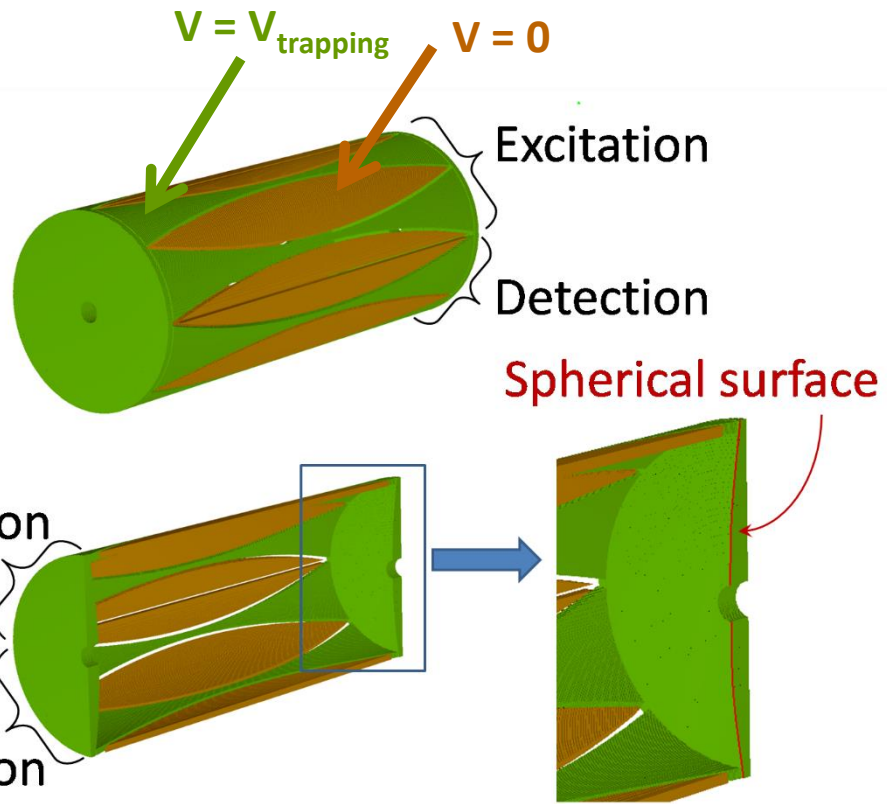


Dynamically harmonized FT ICR cell

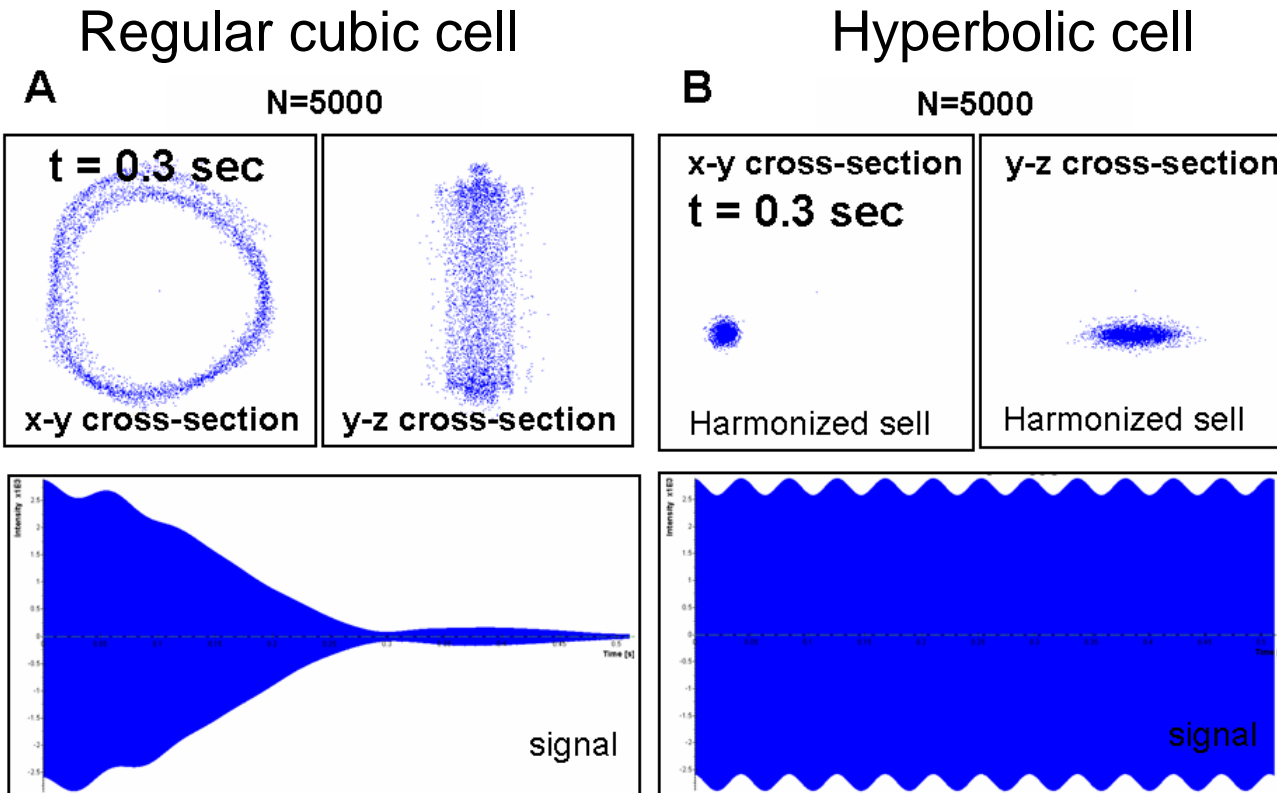


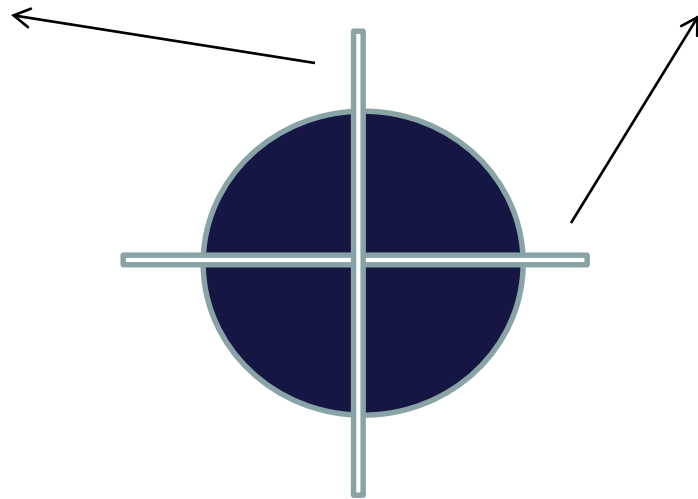
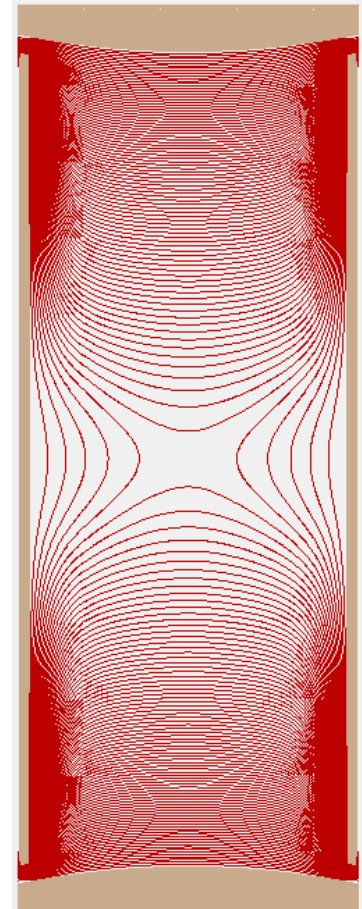
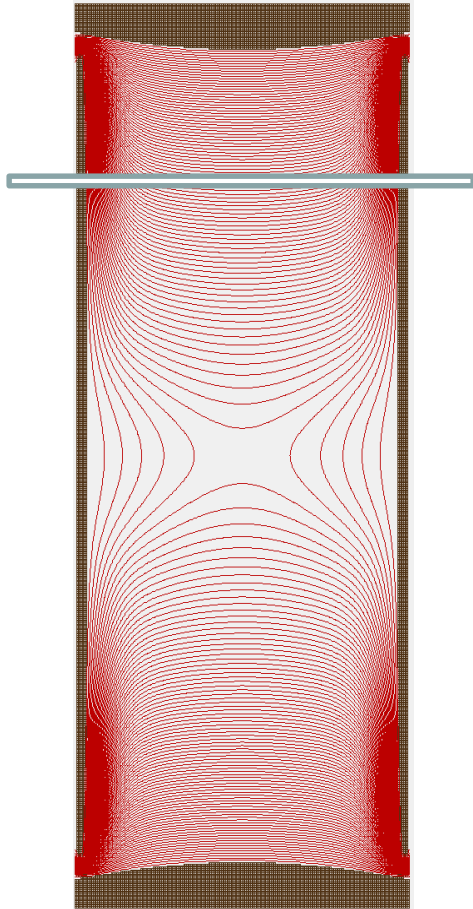
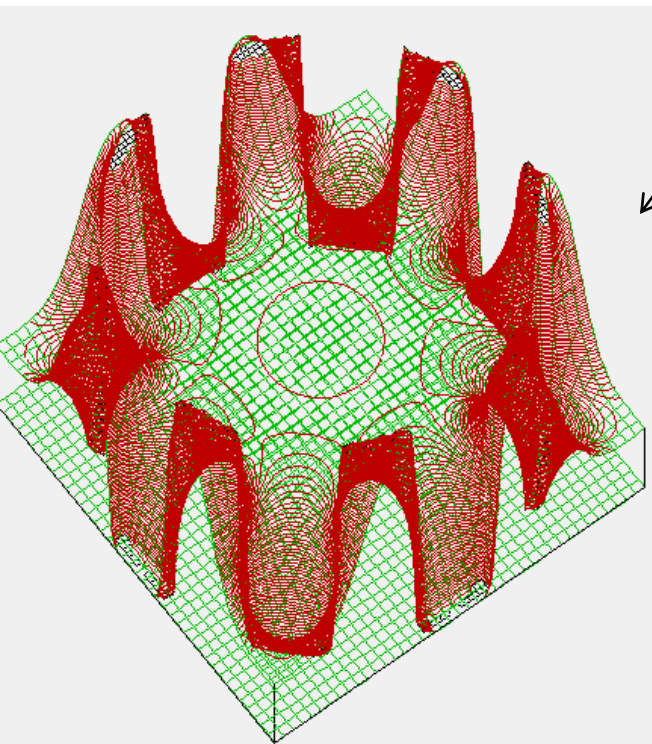
Parabolic shape gaps

$$\alpha = \frac{2\pi}{N} n \pm \alpha_0 \left(1 - \left(\frac{z}{a} \right)^2 \right)$$

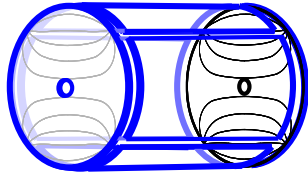
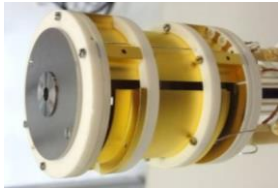


Evolution of ion cloud $m/z = 500$ Da, $Z=1$ in 7 T
0.5 s detection time.

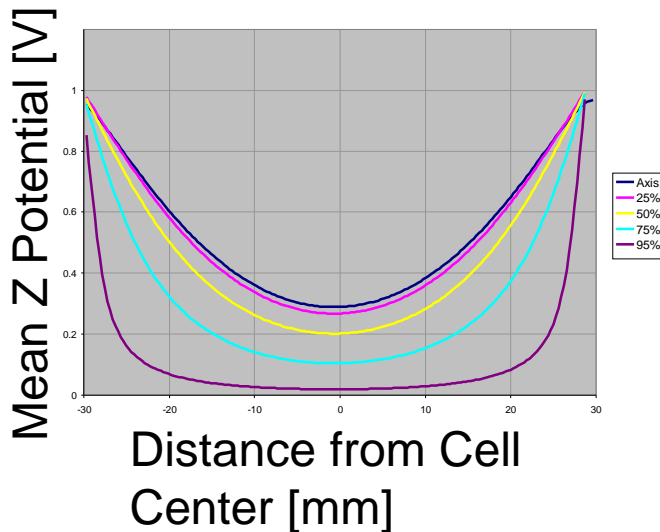




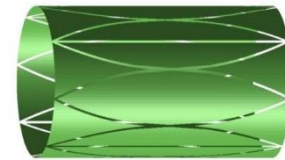
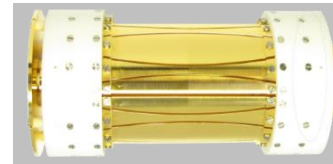
Comparison of averaged axial potential



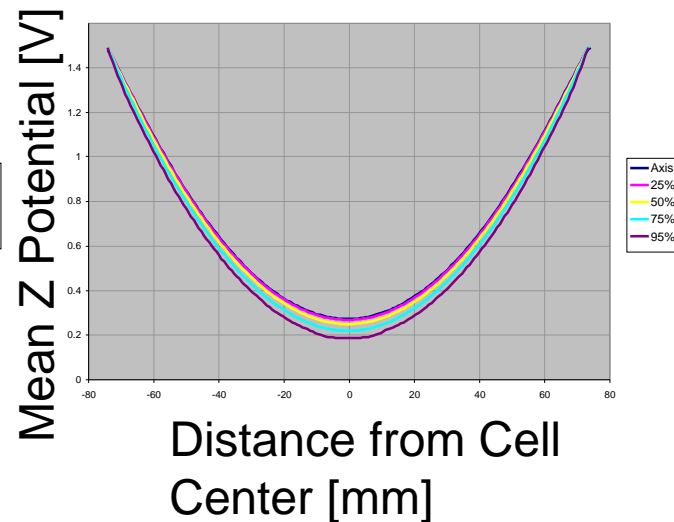
Infinity Cell



Near parabolic potential up to a cyclotron orbit of 50% of the cell radius.



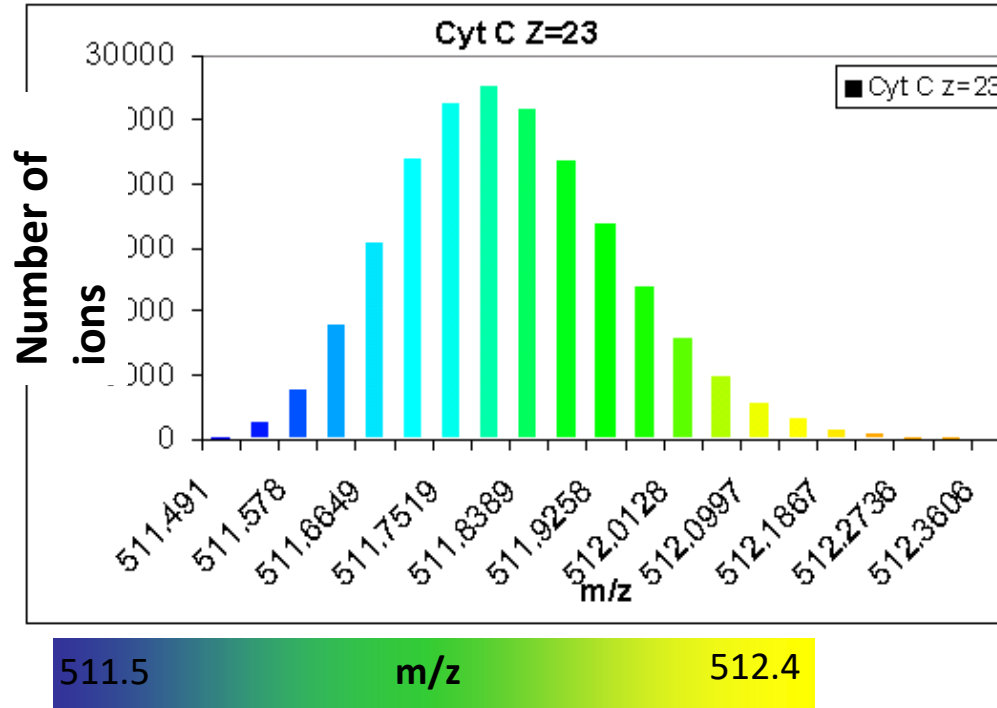
Dynamically Harmonized Cell



Harmonic, parabolic potential at all cyclotron orbits.

Isotopic cluster of Cyt C (charge state Z=23)

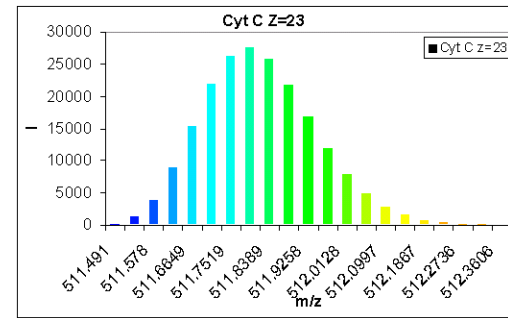
Theoretical isotopic distribution



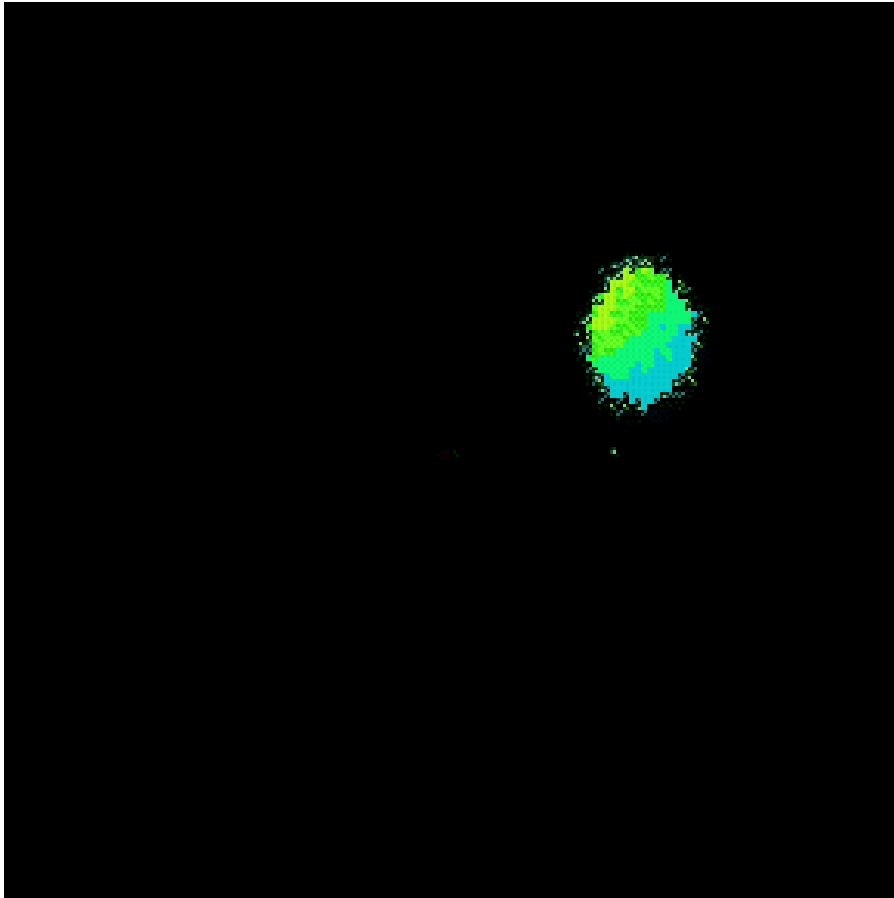
*7T, 21T ; 0.3 sec
detection; >100
steps per
minimal
cyclotron
period;*

*0.0004 sec, 50V
p-p excitation
"chirp"
excitation ; 5V
trapping
potential*

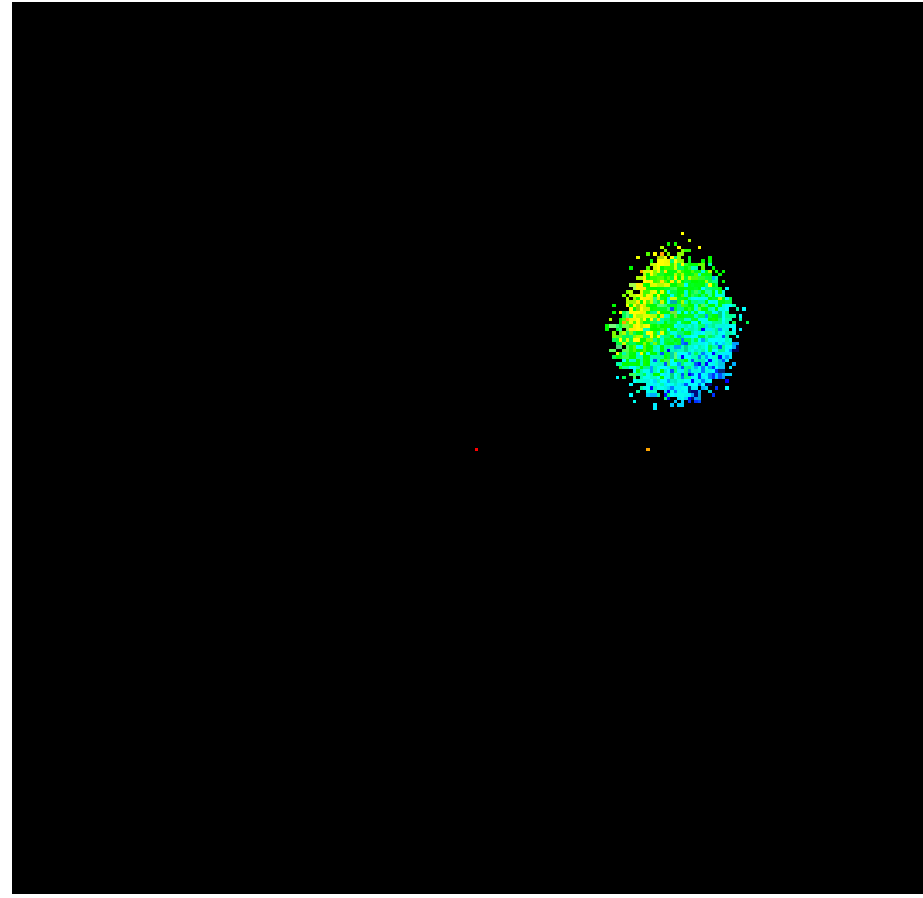
7T Cyt C 100000 charges



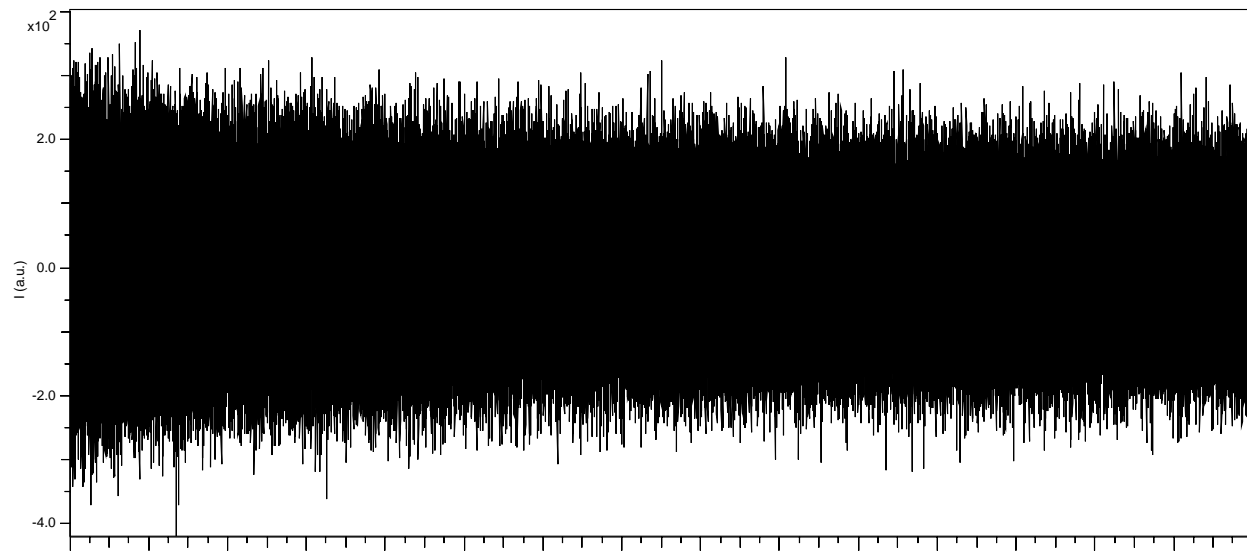
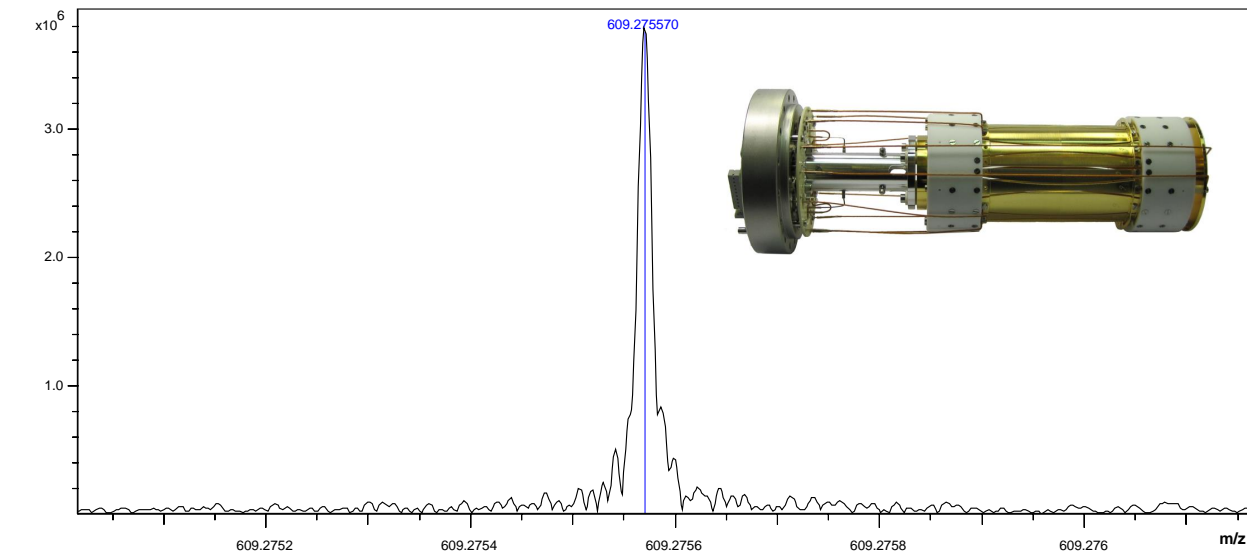
Cylindrical, cubic



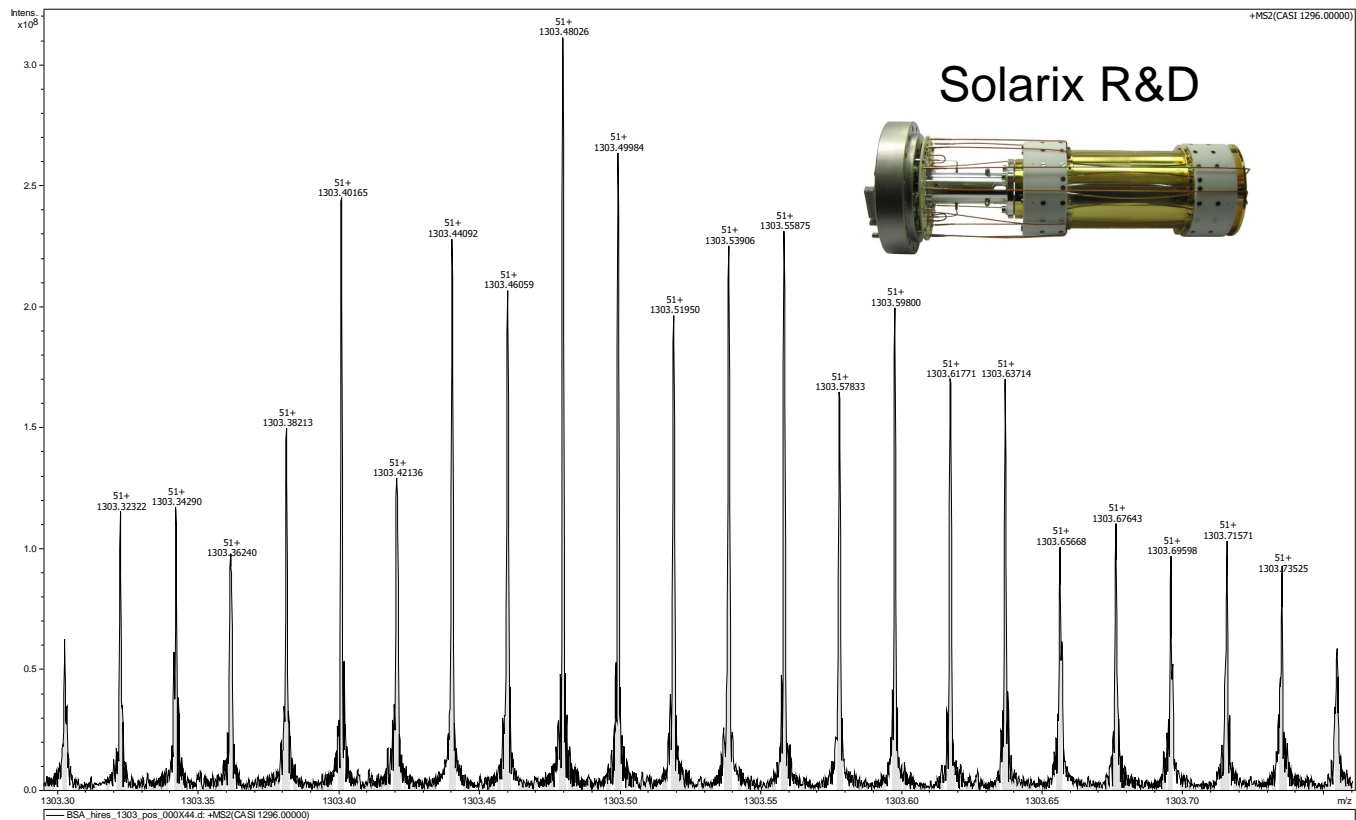
Hyperbolic, dynamically harmonized



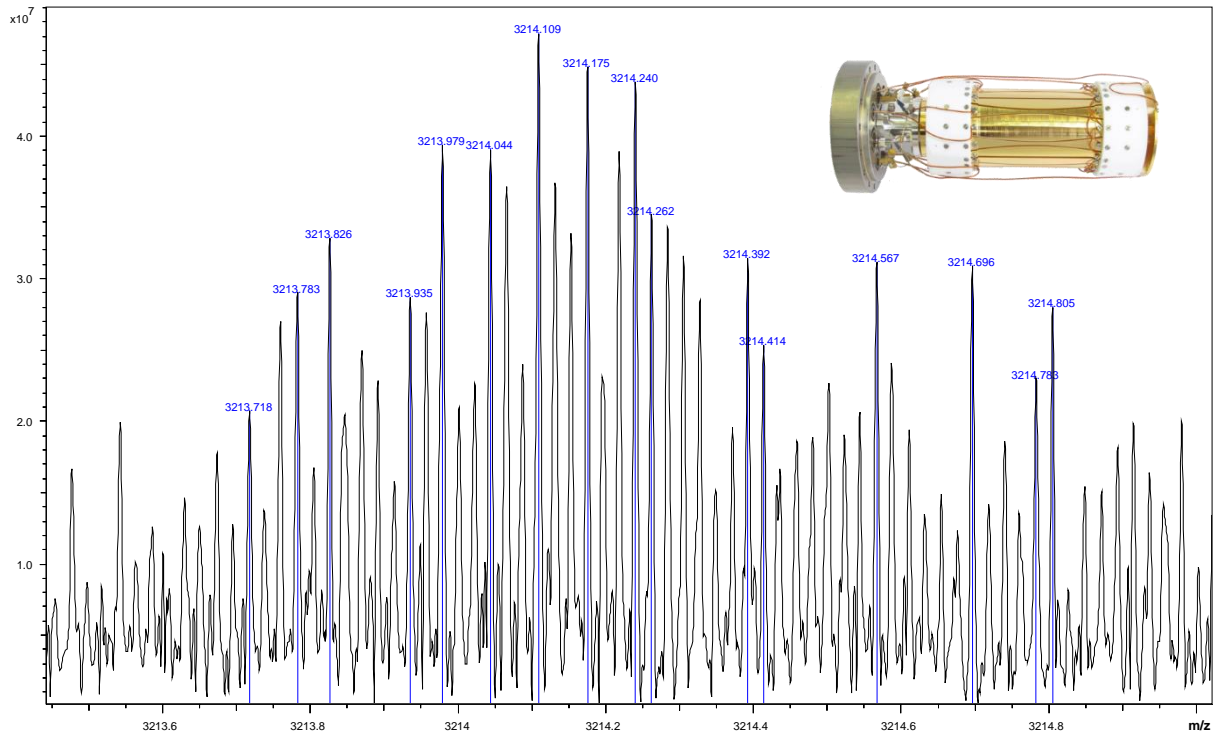
Reserpine. Lab Prototype , Solarix, 300s transient, RP 39,000,000 in magnitude mode



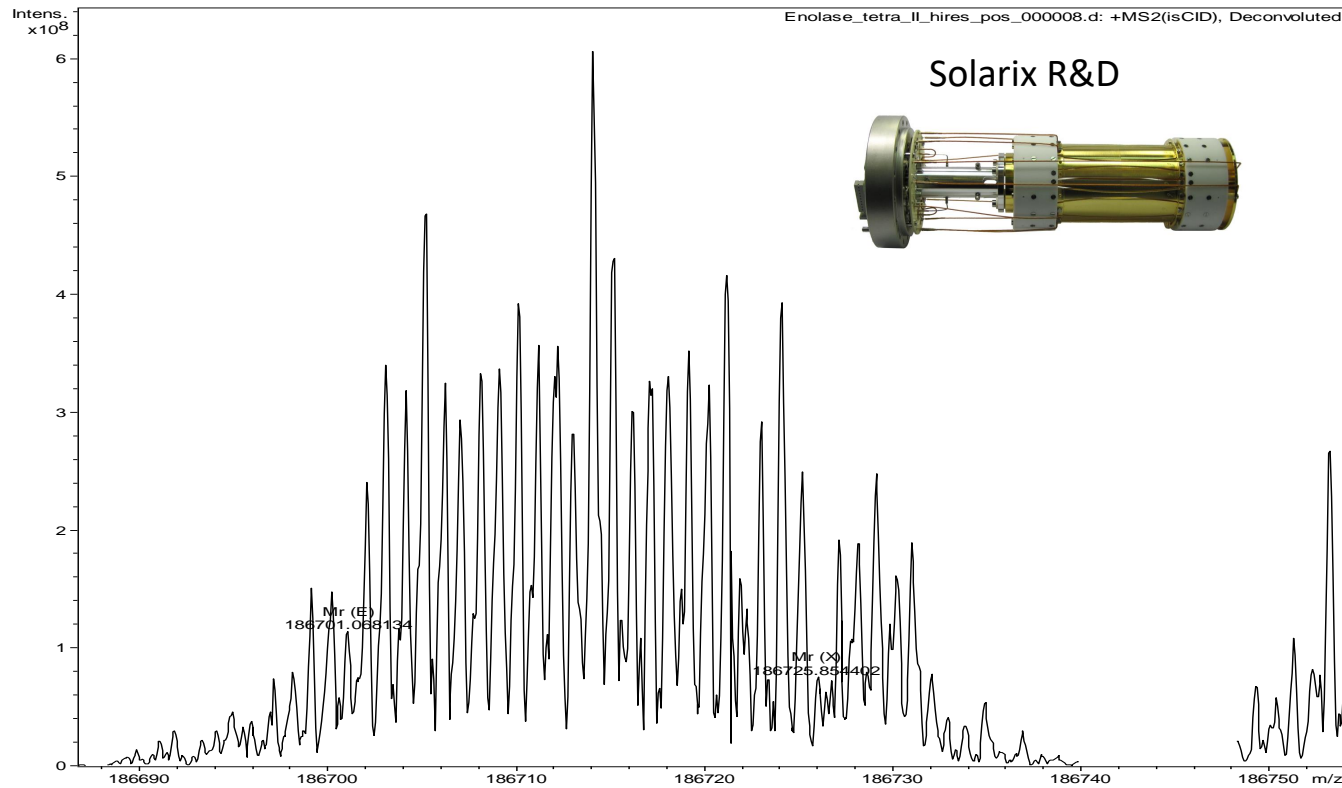
7T R&D, BSA, 51+, RP 1,700,000 28 s transient



IgG1 (MW =147800 Da), 46+, RP 500 000



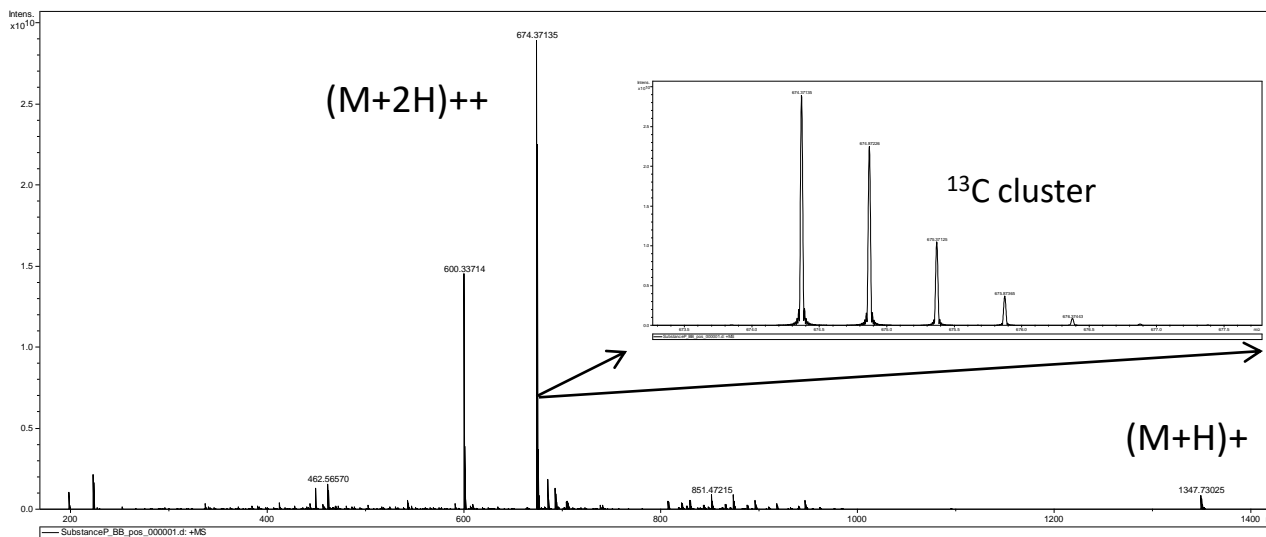
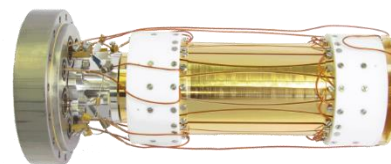
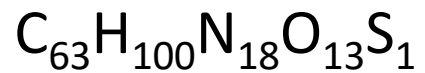
12T R&D, Enolase Tetramer, MW=**186713** Da,
m/z=5835, (6μG/ml) , 32+, deconvoluted



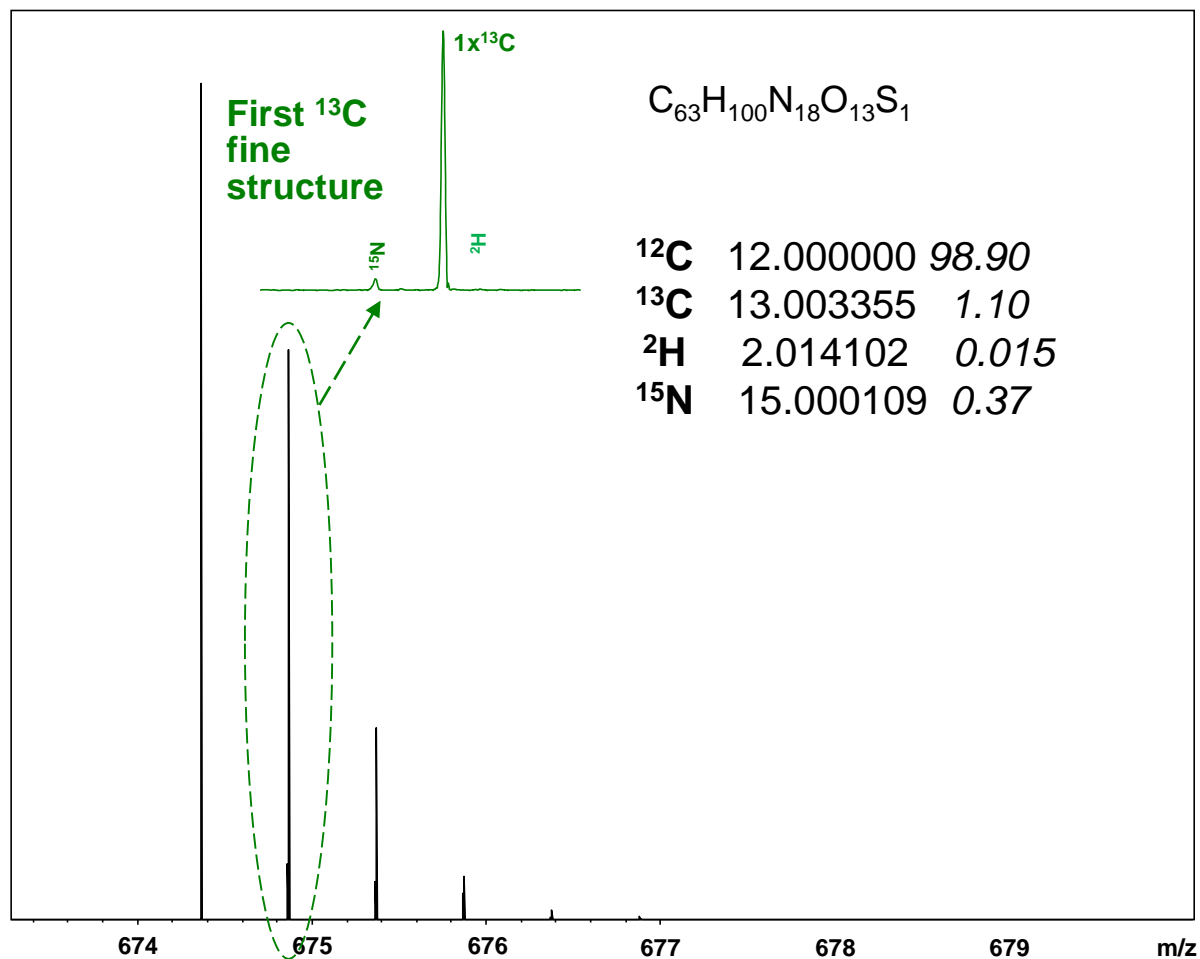
The highest mass protein complex isotopically resolved (2012)

Peptide spectra fine structure

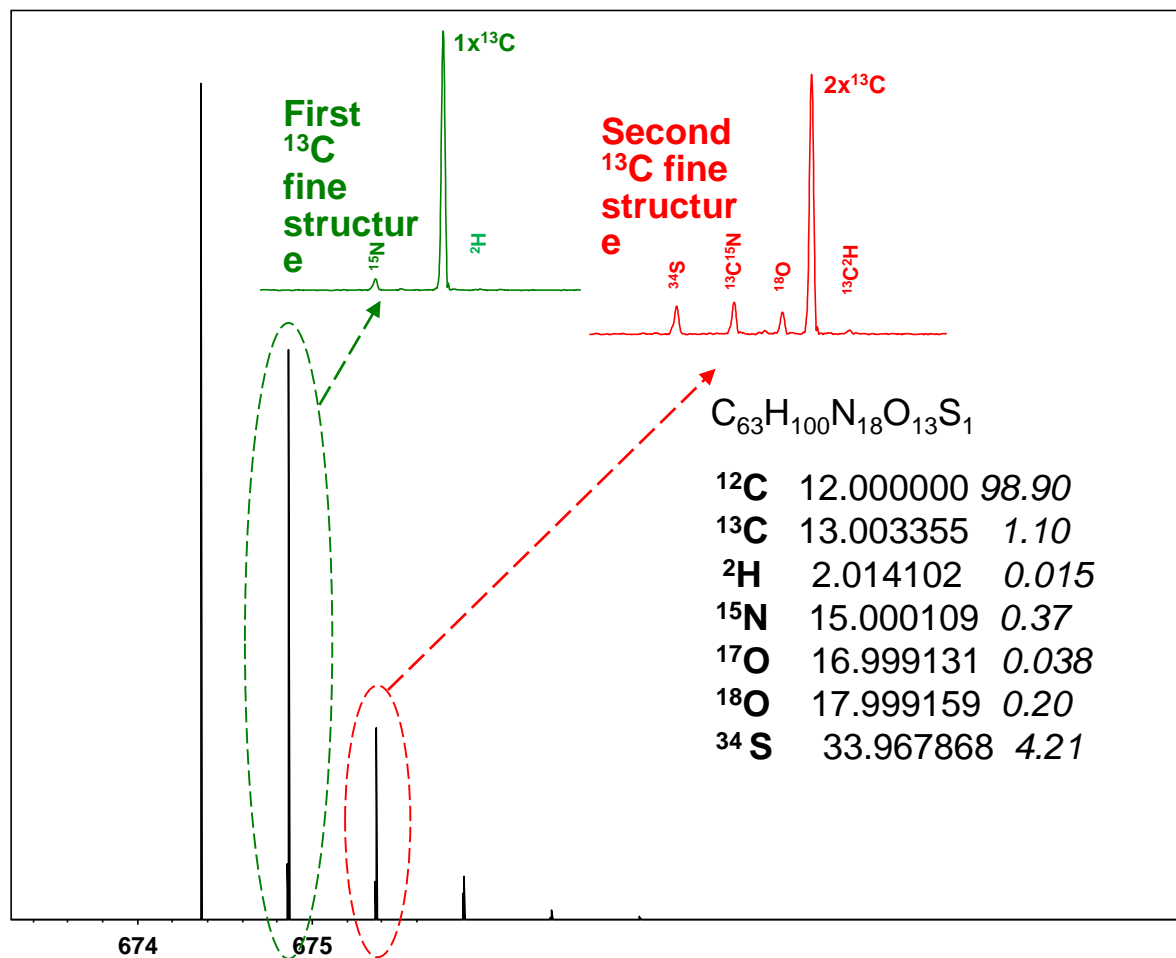
Substance P, broadband spectrum



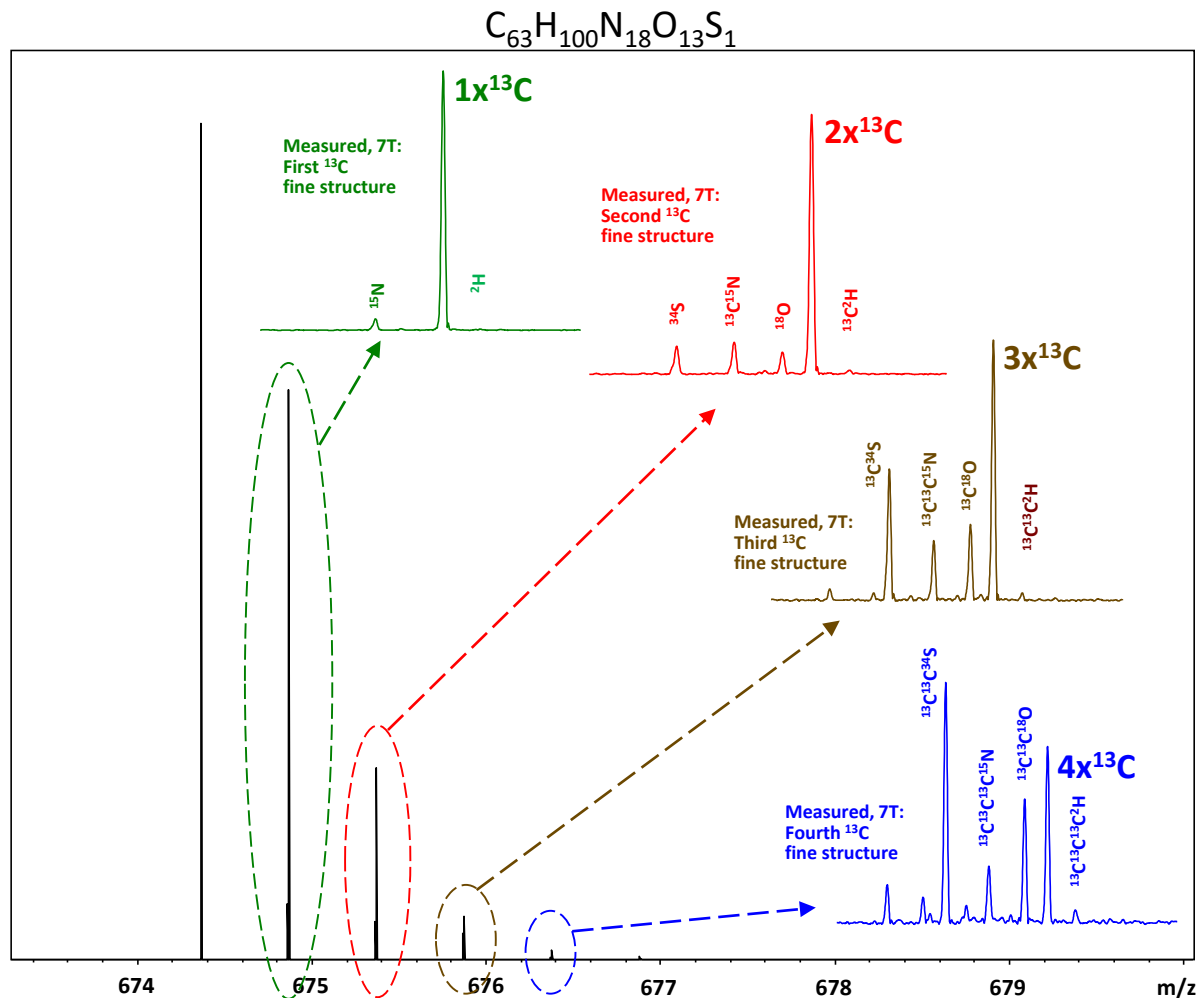
Substance P ($M+2H^+$) on 7 Tesla magnet



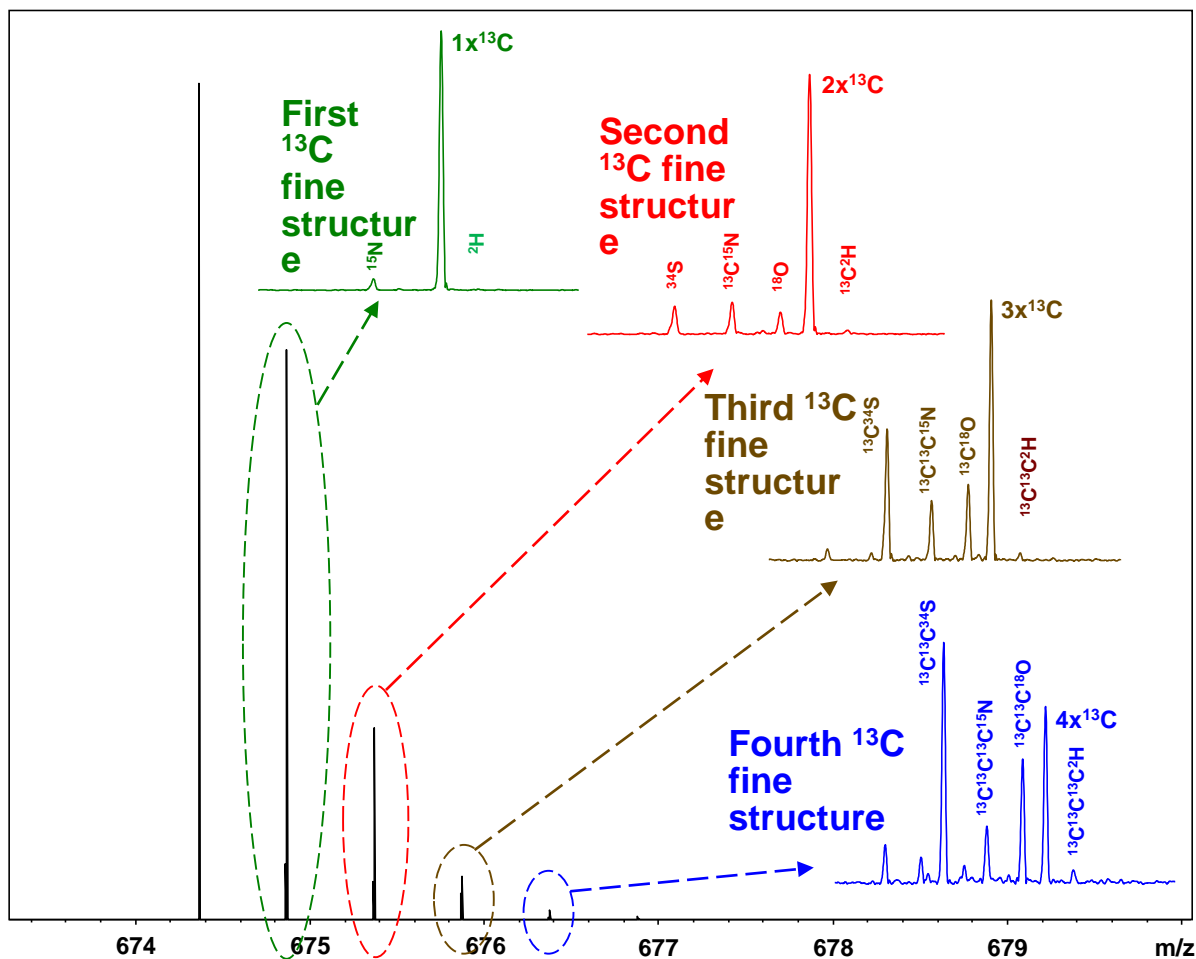
Substance P ($M+ 2H^+$) on 7 Tesla magnet



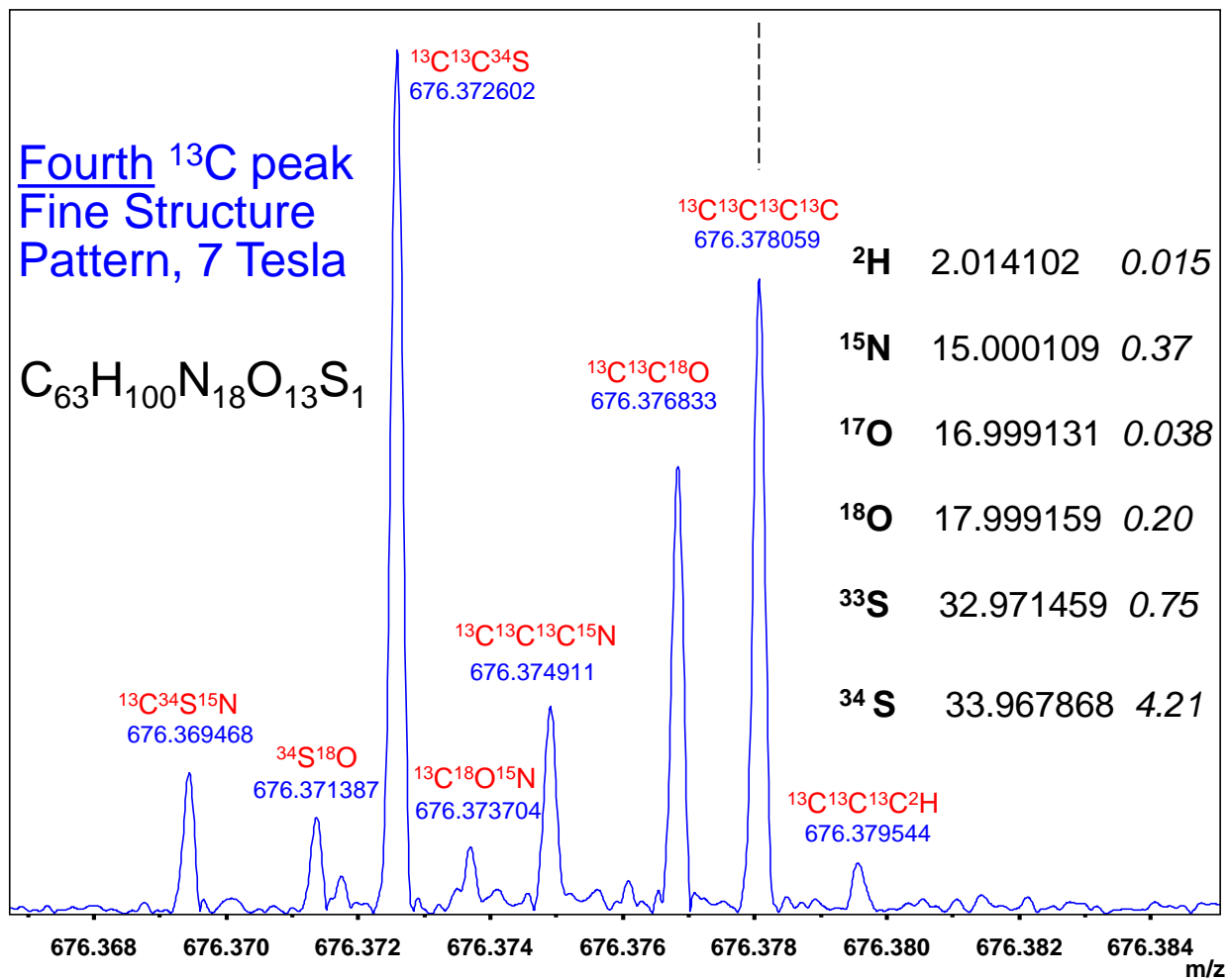
Substance P ($M+2H^+$) on 7 Tesla magnet



Substance P ($M+2H^+$) on 7 Tesla magnet



Substance P (M+ 2H⁺) on 7 Tesla magnet

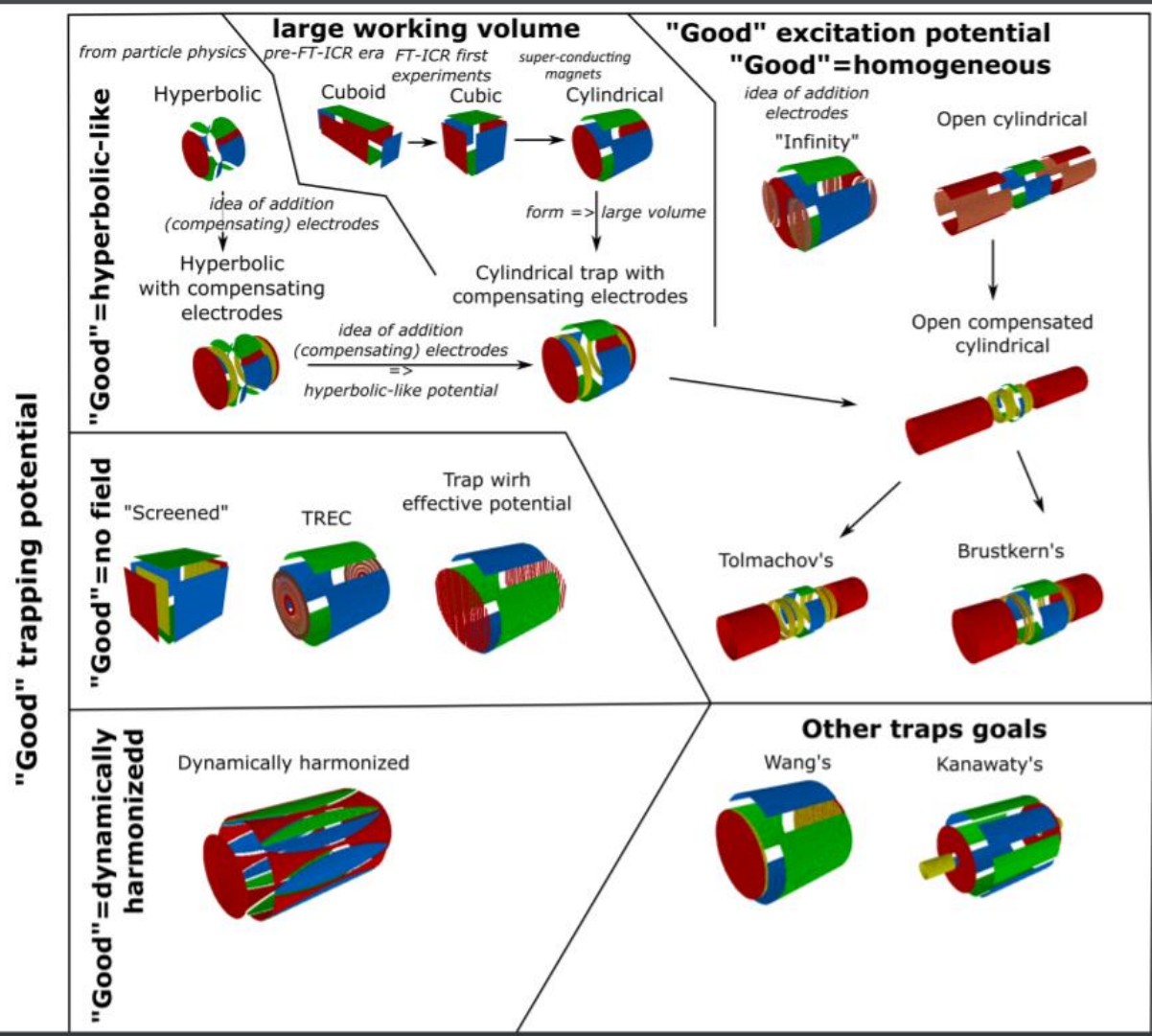


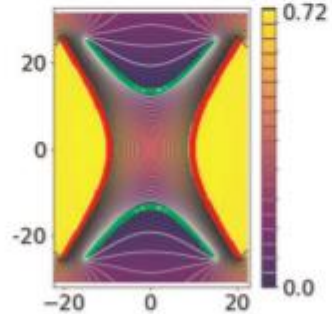
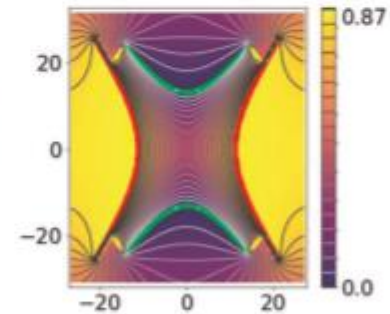
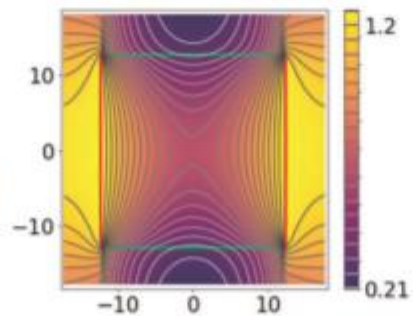
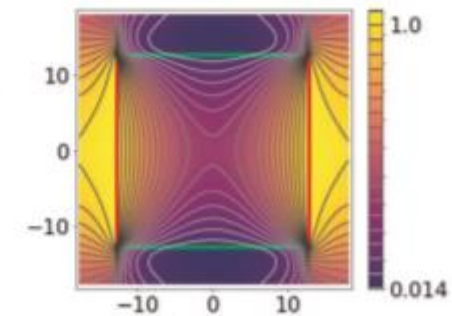
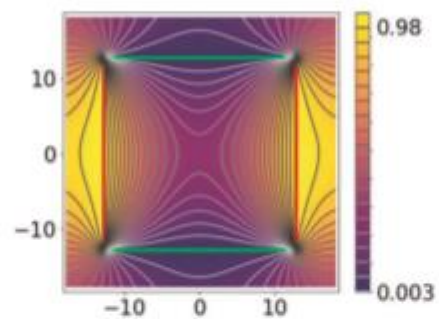
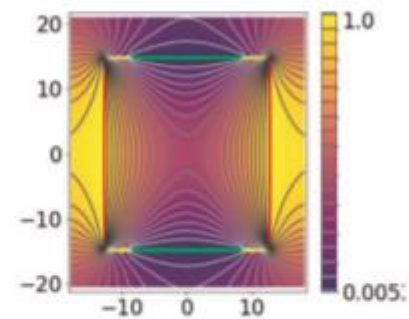
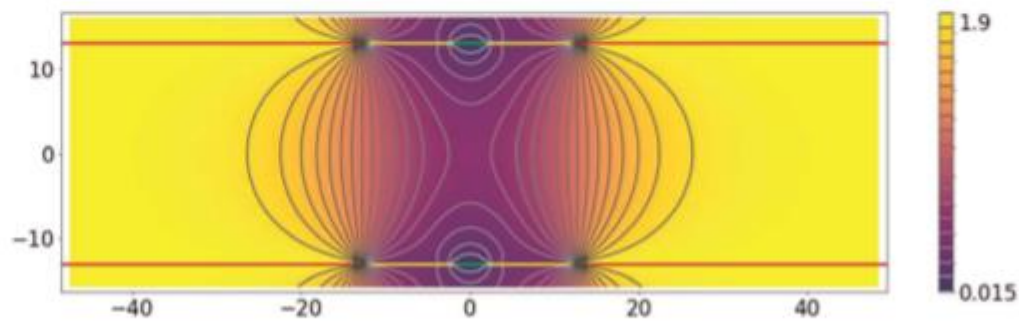
How to evaluate the cell quality?

E.Nikolaev, A.Lioznov

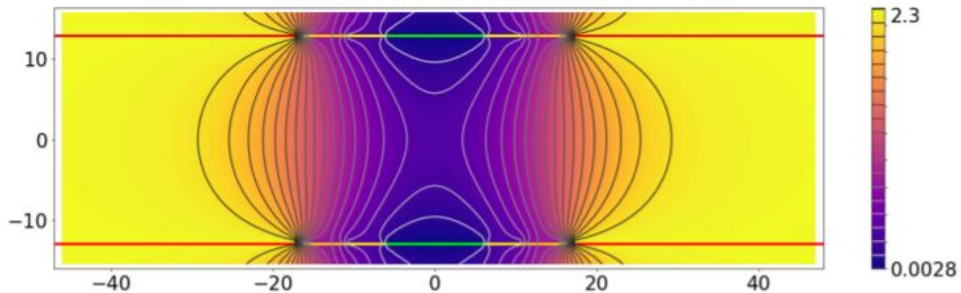
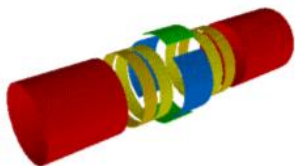
Evaluation of major historical ICR cell
designs using electric field simulations

Mass Spec Rev. 2020;1–22

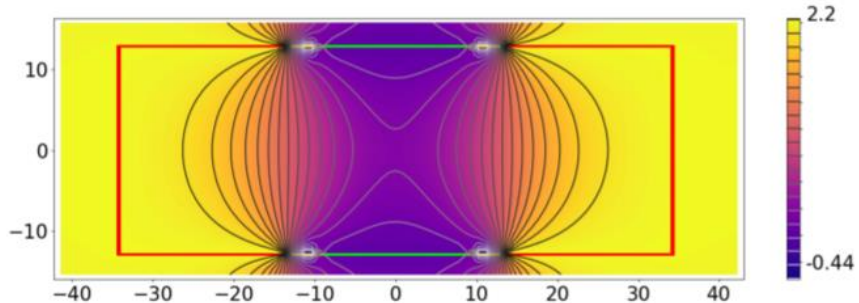
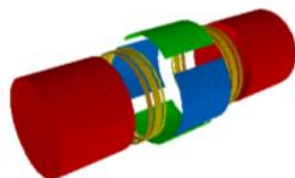


(A)**(B)****(C)****(D)****(E)****(F)****(G)**

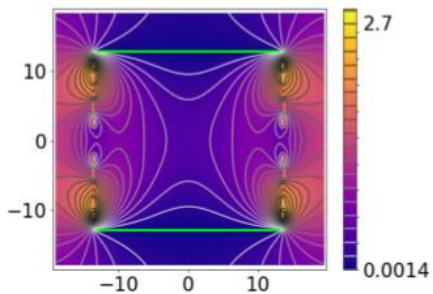
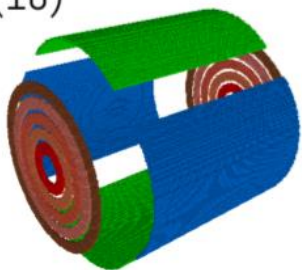
(8)



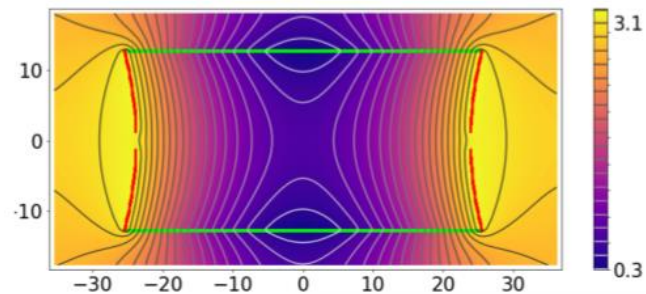
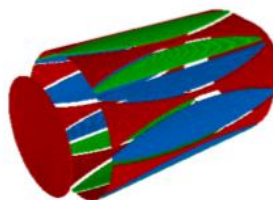
(9)



(10)



(11)



The electric field inside any ion cell may be presented as Spherical Harmonic Decomposition

$$\phi(r, \theta, \varphi) = \sum_{l=0}^{\infty} \sum_{m=-l}^l A_{lm} Y_{lm}(\theta, \varphi) \cdot r^l$$

We take into account only first significant nonzero terms: $A_{20}r^2Y_{20}$, $A_{40}r^4Y_{40}$, $A_{60}r^6Y_{60}$ and present the main mode of rotation ion frequency as

$$\omega_+(\rho, z) = \frac{qB}{2m} + \left[\left(\frac{qB}{2m} \right)^2 - \frac{q}{m} \left\{ A_{20} + A_{40}(48z^2 - 12\rho^2) + \right. \right. \\ \left. \left. + A_{60}(240z^4 - 360z^2\rho^2 + 30\rho^4) \right\} \right]^{1/2}$$

Theory

The time of comet formation can be estimated as

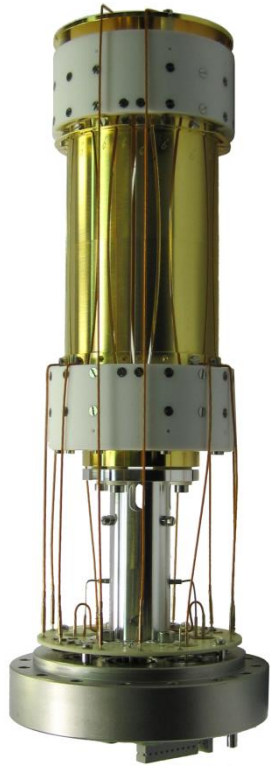
$$T_{\text{comet formation}} = \frac{2\pi}{\max_{r,z} \omega_+ - \min_{r,z} \omega_+}$$



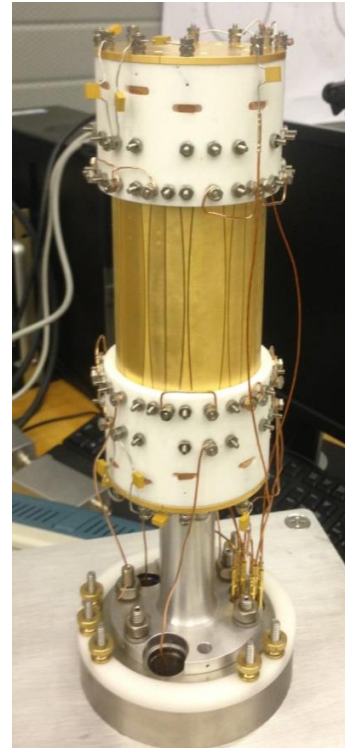
Relative time of synchronized motion of ions in different FT ICR cells

Trap name	A_{20}	A_{40}	A_{60}	t_{comet}, s
Hyperbolic trap	4.3e-01	-2.0e-05	4.5e-06	5.3e+00
Hyperbolic trap with compensating electrodes	4.3e-01	-1.9e-07	2.4e-06	1.8e+01
Cuboid cell	1.9e+00	-2.0e-02	-9.8e-02	3.2e-02
Cubic cell	5.2e-01	4.7e-03	-2.9e-03	2.4e-02
Cylindrical cell	5.3e-01	1.0e-02	-3.6e-03	1.4e-02
Cylindrical trap with compensating electrodes	5.8e-01	2.0e-06	-3.1e-03	3.3e-02
Open cylindrical cell with compensating electrodes	5.3e-01	2.4e-08	-5.9e-04	1.3e-01
Trap with compensating electrodes by Tolmachov	7.6e-01	7.2e-05	-1.3e-03	1.8e-01
Trap with compensating electrodes by Brustkern	5.8e-01	1.6e-02	-3.5e-03	1.3e-02
Dynamically Harmonized Cell or Paracell	1.6e+00	-4.4e-05	2.6e-04	7.0e+00

Dynamically harmonized cells are providing the highest resolving power



Bruker's cell



NHMFL cell

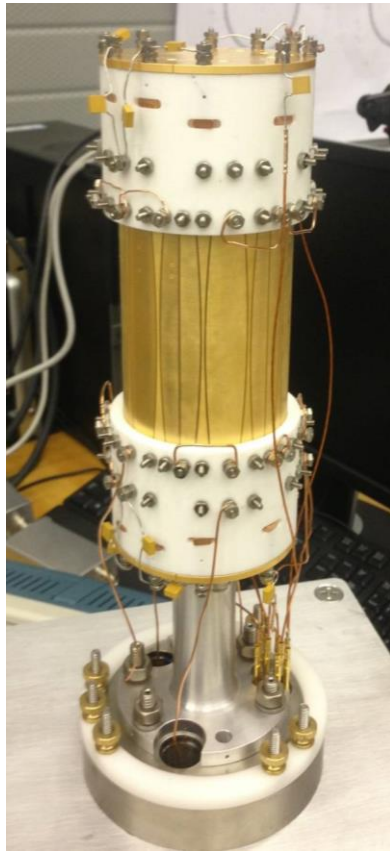
In 2015 we had Milestone events in FT ICR mass spectrometry

Launching two 21 tesla FT ICR mass Spectrometers

In National High Magnetic Field Laboratory
NHMFL (Tallahassee Florida)

and in Pacific North West National Laboratory
PNNL (Richland, Washington)





From Alan Marshall 10th NA FTMS 21 T talk

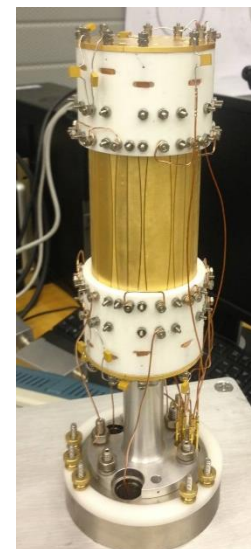
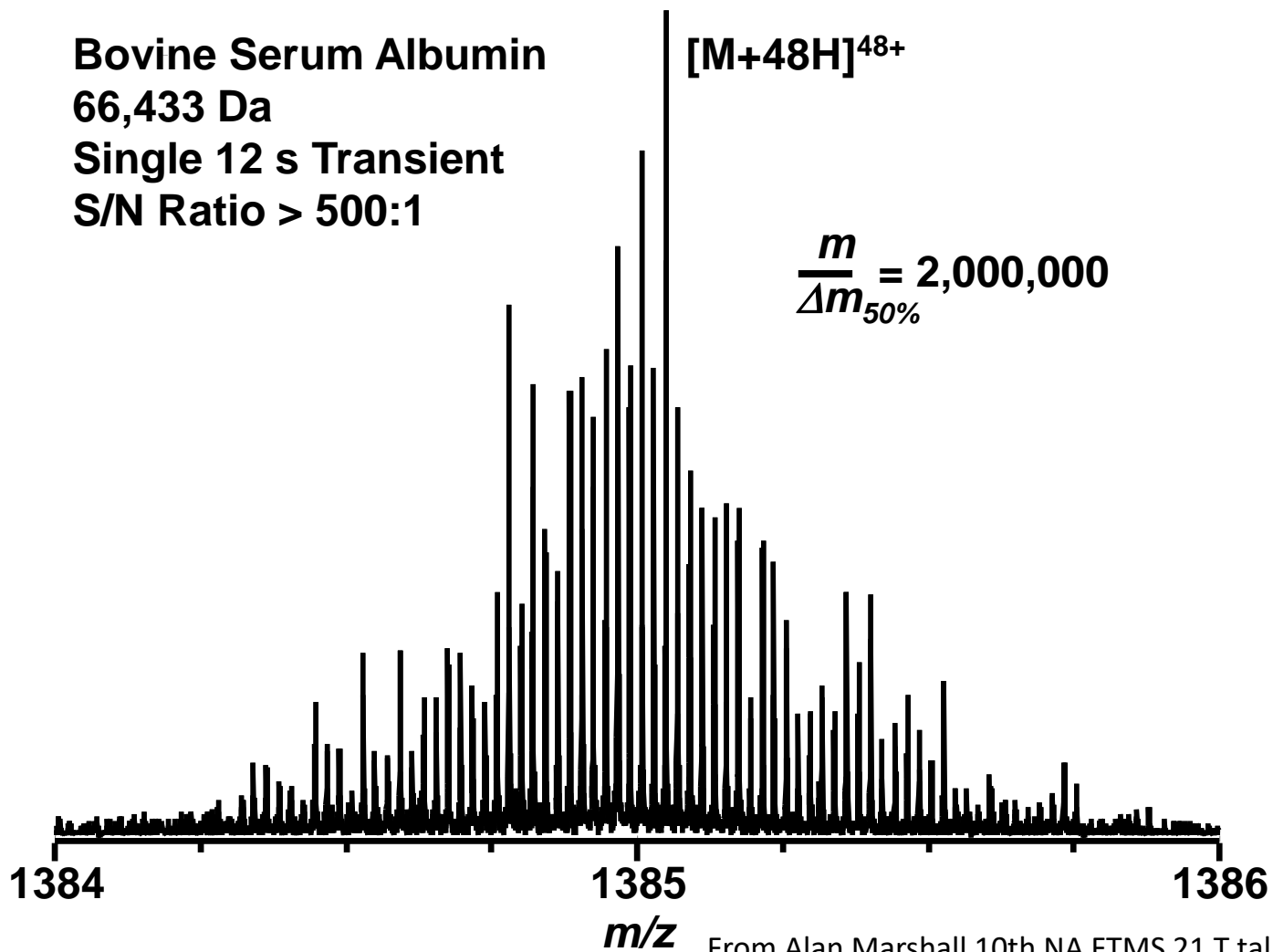


Solarix R&D

Bovine Serum Albumin
66,433 Da
Single 12 s Transient
S/N Ratio > 500:1

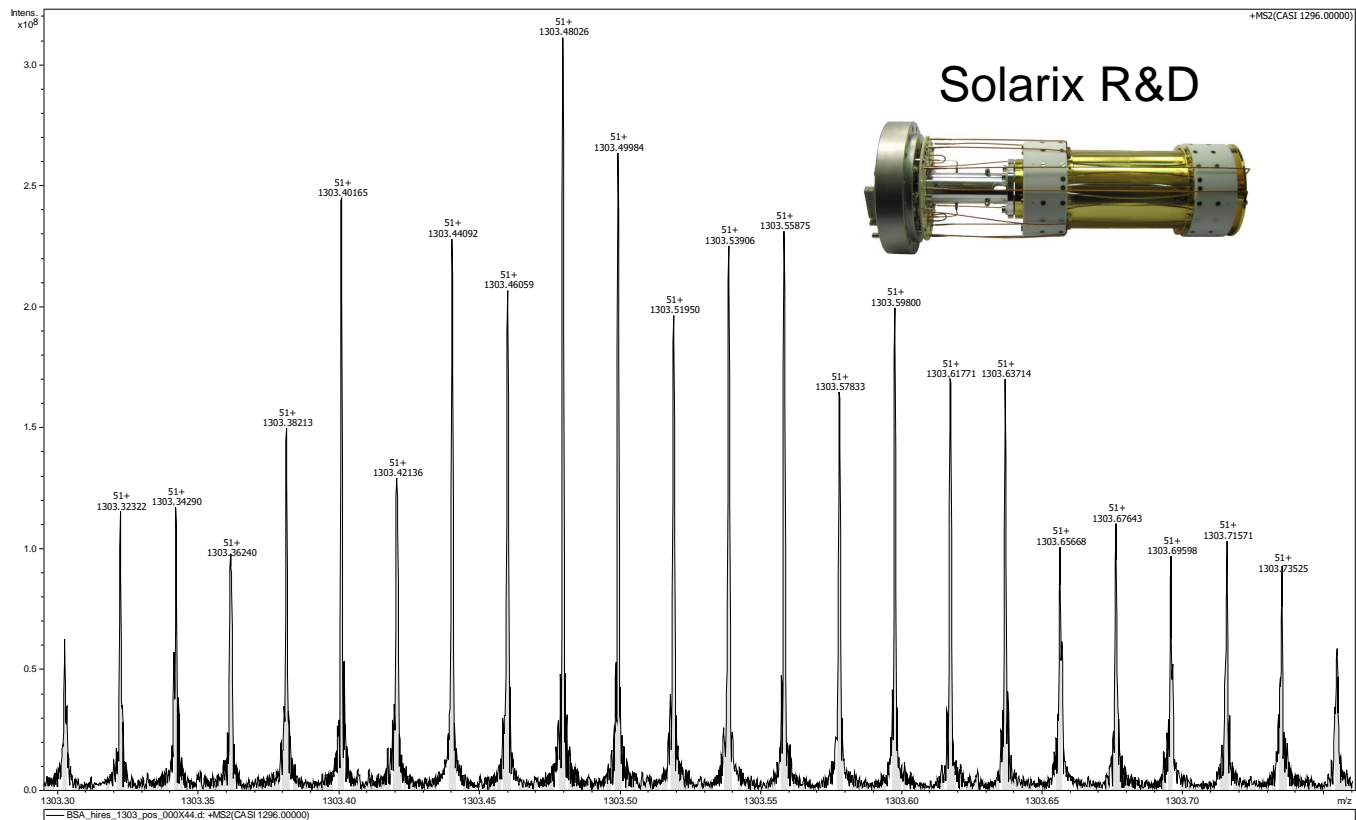
$[M+48H]^{48+}$

$$\frac{m}{\Delta m_{50\%}} = 2,000,000$$



From Alan Marshall 10th NA FTMS 21 T talk

7T R&D, BSA, 51+, RP 1,700,000 28 s transient

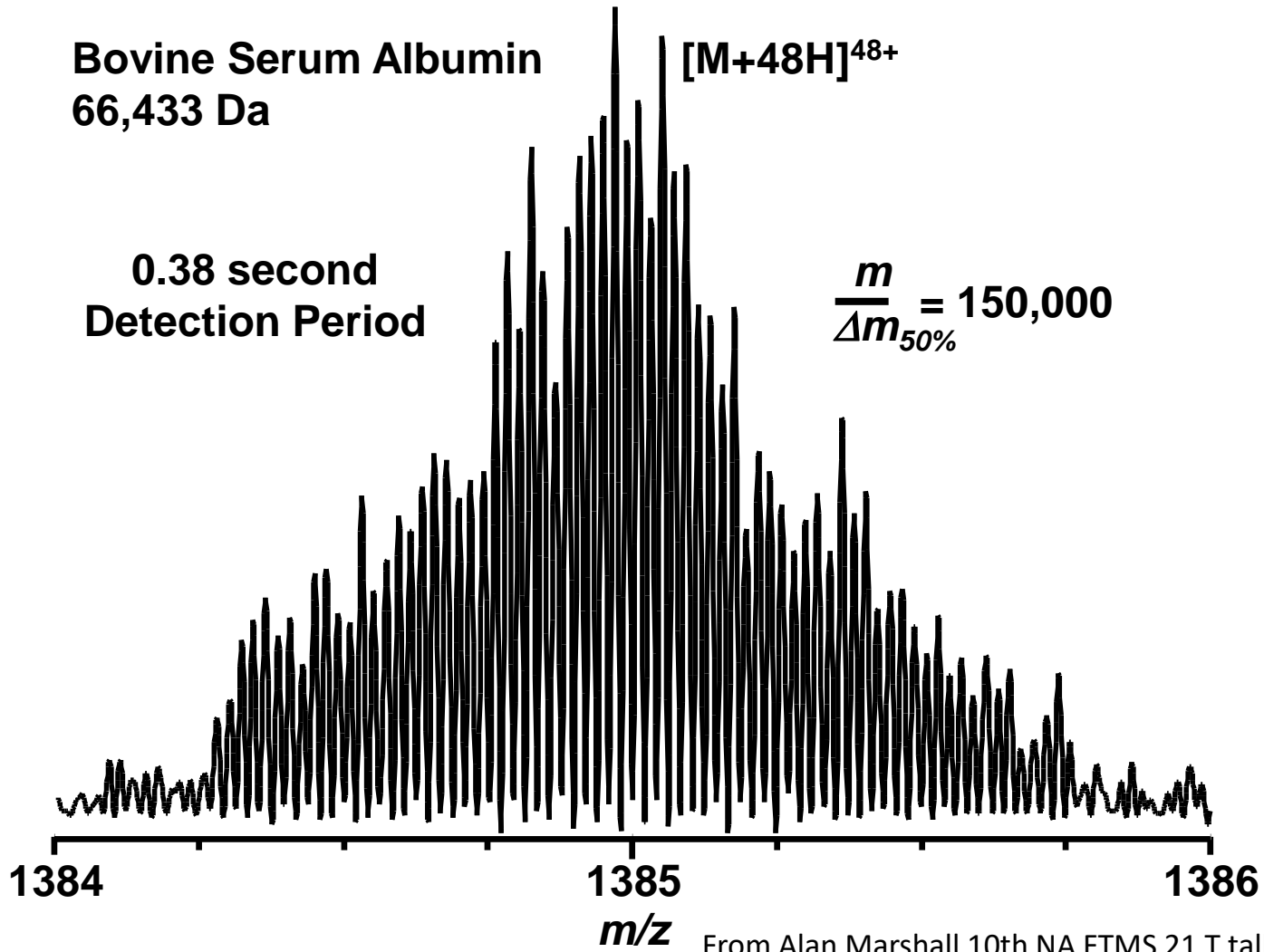


Bovine Serum Albumin
66,433 Da

[M+48H]⁴⁸⁺

0.38 second
Detection Period

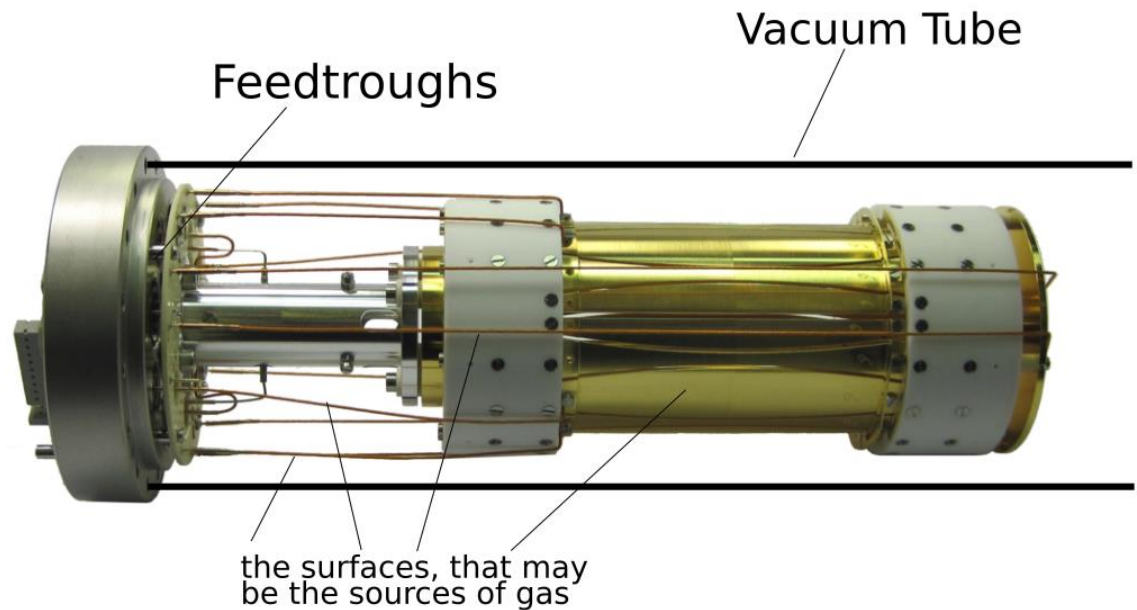
$$\frac{m}{\Delta m_{50\%}} = 150,000$$



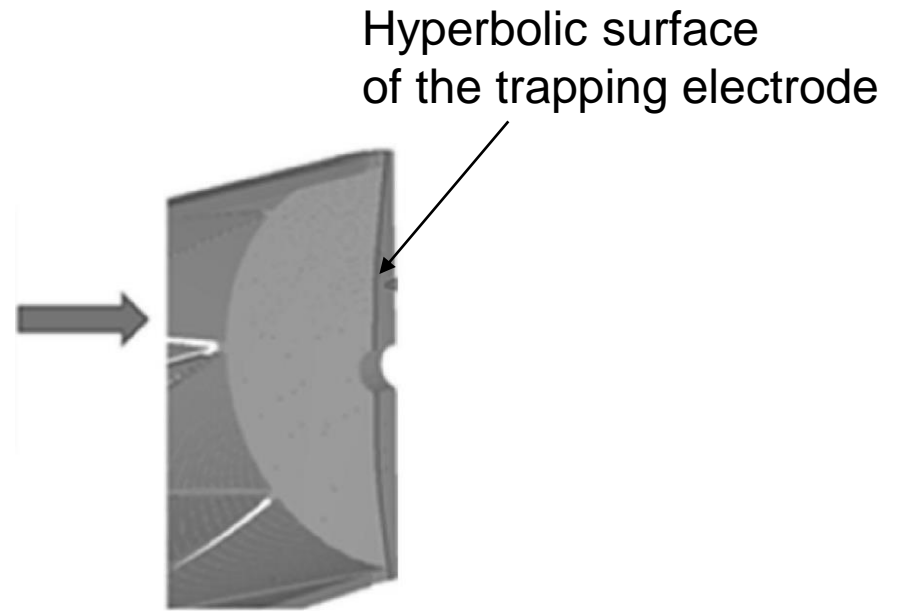
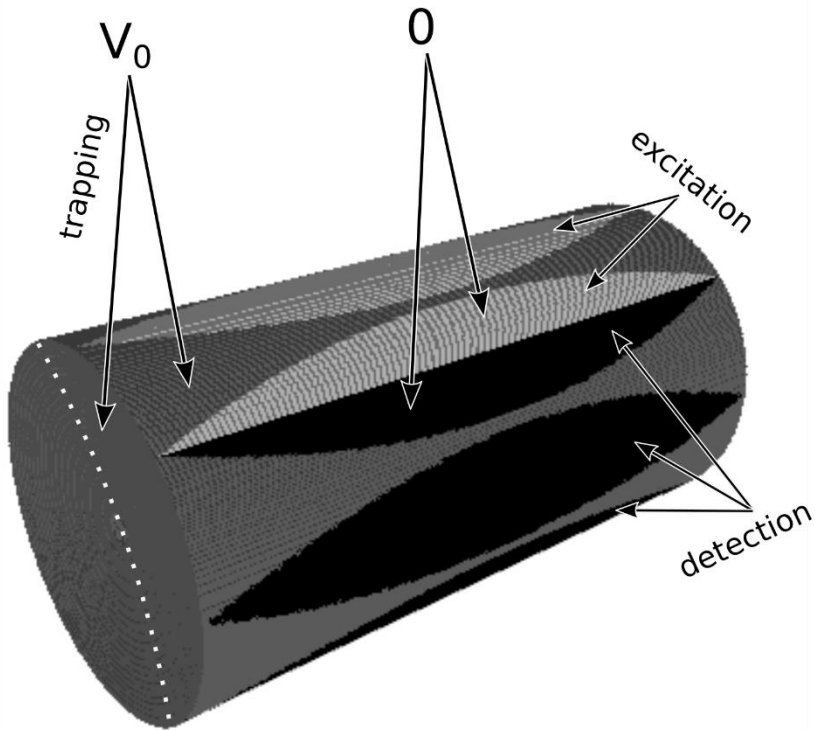
From Alan Marshall 10th NA FTMS 21 T talk

Highly developed surface with large «vacuum memory»

- Long pumping time;
- Not highest available final vacuum;
- Potential leakage in feedthroughs.
- Closed volume of the cell

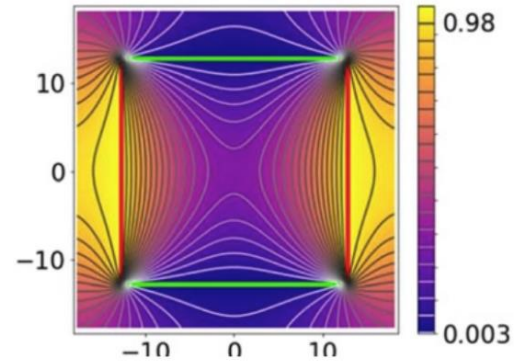
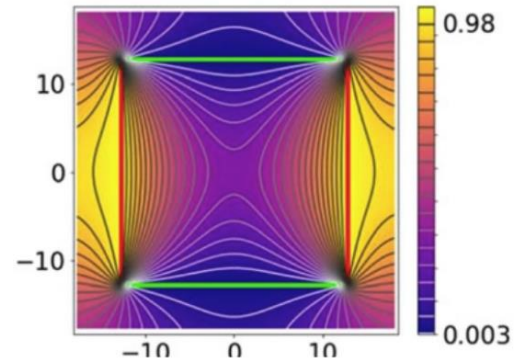
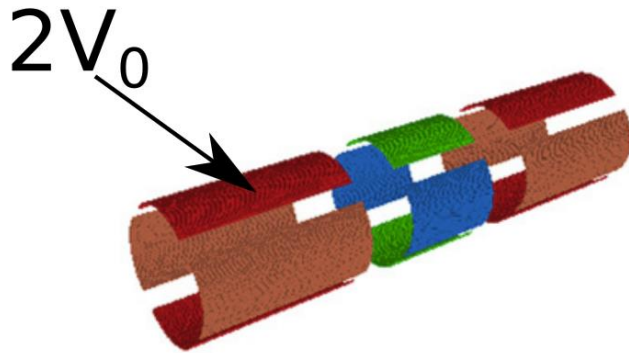
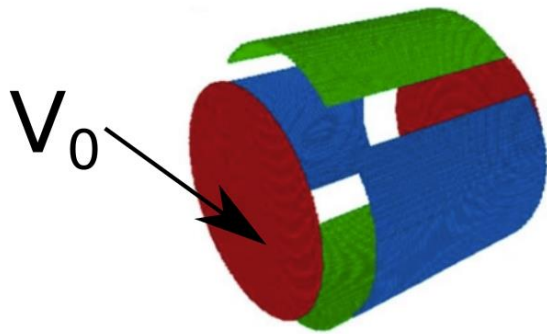


«Standard» (closed) DHC

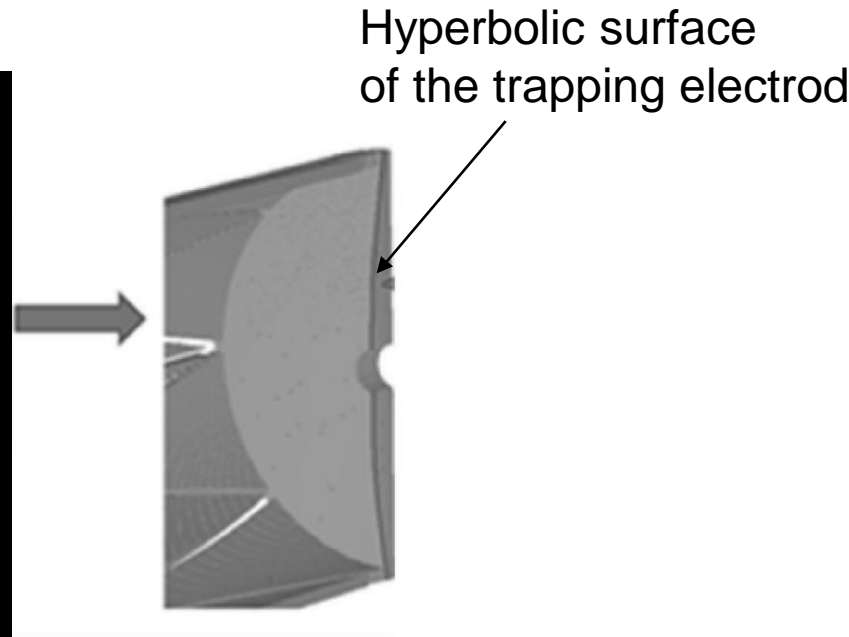
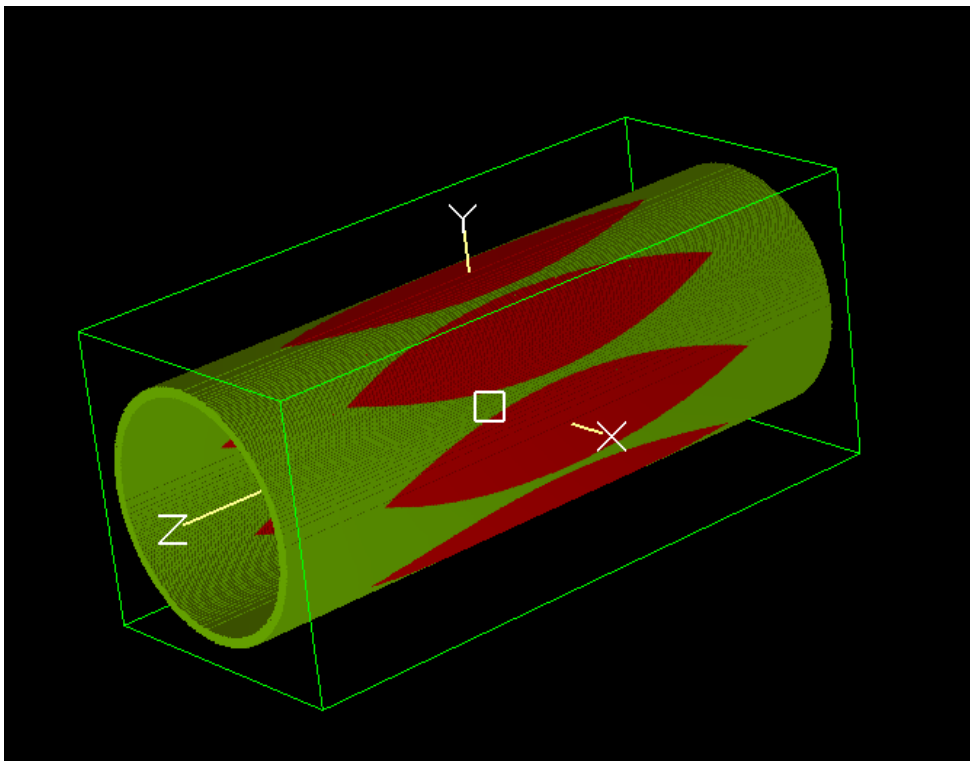


How to “open” dynamically harmonized cell?

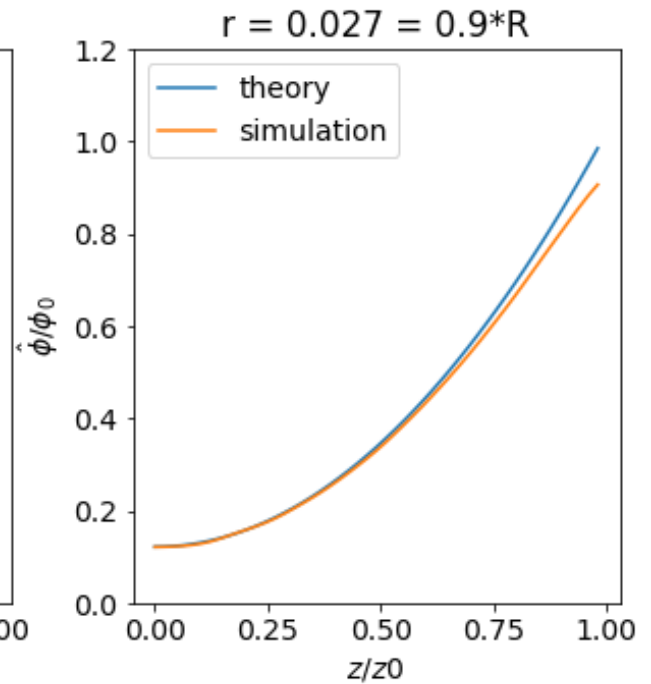
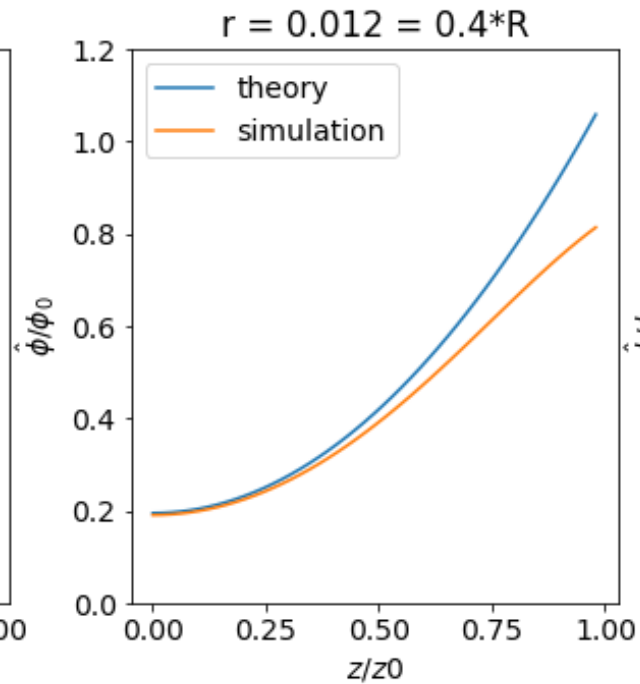
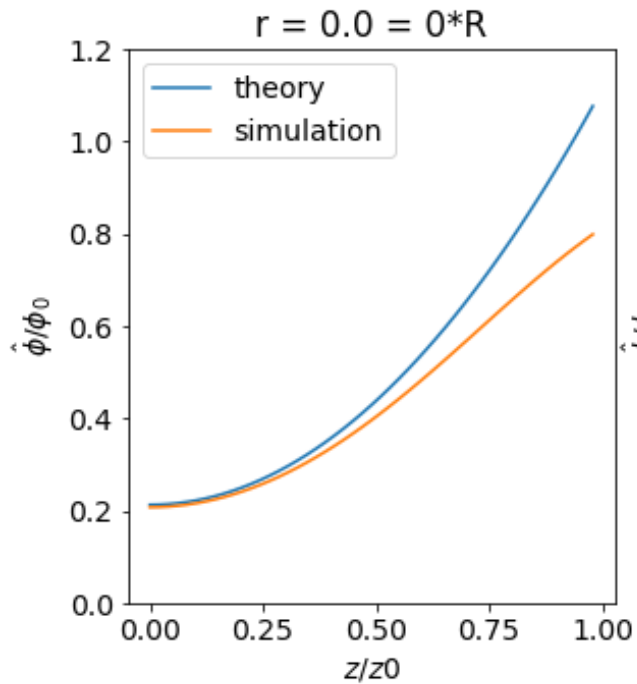
It is easy to «Open» a simple Cylindrical Cell
Substituting flat trapping electrodes by cylinders



If we substitute in DHC the hyperbolic shape trapping electrodes by cylinders...

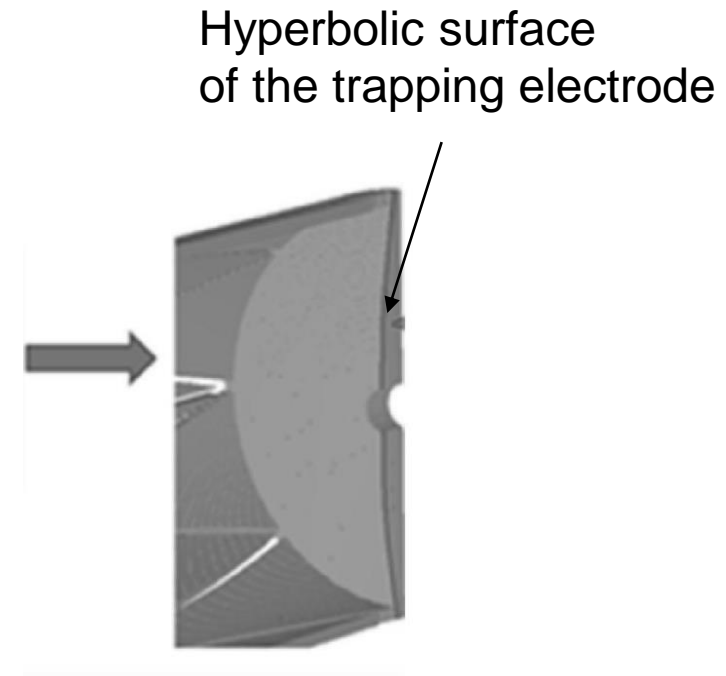
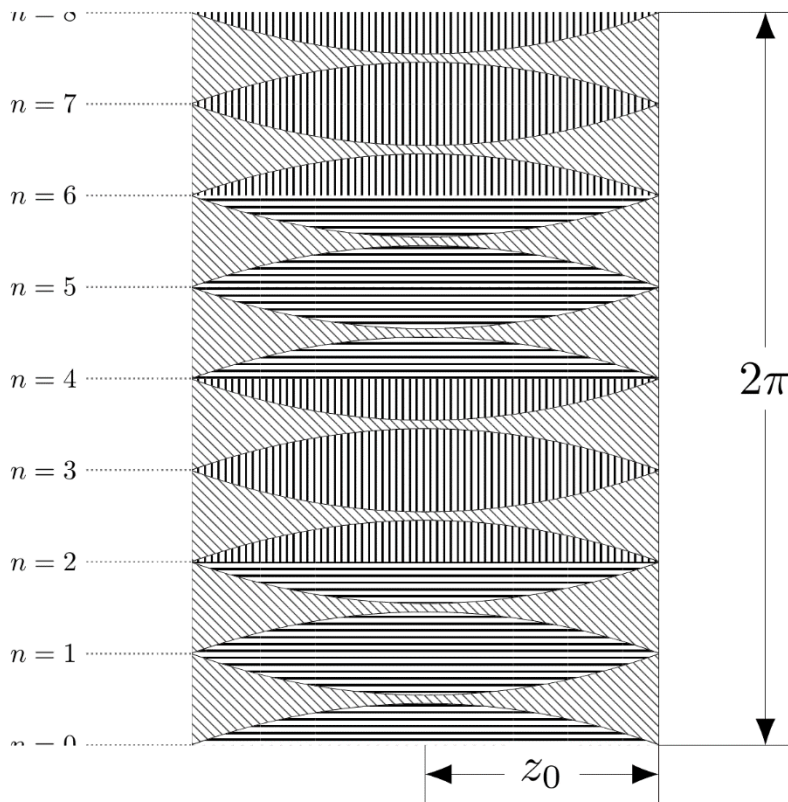


We will not obtain hyperbolic field inside the cell!

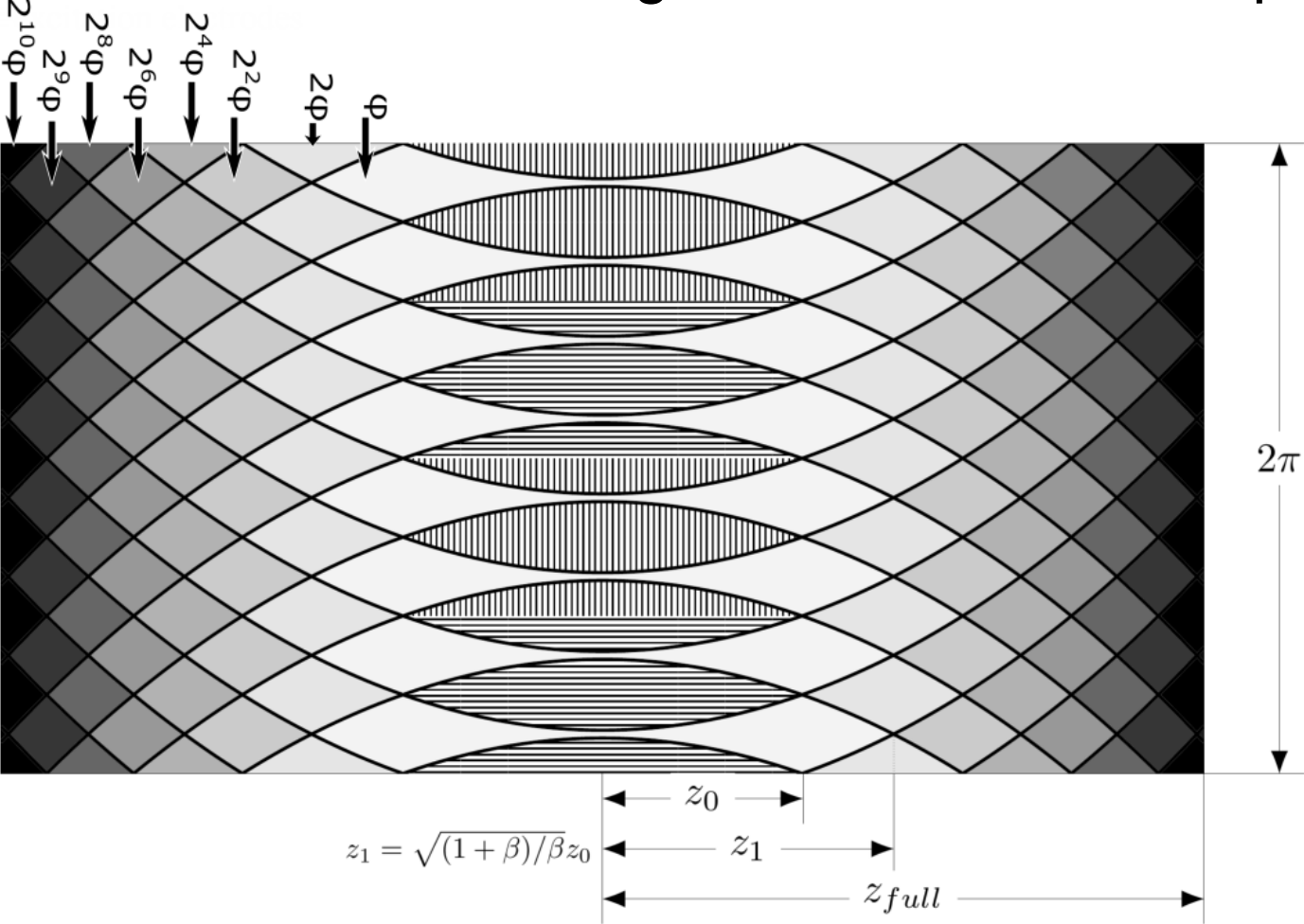


The 2D-unrolled electrode configuration for a closed DHC

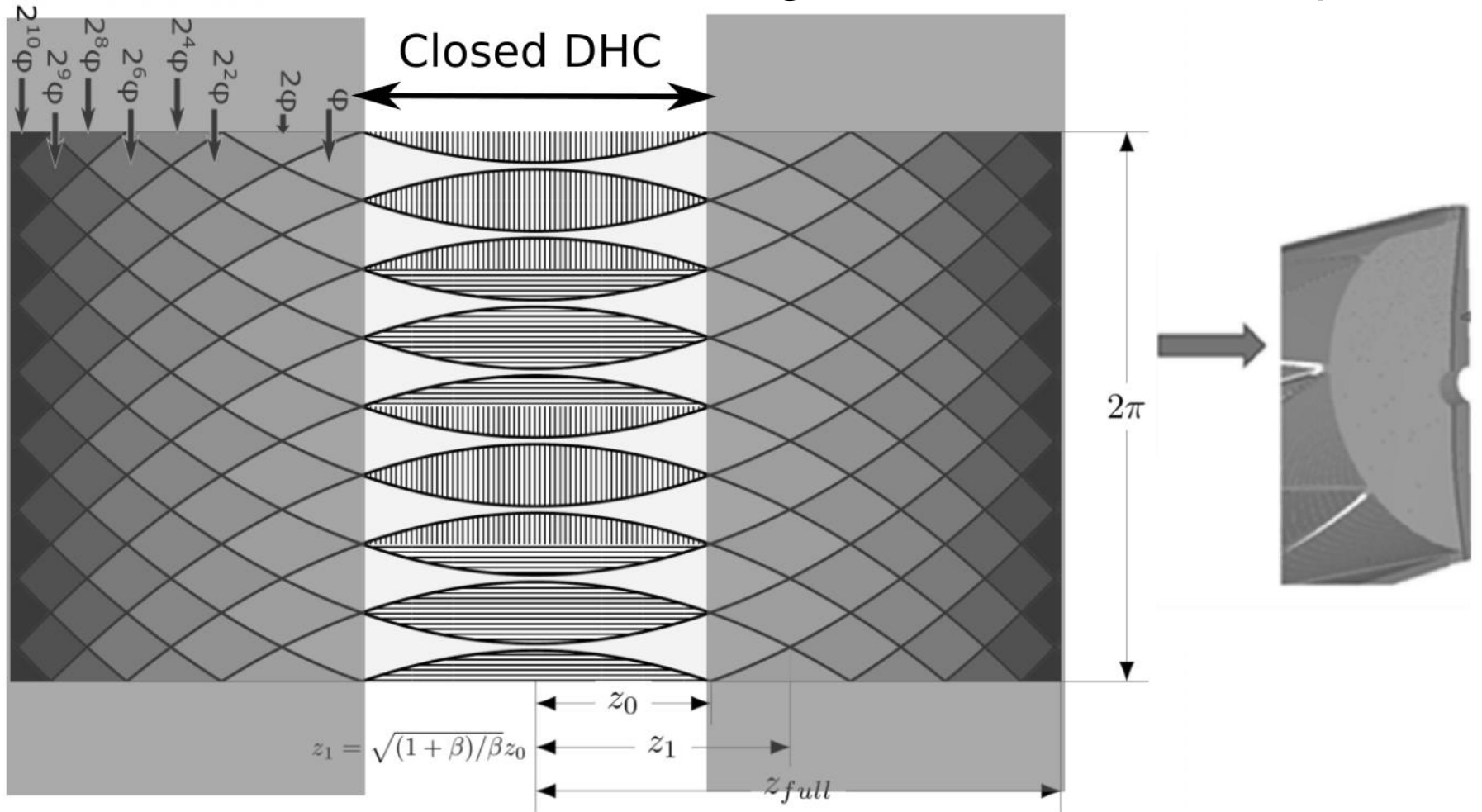
▯▯▯ detection electrodes
▯▯▯ excitation electrodes
▯▯▯ trapping electrodes



The 2D-unrolled electrode configuration for an ideal open DHC



The 2D-unrolled electrode configuration for an ideal open DHC



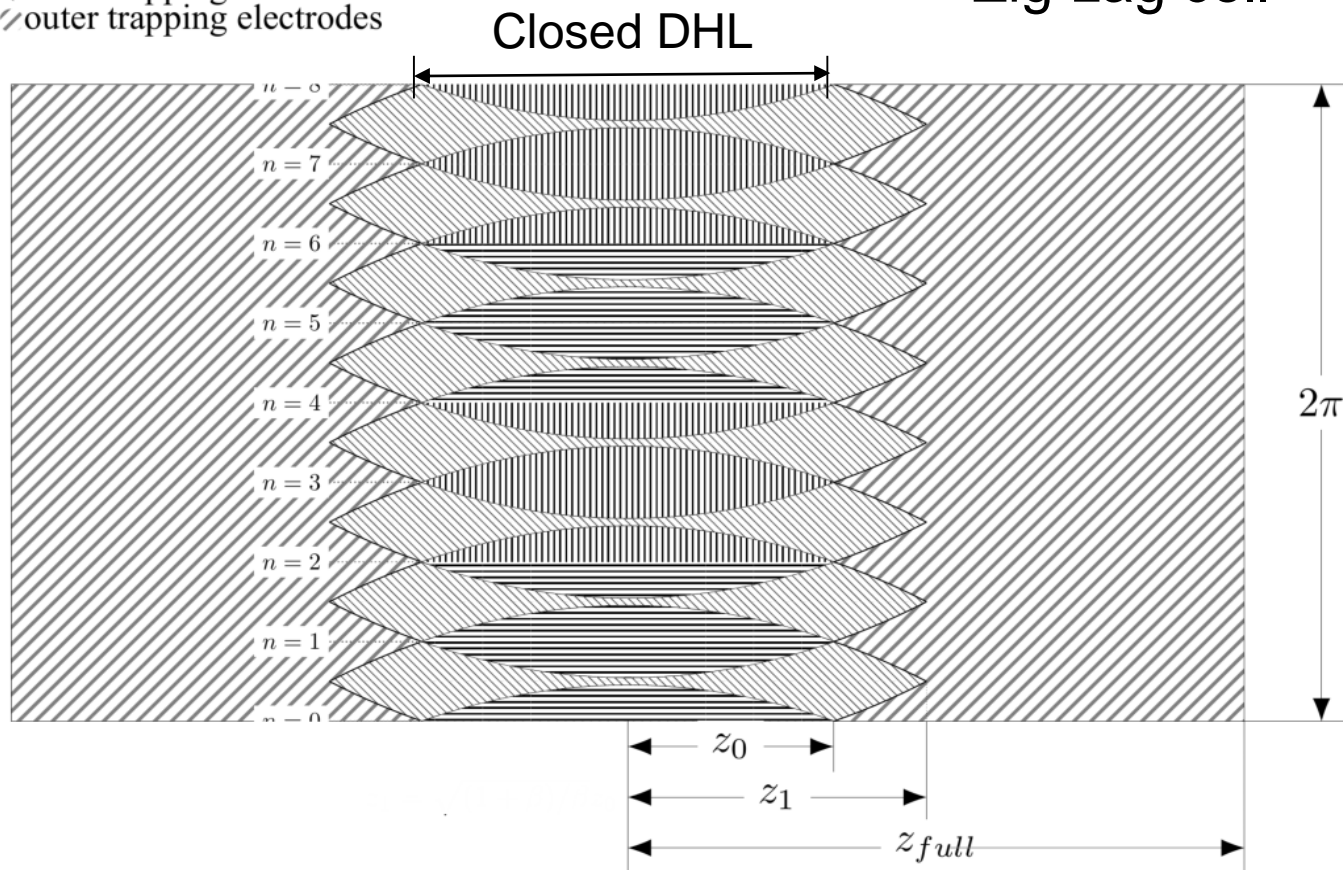
Reducing number of electrodes

- The set of electrodes shown above creates the needed field, but it is hard to build it.
- We have shown that the electrodes located far from the trap center has low effect on the field inside the working volume of the cell. Thus, we can merge all these electrodes into one.

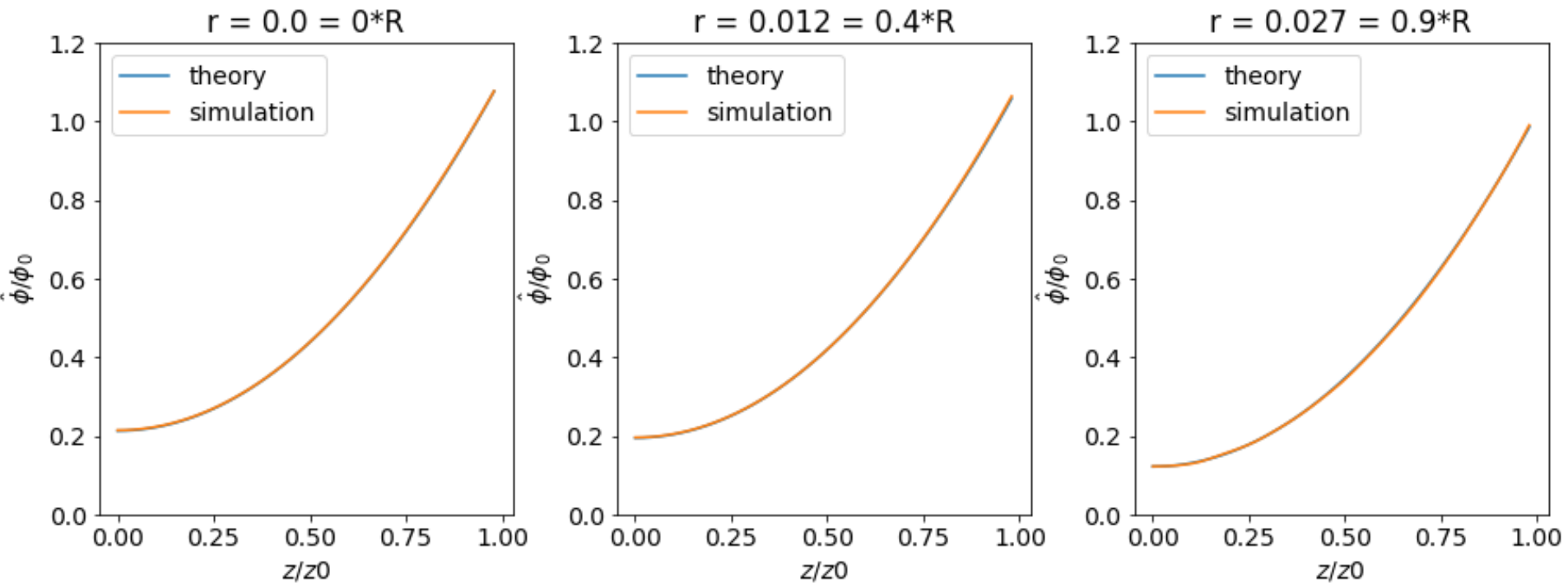
The 2D-unrolled electrode configuration of realizable open DHC

- ▨ detection electrodes
- ≡ excitation electrodes
- ▨ inner trapping electrodes
- ▨ outer trapping electrodes

Zig-zag cell



The ideal and simulated distribution of the electric potential inside the open DHC



Z-component of electric field at different distance (r) from the cell axis

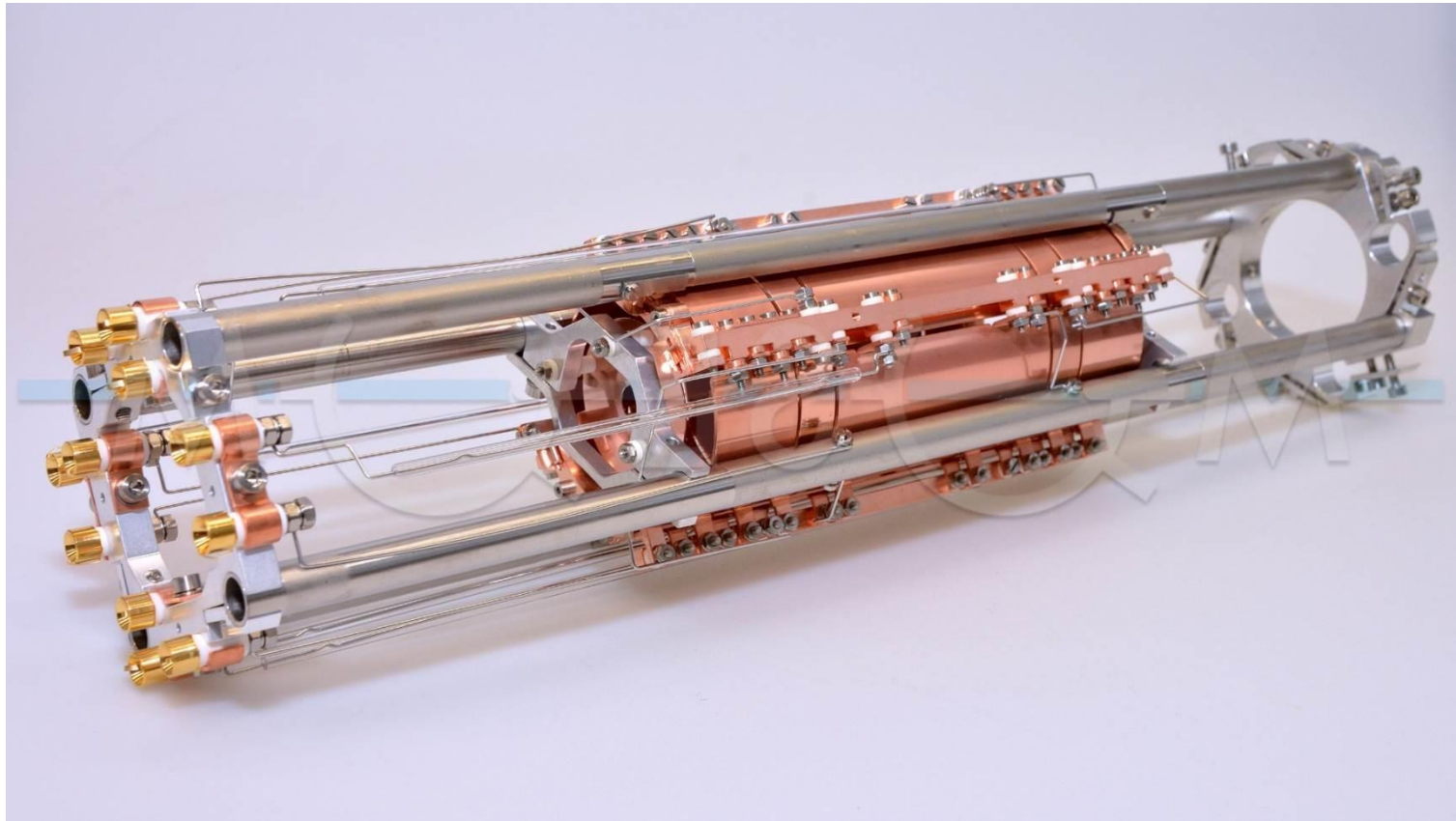
The deviations from the ideal field

The electric field distribution inside the Open Dynamically Harmonized «Zig-Zag» Cell is not absolutely ideal. But the field deviation is below numerical errors of simulations.

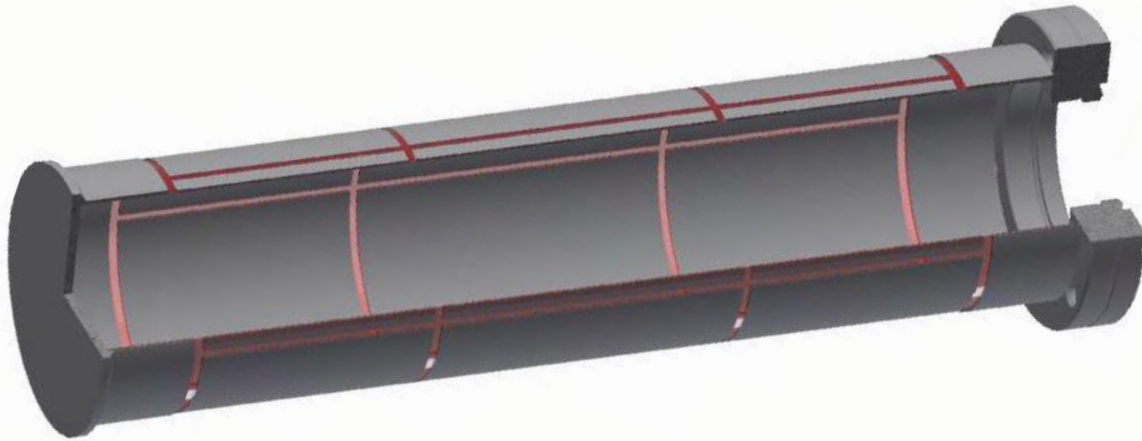
▪

Tired of cells...

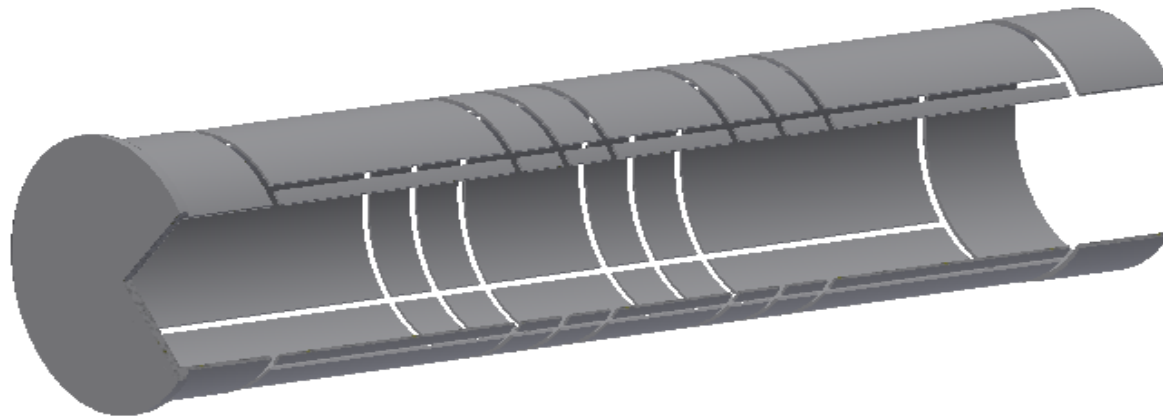
Is it possible to get rid of the cell as a **separate** element of FT ICR mass spectrometer?



Trap walls are the walls of the vacuum chamber:
Different geometries could be implemented



Open cylindrical cell



Open compensated cylindrical cell

Advantages of vacuum system wall imbedded cell

No feedthroughs (can apply voltages from outside)

No wires inside

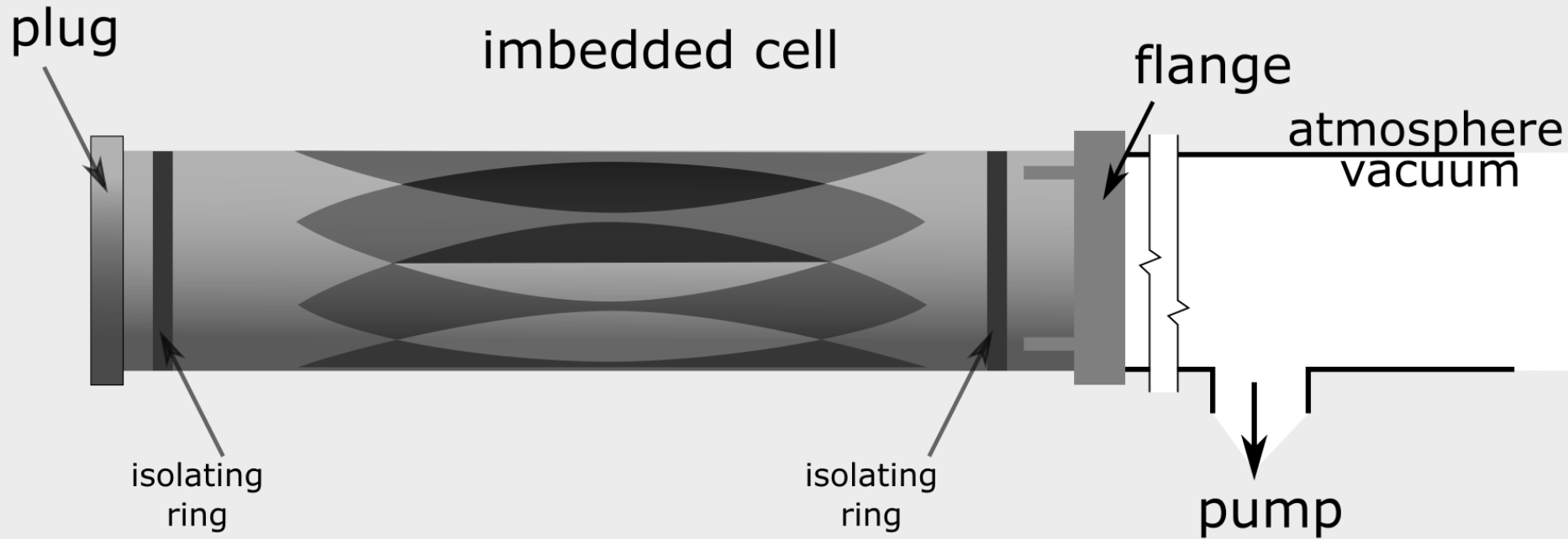
Extremely low surface (only surfaces of the electrodes)

Easy to align to magnetic field

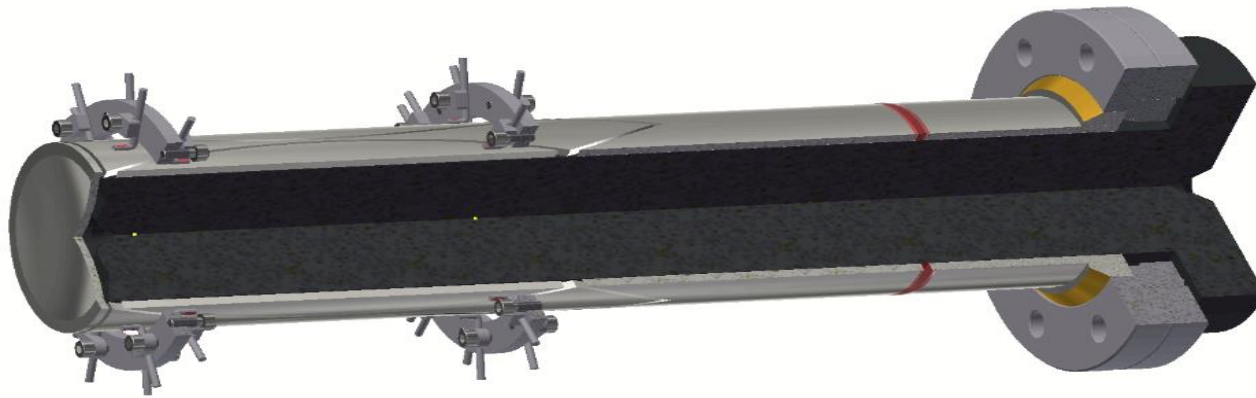
Low diameter of room temperature bore magnet could be used

Is it possible to incorporate an open DHC into the vacuum tube wall?

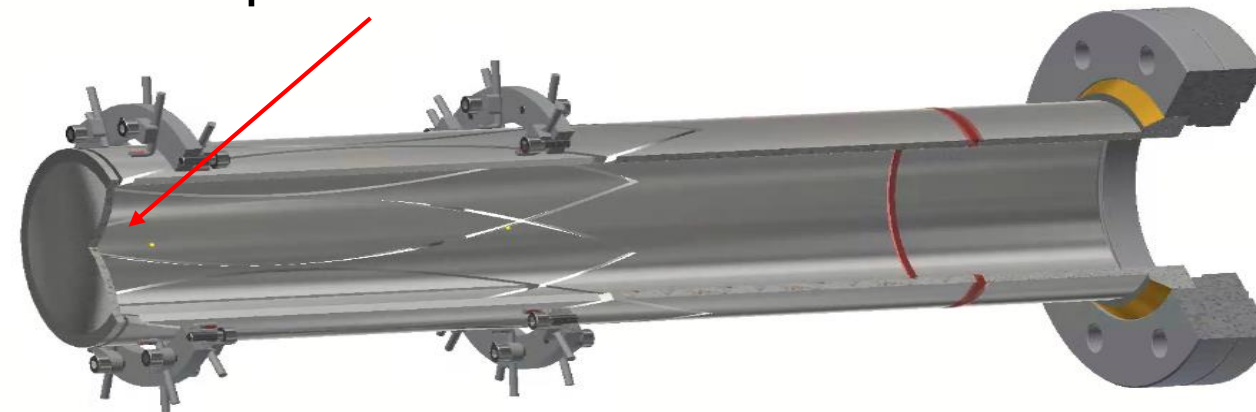
New Open DHC



The open dynamically harmonized cell
could be made from a single cylinder



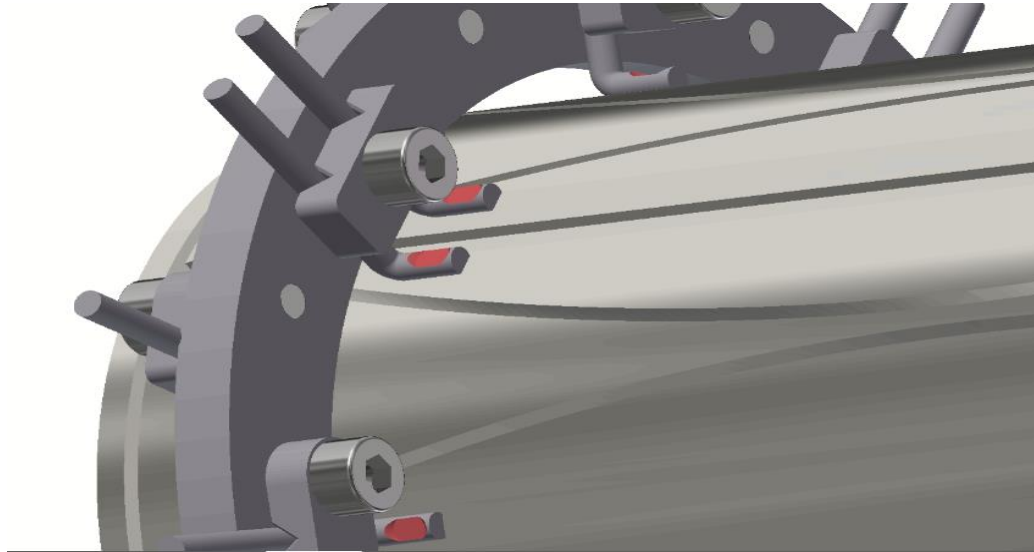
Spherical surface



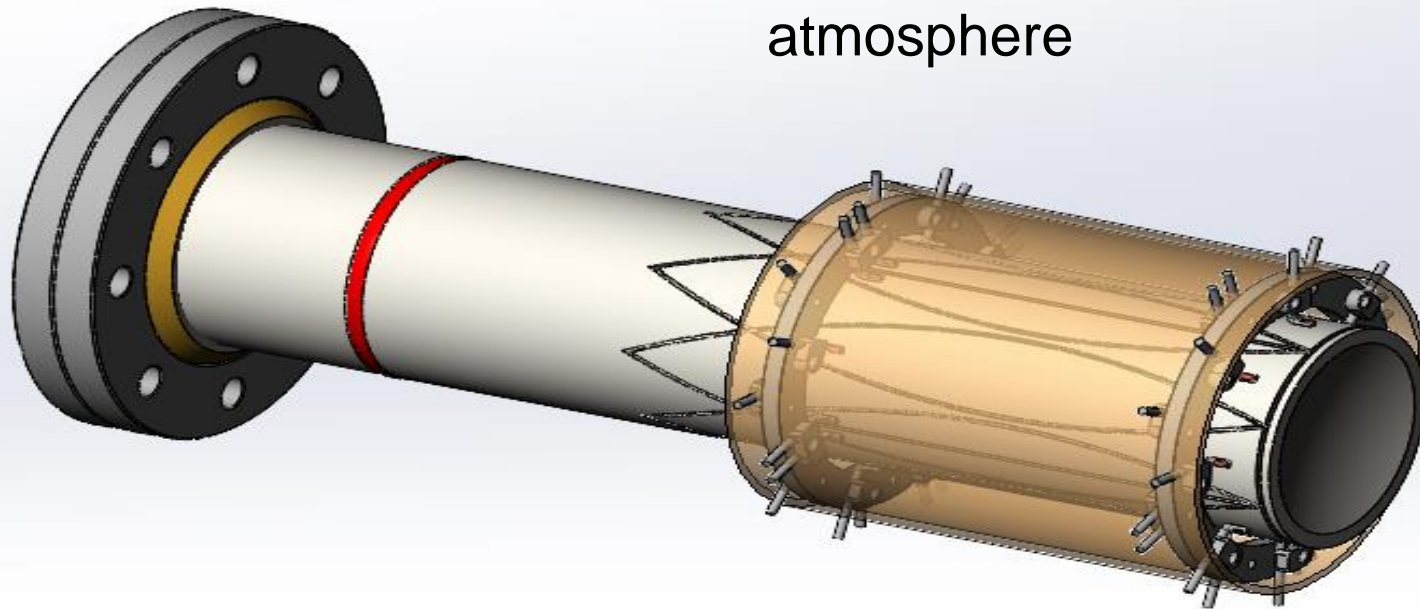
The cell opened from one side

- Fabrication of ICR trap-vacuum chamber consists of the following steps
- 1) A titanium adapter for a CF63 flange is welded to a 62 mm diameter BT1-0 titanium tube
- 2) In certain places on the tube by means of contact welding, pieces of 2mm BT1-00cb titanium wire are welded
- 3) The pipe is cut into individual electrodes
- 4) Temporary fasteners are installed to hold the electrodes
- 5) A graphite insert is placed inside the pipe, and then the cut points are filled with a special ceramic powder. Then the billet is annealed in the furnace.

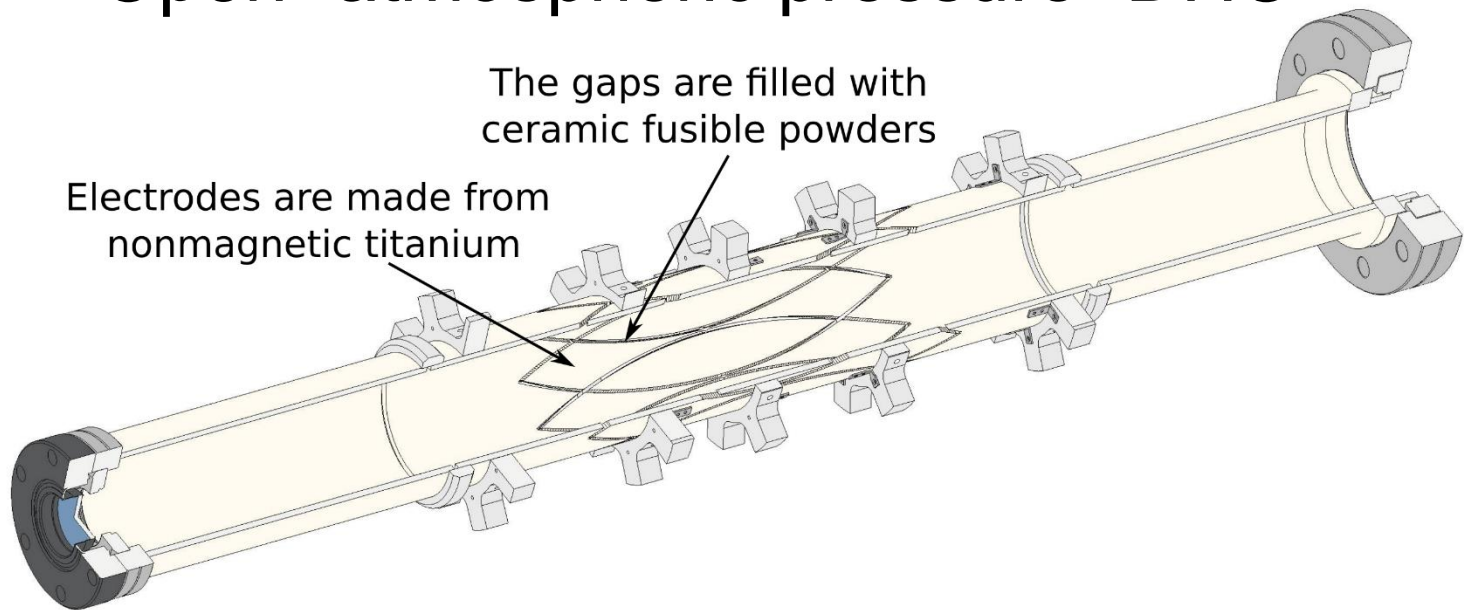
The voltage to the cell electrodes could be applied from outside



Amplifier could be installed directly on ICR trap using Flexible PCBs



Open “atmospheric pressure” DHC



The titanium and the ceramics have the similar coefficient of thermal expansion, which allows annealing a vacuum system

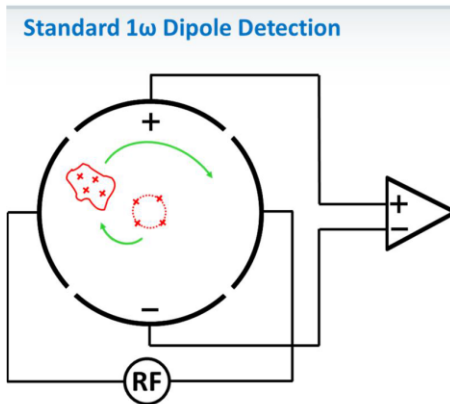
Detection at multiple frequencies

Detection with more than two electrodes

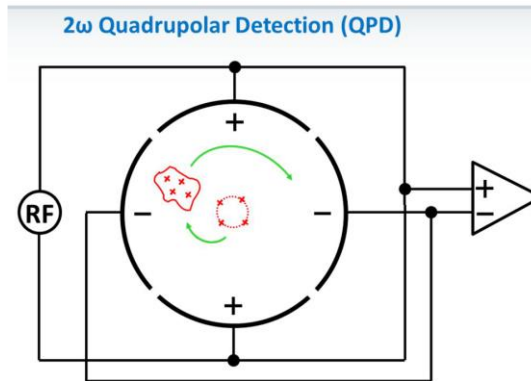
4 electrode FT ICR cell dipolar detection

4 electrode FT ICR cell quadrupolar detection

2N electrode FT ICR cell multipolar detection

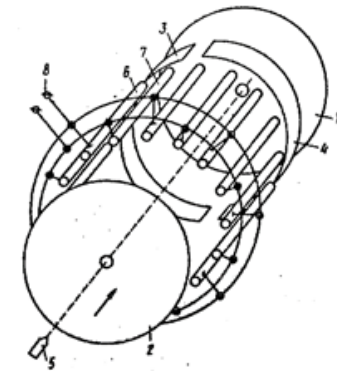


$$\omega_{\text{signal}} = \omega_{\text{cyclotron}}$$



$$\omega_{\text{signal}} = 2 * \omega_{\text{cyclotron}}$$

Double resolution
or double speed



$$\omega_{\text{signal}} = N * \omega_{\text{cyclotron}}$$

N times higher resolution
or speed

Detection on multiplied frequencies and on harmonics

$$R = \omega / \Delta\omega$$

$$\Delta\omega \sim 1/T$$

T is signal duration

$$\text{If } \omega' = n * \omega, \quad R' = n * R$$



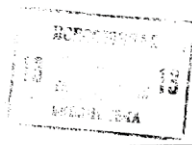
СОЮЗ СОВЕТСКИХ
СОЦИАЛИСТИЧЕСКИХ
РЕСПУБЛИК

(19) SU (11) 1307492 A1

(SD) 4 Н 01 J 49/38

ГОСУДАРСТВЕННЫЙ КОМИТЕТ СССР
ПО ДЕЛАМ ИЗОБРЕТЕНИЙ И ОТКРЫТИЙ

ОПИСАНИЕ ИЗОБРЕТЕНИЯ К АВТОРСКОМУ СВИДЕТЕЛЬСТВУ



(21) 3922733/24-21
(22) 05.07.85
(46) 30.04.87. Бюл. № 16
(71) Институт химической физики АН СССР

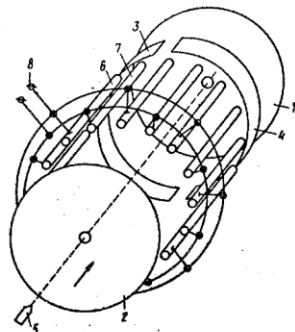
(72) Г.Н.Николаев, М.В.Горшков,
А.В.Мордехай и В.Л.Тальрозе
(53) 621.384.6 (088.8)
(56) Леман Т., Берси М. Спектрометрия
ионного циклотронного резонанса. М.:
Мир, 1980, с.13-41.

Патент США № 3742212, кл.250-291,
1973.

(54) ИОННО-ЦИКЛОТРОННЫЙ РЕЗОНАНСНЫЙ
МАСС-СПЕКТРОМЕТР

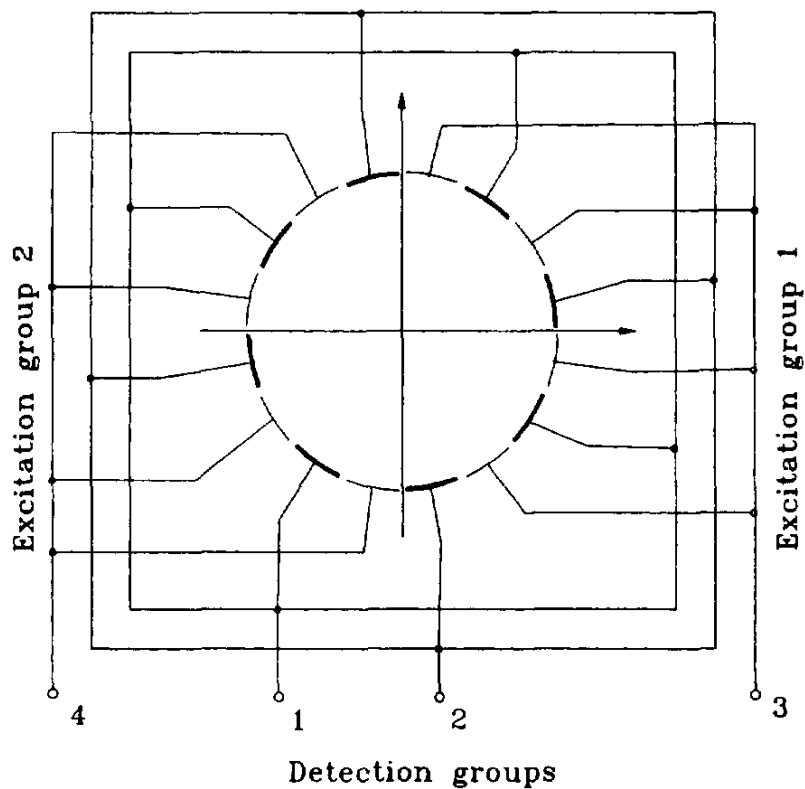
(57) Изобретение относится к области
ионноплазменной техники. Ионно-цикло-
тронный резонансный масс-спектрометр
(ИЦМС) содержит пластины 1, 2 удержи-
вания ионов (И), расположенные по тор-

цам перпендикулярно оси ИЦМС, электроды (Э) 3, 4 возбуждения И в виде полуцилиндров, установленных в одной плоскости торцами друг к другу, детектор 5 И и электронную систему управления и обработки данных. Выполнение детектора 5 И в виде четного числа Э 6, 7, размещенных по окружности с центром на оси ИЦМС и гальванически соединенных в две группы таким образом, что два соседних Э расположены в разных группах, позволяет расширить диапазон исследуемых масс и увеличить разрешающую способность ИЦМС за счет детектирования сигнала на частоте, кратной циклотронной. Изобретение позволяет исследовать ионно-молекулярные реакции в газовой фазе, особенно И тяжелые биологических молекул. 1 ил.



Soviet Union patent
Priority 05.07.1985
Nikolaev, Gorshkov, Mordehai,
Talroze
Multi-electrode detection FT
ICR cell

(19) SU (11) 1307492 A1



E.N. Nikolaev, M.V. Gorshkov, A.V. Mordehai and V.L. Talrose, *Rapid Communications in Mass Spectrometry*, 4 (1990) 144.

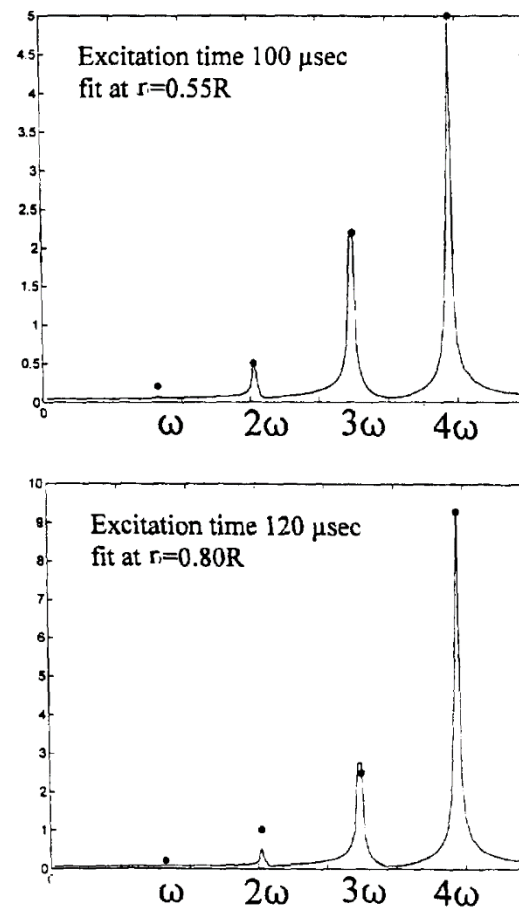
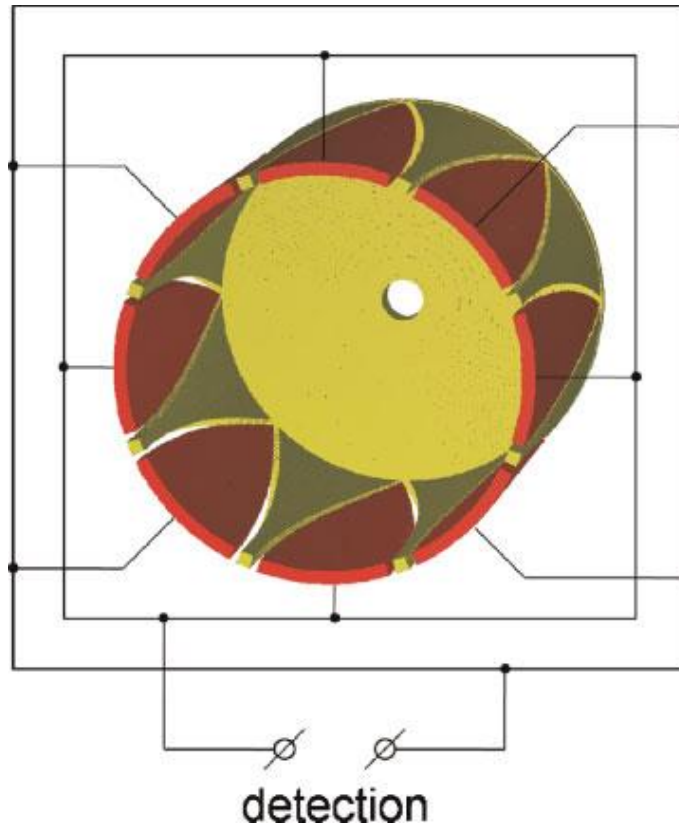
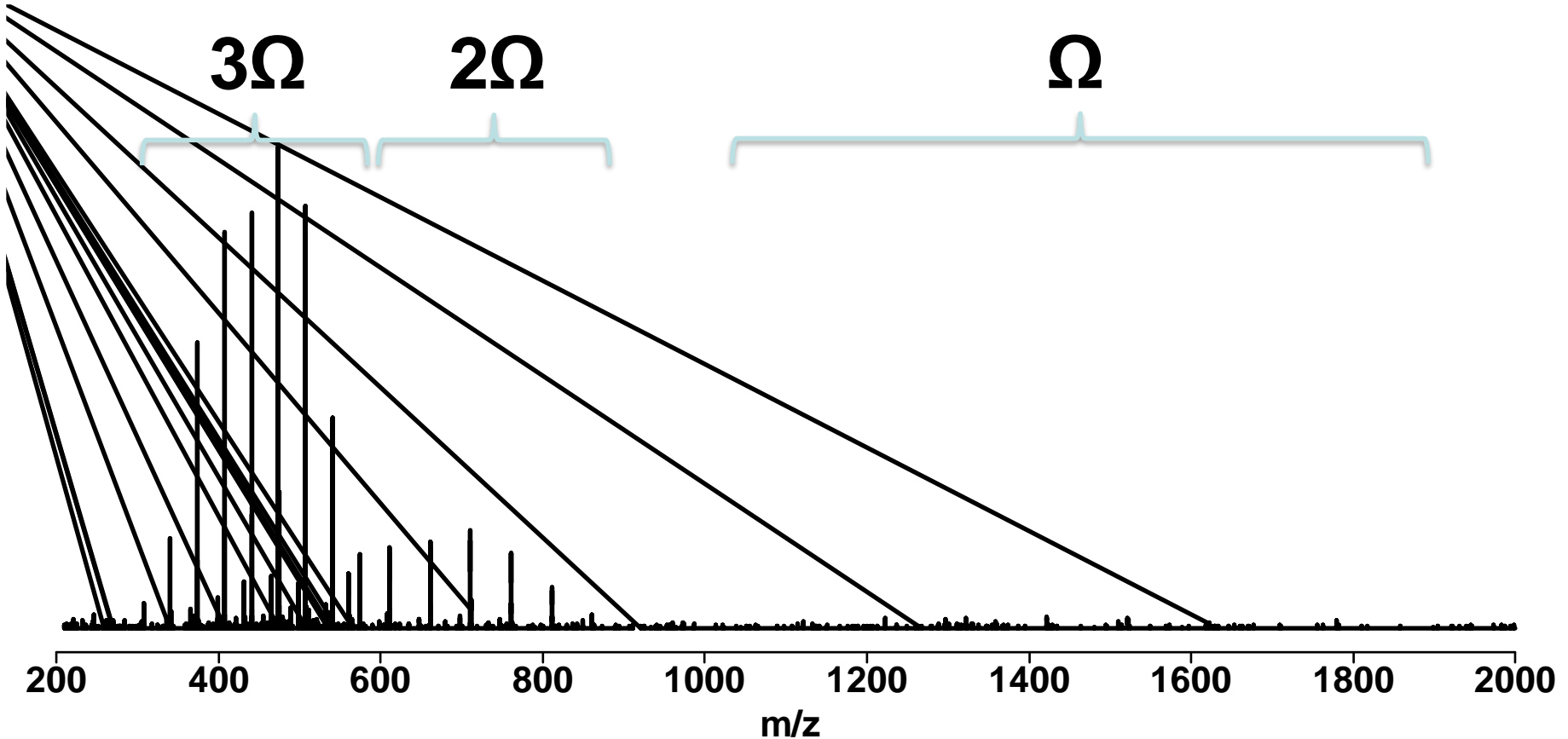


Fig. 11. Simulation for 16-electrode cell shown in . Cells radius $R = 1$. •, experimental amplitudes obtained in [7] for first four harmonics; —, the result of computer simulation for fixed cyclotron radius, $\rho = 0.1$ and several magnetron radii. Correlation between excitation time and magnetron radius is pronounced.



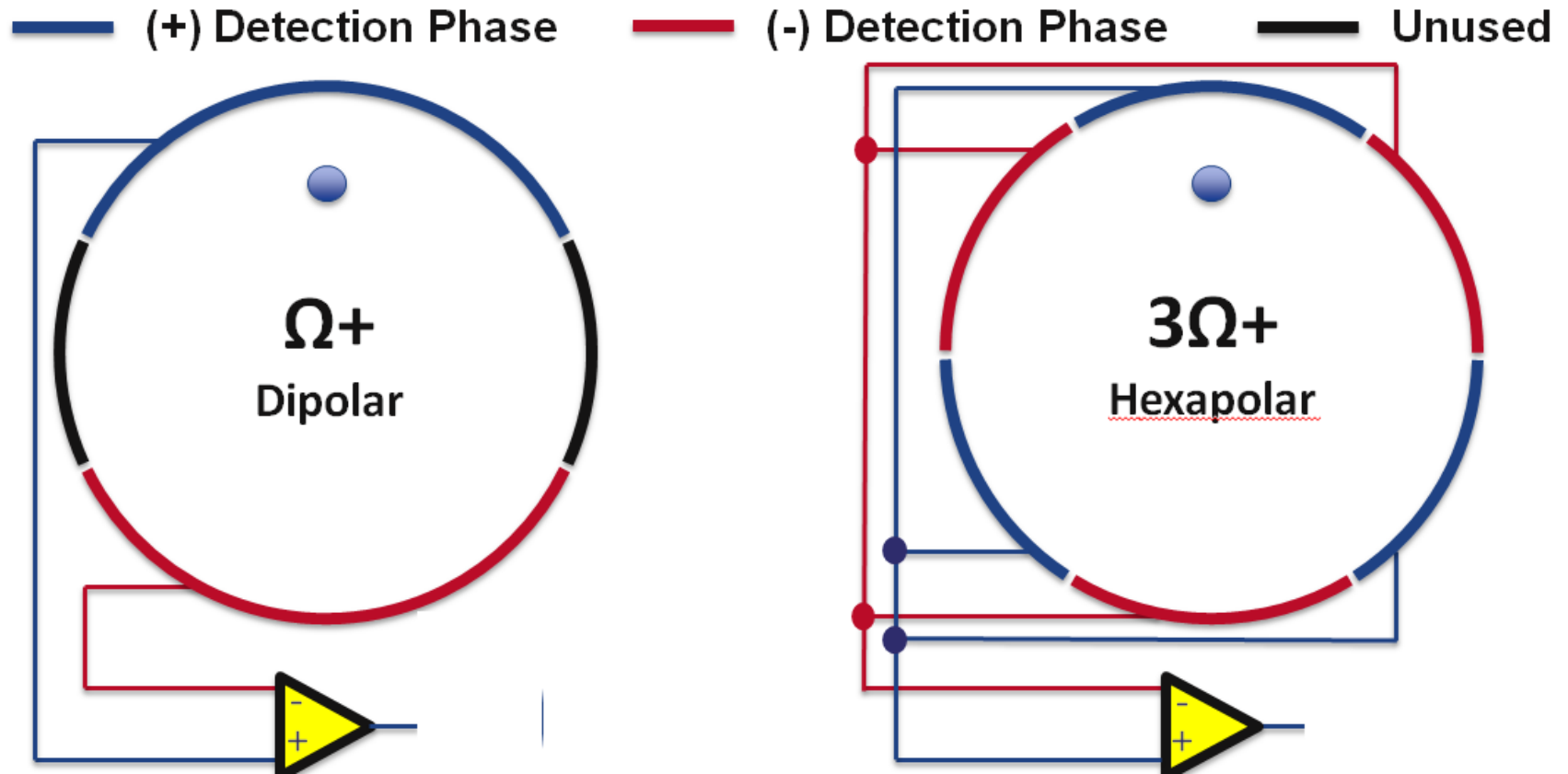
$$\omega_{\text{signal}} = 4 * \omega_{\text{cyclotron}}$$

Spectral Acquisition at 3Ω (14.5 T)



Alan Marshall 13th European FT MS Workshop (Freising)
26 April, 2018

3 Ω Detection Geometry



Alan Marshall 13th European FT MS Workshop (Freising) 26 April, 2018

Thank you!

Acknowledgement to

HORIZON 2020 FT ICR
network programm